Università degli Studi di Torino
Department of Life Sciences and Systems Biology
PhD Programme in Biological Sciences and Applied Biotechnologies

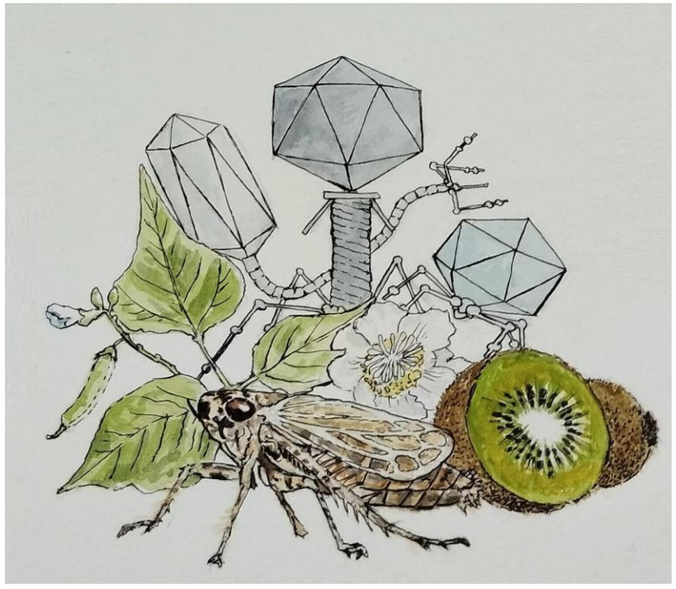

Bacteriophage-Based Biocontrol Methods in Two Model Crops

Gabriele Martino

PhD Programme Coordinator: Prof. Silvia Perotto

Academic Years: 2019–2022

Tutor: Prof. Luisa Lanfranco

Co-Tutor: Dr. Massimo Turina

Academic Discipline (SSD): BIO/01

Università degli Studi di Torino

Tesi di Dottorato di Ricerca in Scienze Biologiche e Biotecnologie Applicate

PhD Thesis in Biological Sciences and Applied Biotechnologies

Bacteriophage-Based Biocontrol Methods in Two Model Crops

Gabriele Martino

Academic Tutor: Prof. Luisa Lanfranco
Non-academic Tutor: Dr. Massimo Turina

XXXV Cycle: 2019 – 2022

Contents

1 INTRODUCTION

Bacterial diseases of plants are becoming more and more a limiting factor in some specific crops, because of the very limited options available for containing their impact. Furthermore, some of the most destructive recent emergencies in crop protection are indeed due to introduction of new bacterial diseases as the CoDIRo diseases caused by *Xylella fastidiosa* in Southern Italy on olive trees, and the HLB (huánglóngbìng) disease in citrus worldwide. Mimicking the recent revival of phage therapy against human bacterial infections (particularly those caused by antibiotic resistant bacteria), phages have been at the center of attention of many research groups as a feasible alternative to contain plant bacterial disease. Here in our work, we will consider two important crops (a woody one and an herbaceous one) that face considerable production limitation from bacterial diseases: Kiwifruit and beans. We will start describing the two cropping systems and their bacterial diseases, and we will then present a background knowledge on phage therapy approaches for biocontrol for such threats.

1.1 Kiwifruit

Kiwifruit is a fruit known for its sweet acidic taste and for its high content in ascorbic acid. (Ferguson & MacRae, 1991). Its domestication is relatively recent: it started a little more than 100 years ago and the crop raised to a worldwide cultivation only in the 1970s (Huang, 2016). Its production rose from 1.5 million to about 4 million tons per year from 2000 to 2020. As a crop it has a value of three billion euros annually and a retail market value of ten billion euros with Italy listed as the third world producer after China and New Zealand (http://faostat.fao.org). In Italy in the last 20 years registered a decrease of the culture in the northern regions, and an increase in central and southern Italy, and the rise of var. *chinensis* that is substituting var. *deliciosa* (https://terraevita.edagricole.it/frutticoltura-orticoltura/kiwi-landamento-della-coltura-in-italia-negli-ultimi-20-anni/). The kiwifruit taxonomic hierarchy is: Order *Ericales*, Family *Actinidiaceae*, Genus *Actinidia* Lindl. The genus *Actinidia* Lindl. groups 54 species of dioecious woody plants, mostly with a Southwest China origin area, distributed from tropical to cold temperate areas with a high degree of biological diversity. Its variability is partly due to its large geographical distribution (Chou-Fen & Ferguson, 1986).

Under natural conditions, kiwi fruit develops as a strong vine if it is supported, or if it is not as a large shrub, and can last over a hundred years. The root system is shallow, with a horizontal distribution greater than the vine crown and it is composed of a fibrous system of fleshy roots (Cui, 1993; Huang, 2016). The kiwifruit wood has a intersperse, or diffuse-porous xylem, with no clear rings visible. In the old stems xylem rays are obvious. Xylem tissue is loose with large vessels, on the contrary the phloem layer is thin. (Ferguson, 1984; Huang, 2016).

The two varieties of kiwifruit *Actinidia chinensis* Planch var. *deliciosa* and *Actinidia chinensis* var. *chinensis* (A. Chev.) are the most cultivated and commercially relevant ones. A third variety of *Actinidia chinensis*, var. *setosa*, has a lesser economic importance (Huang, 2016). The first one, var. *deliciosa,* has mainly green-fleshed cultivars while the second, var. *chinensis*, includes yellow- or red-fleshed fruit cultivars (Huang, 2016). Another species of kiwifruit economically relevant is *Actinidia arguta* that comprises two different varieties (*A*. *arguta* var. *arguta* and *A*. *arguta* var. *giraldii*). The species is distinguishable from *Actinidia chinensis* mainly for the fruit shape and size. The fruits are globose or ovoid, glabrous and smaller than *Actinidia chinensis* (4 cm long, 2.5 cm of diameter) (Huang, 2016). The two *Actinidia chinensis* varieties differ in vegetative morphology, flower and fruit morphology and in chromosome number (Chou-Fen & Ferguson, 1986; Gui, 1981; Jie & Beuzenberg, 1983; Zhi-Yu, 1983). The two varieties have also phenological differences such as a different flowering time and a consequently different susceptibility to pathogens and insects (Mauchline & Hill, 2005).

Although at the beginning of its cultivation in New Zealand kiwifruit orchards were almost disease free, excluding the common root rot (*Phytophthora cactorum*), the increasing span of kiwifruit commercialization took to the adaptation of disease of other plants to kiwifruit and to the emergence of diseases specific to kiwifruit. Concerning insect pests, more than 16 leafhoppers were signaled to damage kiwifruits, with *Empoasca rufa* and *Erythroneura sudra* as the most frequent (Huang & Ferguson, 2001) (H. Huang, 2016). In the last years the brown marmorated stink bug, *Halyomorpha halys,* is posing a threat to kiwifruit production in Italy (Francati et al., 2021). Diseases of microbiological origin of kiwifruit can be divided in four broad categories: i) bacterial diseases as bacterial canker caused by *Pseudomonas syringae* pv. *actinidiae*, bacterial blossom blight and crown gall; ii) fungal diseases as *Armillaria* root rot, collar rot, fruit rip rot, leaf spot, fruit storage rot and black spot; iii) virus diseases as tobamovirus and chlorotic leaf spot virus; iv) nematode-caused diseases consisting of *Meloidogyne hapla*, *M*. *arenaria* and *M*. *javanica* agents of northern root rot (Huang, 2016). Since 2012 a new disease emerged in northern Italy, named kiwifruit vine decline syndrome a disease with a still unknown etiology and suspected to be multifactorial in its causes, presenting characteristics of a fungal disease and of a physiological disorder (Donati et al., 2020; Tacconi et al., 2019). In Kiwifruit cane decay changes in root morphology associated to anoxy are observed, but symptoms cannot be reproduced if the anoxic conditions are applied to sterilized soil (D'Ippolito et al., 2021; H. Huang & Ferguson, 2001; Savian et al., 2020).

1.2 Beans

Beans, or pulses, dry seeds of edible legumes, are one of the basilar crops for human dietary supply, source of proteins, vitamins, minerals and starch (Carvalho et al., 2012). The production of dry beans deincreased from 18 million to 17 million tons per year from 2000 to 2020, and the production of string beans was 146,000 tons in 2020. *P. vulgaris* is

cultivated worldwide in tropical, semitropical and temperate climates with the main part of the production concentrated in Latin America and sub-Saharan Africa (http://faostat.fao.org).

The common bean taxonomic hierarchy is: order *Fabales*, family *Fabaceae*, subfamily *Faboideae*, tribe *Phasoleae,* genus *Phaseolus* L., species, *Phaseolus vulgaris* L.. The genus *Phaseoulus* contains about 70 species five of which were domesticated (*P. vulgaris, P. dumosus, P. coccineus, P. acutifolius, P. lunatus*)(Bellucci et al., 2014).

The *Phaseolus vulgaris* species, one of the most ancient crops in the world, owns a great variety of different cultivars specialized in the production of dry beans or string beans, among which borlotti beans, green beans, pink beans, white beans, yellow beans, black turtle beans, cranberry beans, kidney beans and flageolet beans are just some of the more represented.

Both the domesticated and wild forms of *Phaseolus vulgaris* are self-pollinating, autogamous, diploid species, with 2n = 2x = 22 chromosomes. Hybridization between domesticated and wild plants of *P. vulgaris* is common (Salinas et al., 1988; Singh et al., 1991).

Different methods were used to obtain common bean genetic content and the first results obtained were a linkage map, (Expressed Sequence Tags (EST) collections, and a physical map (Gepts et al., 2008; McClean et al., 2008). The first complete reference genome covered 487 Mb of the total 630 Mb (Schmutz et al., 2014). Today 4 other different assemblies are available (https://www.ncbi.nlm.nih.gov/genome/browse/#!/overview/Fabaceae)(Kagale & Close, 2021; Nadeem et al., 2021). Natural crossing events between *P. vulgaris* and other members of the genus are rare, due to various incompatibility mechanisms (Broughton2003).

Two geographical gene pools were formed before the domestication of the wild common bean (Bellucci et al., 2014). In 1995 a third gene pool with intermediate molecular and morphological characteristics was identified in northern Peru and Ecuador, distinct for the production of type I phaseoli. The other two groups were probably originated from the latter group, expanding to north and south (Kami et al., 1995). However, this hypothesis was substituted by a Mesoamerican origin of the first plants, as a higher diversity was detected in central America, with a distinction into four groups, B1-B4 (Bitocchi et al., 2012). It was possible to identify six races of domesticated common bean, three from Middle America, and three from Andean South America (Singh et al., 1991).

Common bean growth stages can be divided, as other *Fabaceae*, in emergence and early vegetative growth, branching and rapid vegetative growth, flowering and pod formation, and pod-fill and maturation. The first stage of emergence and early vegetative growth is a

critical stage for possible infection or systematic invasion of pathogens already present on the surface of the seed or present in the soil and water surrounding the seed. This stage can be further divided in VE (hypocotyl emerged from soil, crook stage), VC (two cotyledons & primary leaves at nodes 1 and 2), V1 (Figure 1.1), V2 and V3 (1st, 2nd and 3rd trifoliate leaf unfolded at nodes 3, 4 and 5) (https://beanipm.pbgworks.org/common-bean). The major bacterial diseases of dry beans are bacterial wilt, brown spot, common blight and halo blight. Fungal diseases, such as fusarium root rot, fusarium wilt, rhizoctonia root rot and rust are also of concern. Regarding insect pests, thrips, as *Thrips tabaci* and *Frankliniella occidentalis*, can cause damages to growing tips and leaves (OECD, 2016).

Figure 1.1: *Phaseolus vulgaris* growth stage V1

1.3 *Pseudomonas syringae*

Taxonomically the *Pseudomonas syringae* (P.s.) species complex, also called *P. syringae* sensu *lato* belongs to Proteobacteria, gamma subdivision, order *Pseudomonadales*, family *Pseudomonadaceae*, genus *Pseudomonas*. Members of this species complex are equally found in agronomical and water habitats, with a wide range of niches from salty or fresh water to the rhizosphere of wild and crop plants, associated to the soil fauna, to fungi and plants (Berge et al., 2014; Goldberg, 2000). *Pseudomonas syringae* species complex can be divided in three different ecotypes, one specifically found in crops, one water-specific and the third, the most abundant, found in both habitats. The epidemiology of P.s. is likely to be linked to the possibility to adapt to the water cycle, using its ice-nucleation ability. The diversity of the pathogen can be due to the exchange of population between agricultural and water habitats, that can play a role as environmental reservoirs (Morris et al., 2010; Morris et al., 2008). *Pseudomonas syringae* species complex gathers closely related

pseudomonads and it can be divided in nine genomospecies, 13 phylogroups and more than 60 pathovars.

Phylogroups classification was defined on basis of genetic distance of less than 5% in conserved housekeeping genes. *Pseudomonas syringae* species complex was initially divided in 7 phylogroups (Parkinson et al., 2011) and then in 23 clades distributed in 13 phylogroups Through Multi Locus sequence Typing (MLST)(Berge et al., 2014). The sequence of the Citrate synthase (*cts*) in this study was indicated as highly predictive of the phylogroups of a *Pseudomonas syringae* strain, and was used in a successive study to recognize *Pseudomonas syringae* sensu *lato* species (Guilbaud, et al., 2016).

Another existing division of the *Pseudomonas syringae* species complex was based on Average Nucleotide Identity tetranucleotide (ANI/TETRA) analyses combined with multilocus sequence analysis (MLSA). In this way nine different genomospecies were individuated. Each genomospecies groups strains, with at least 70% DNA-DNA homology and with the presence of different phenotypic characteristics compared to other genomospecies. Genomospecies 8 includes *P. s*yringae pv. *actinidiae*, *P. syringae* pv. *theae* and *P. avellanae.* Genomospecies 2 includes *P.syringae* pv. *phaseolicola*, *tabaci*, *aesculi*, *glycinea* and *mori* (Marcelletti & Scortichini, 2014).

On a finer scale pathogenic variety (abbreviated pathovar or pv.) distinction was made accordingly to the host range of plants infected by different strains. *Pseudomonas syringae* species complex counts more than sixty different pathovars, able to cause disease in a large number of monocotyledon and dicotyledon plants with a broad range of symptoms as cankers, speck, spot and blight (Young, 2010). The division in pathovars is not applicable to saprophytes found in the environment belonging to the species complex (Berge et al., 2014).

Races are established depending on 'avirulence' Avr genes interaction with R proteins in plants (Taylor, et al., 1996). *Pseudomonas syringae* pv. *phaseolicola* (Pph) like other *P.s*. pathovar can be subdivided in races.

As a general mechanism of infection, the bacteria in the species complex enter the host plants through natural openings (stomata and hydathodes) and wounds in the epidermis (Melotto et al., 2008). Humidity is a key factor for occupying the phyllosphere and *Pseudomonas syringae* cells are able to change the leaf surface and water availability by producing and releasing surfactants, increasing their virulence (Koskella 2020). Ice nucleation is a characteristic owned by some members of the species complex (present in Psa, but not in Pph) that allows the bacteria suspended in air to function as start nuclei to form rain drops, snowflakes or hail and therefore return to the soil and plants surfaces. Ice nucleation can help to create wounds on the plant surface and increase the possible access points. *Pseudomonas* genus members can use aggregations as biofilm to protect themselves from environmental stresses (Danhorn & Fuqua, 2007). Once entered in the

host *Pseudomonas syringae* pathogenicity is caused by two main mechanisms, the inhibition of the host immunity machinery and the creation of a humid niche in the host phyllosphere to help bacteria feeding and diffusion (Xin et al., 2018). The pathogenicity of *P.s.* is linked to *hrp* genes linked to the expression and assembly of Type III Secretion systems (T3SS) (Arnold, et al., 2011).

1.4 *Pseudomonas syringae* pv. *actinidiae* (Psa)

The kiwifruit bacterial canker (KBC) caused by *Pseudomonas syringae pv. actinidiae* (Psa) is a highly virulent and quickly spreading phytopathogen, able to infect kiwifruit belonging to different cultivars and of different ages. It is considered the main hindrance for the possibility to cultivate kiwifruit worldwide (Donati et al., 2014; Scortichini, et al., 2012; Vanneste, 2017). It belongs to genomospecies 8 (Marcelletti & Scortichini, 2014) and phylogroup 13 (Berge et al., 2014).
Psa is a Gram-negative rod-shaped bacterium. It is an obligate aerobe, motile (with one or more polar flagella), oxidase-negative and arginine dihydrolase-negative. It is not able to develop resistance spores and to produce fluorescent substances (H. Huang, 2016).

The first reported genomes of Psa were published in 2011 from an Italian strain (Marcelletti et al.,2011) and a strain isolated in Asia (Baltrus, 2011).

The pathogen was firstly reported in California, USA and in Shizuoka, Japan in 1980 and then identified and reported formally in 1983 and 1984 (Opgenorth et al.,1983; Serizawa, et al., 1989). Soon after it was reported in Italy (Scortichini, 1994) and Korea (Koh, 1994). The isolated Psa strains initially isolated didn't have a strong impact on the world production of kiwifruit (Onorato et al., 2010). The situation changed in in 2008 when a pandemic outbreak of Psa started in Italy and quickly spread to most of the countries cultivating kiwifruit (Vanneste, 2012; Kim et al., 2016) and reaching a global scale (Donati et al., 2014; Ferrante & Scortichini, 2009; Ferrante & Scortichini, 2014; Scortichini et al., 2012; Vanneste, 2017). In Italy, Korea and New Zealand Psa is still endemic today (Chapman et al., 2012; Kim et al., 2016; Vanneste, Yu, et al., 2013).

The original strains of Psa seemed to come mainly from China but not as the only country of origin. The main degree of variation in isolated Psa strain was reported in Japan and Korea (McCann et al., 2017). In China the pathogen was observed as relatively weak and did not caused outbreaks in the last 35 years, maybe because of the high number of different cultivars used for kiwifruit production in China (H. Huang, 2016). The economic impact for farmers in Italy was estimated as € 20,000/ha/year in production losses, € 5,000/ha for orchard investments and € 15,000/ha for the elimination of plants in order to stop spread of infection

(http://www.kiwiinforma.it/jm/images/stories/articoli/art_storia_della_batteriosi_2013.pdf). Psa is expected to further spread in Europe in the next years (EFSA et al., 2020). In the next years, due to the presence of the optimal climatic conditions, the areas fit for the insurgence of the bacterial canker of kiwifruit could increase. Accordingly, to the use of three modelling methods (MaxEnt, CLIMEX and a Multi-Model Framework, including Support Vector Machine or SVM) Psa establishment will be possible in California (USA), northern Iran, and areas still not affected in Greece, Belgium, Denmark and South Africa (Narouei-Khandan et al., 2022)

The *actinidiae* pathovar is now divided in 5 subgroups with different virulence, called biovars. Psa biovar 1 or Psa1 was isolated in Japan and Asia in 1984 only from infected var. *deliciosa* kiwifruit plants and it is able to produce phaseolotoxin. Psa2 was isolated in 1992 In Korea and was detected in the following years in Italy, in Lazio region. Psa2 was detected only from diseased var. *deliciosa* individuals and it is a coronatine toxin producer. Psa biovar 3, formerly known as Psa V, was the cause of the global outbreak of Psa in 2008 in both var. *deliciosa* and var. *chinensis* hosts (McCann et al., 2017). It is not able to produce phytotoxins (Donati et al., 2014; Ferrante & Scortichini, 2009; Huang, 2016; Vanneste, 2017). Psa Biovar 4 (also named Psa-LV) was isolated in New Zealand and its strains are spread in Australia and New Zealand. It showed a less virulent behavior, causing only leaf spots as symptoms or even absence of symptoms. Biovar 4 is now considered a new separate pathovar, *P. s.* pv. *actinidifoliorum* (Cunty et al., 2015). Psa biovar 5 and biovar 6 were identified in Japan in 2015. Psa biovar 5 phylogenetic position is near to biovar 2 although no genes associated to the production of coronatine were detected in its genome. It has a specific composition of 45 T3SE genes that distinguish it from the other biovars (Fujikawa & Sawada, 2016). Psa Biovar 6 genome showed the greater similarity with Psa Biovar 3 genome, but differently from biovar 3 it has both the gene cluster necessary for the biosynthesis of coronatine and phaseolotoxin. It has 29 T3SE genes, two of which, unique to this biovar (Fujikawa & Sawada, 2019).

Regarding plant sensitivity to the pathogen, kiwifruit species and varieties from the less sensitive to the most sensitive can be listed as follow: *A. arguta*; *A. chinensis* var. *deliciosa* 'Hayward'; *A. chinensis* var. *chinensis* – 'Zesy002'; *A. chinensis* var. *chinensis* – 'Jintao'; *A. chinensis* var. *chinensis* – 'Hort16A' (I. Donati et al., 2020). The two varieties *chinensis* and *deliciosa* differ in their susceptibility to Psa with *A. chinensis* var. *chinensis* cultivars more susceptible, with more severe symptoms, a greater spread and faster dieback (Young, 2012). Explanations of this can be found in plant morphology (Miao et al., 2005) as density of trichomes (in var. *chinensis,* in resistant *A. arguta* trichomes almost absent) (Donati et al., 2020) or also in leaves microhabitat conditions (Balestra & Varvaro, 1995, 1997). Moreover, regarding the plant defense mechanisms against Psa, In *Actinidia chinensis* var. *deliciosa* acibenzolar-S-methyl is more effective in producing resistance associated pathways than in var. *chinensis* (A Cellini et al., 2014). Taking in account the microbiome of the phyllosphere the most dramatic change in its composition following Psa infection was

observed on the leaves of *A. chinensis* var. *deliciosa* (Purahong et al., 2018). *A. arguta* kiwifruit species is the less sensitive to Psa and economic damages on these cultures are considered negligible (Cotrut et al., 2013; Vanneste, et al., 2014). This difference in sensitivity can be explained partially by a morphological difference in the plant surfaces. Trichomes are more abundant in *A. chinensis* var. *chinensis* leaves and in younger leaves of both var. *chinensis* and *deliciosa*, while are very scarce on leaves surface of *A. arguta.* This lower number of trichomes make the *A. arguta* phyllosphere a more difficult microhabitat, able to retain less humidity, necessary for the epiphytic life and the infection of Psa (He et al., 2000; Huang, 2016). *A. arguta* greater tolerance to the disease seems also to be linked to a difference in the activation of defense systems compared to *A. chinensis* var. *deliciosa.* In the green fleshed kiwi, following Psa infection are activated the JA-mediated and SA-mediated defensive pathways, whereas in *A*. *arguta* was registered a downregulation of the ABA pathway. In *A. chinensis* var. *deliciosa* Psa attack cause the upregulation of sucrose metabolism and transport related genes, with an accumulation of sugars in plant tissues that might facilitate Psa colonization. *A*. *arguta* on the other hand activates more specific defense-related genes (Nunes da Silva et al., 2022).

1.4.1 Psa infection cycle

Psa bacteria are able to colonize different organs of kiwifruit each with different specific symptomatology. Psa, as other pathovar of *P.s.* species complex, is able to conduct an epiphytic phase before entering the plant. The bacterial cells penetrate in the plants through wounds and natural openings. Psa causes primary external infections entering by wounds caused by frost, wind and rain, pruning cuts, broken trichomes (Renzi et al., 2012; Spinelli et al., 2010) abscission scars, and natural openings as lenticels, stomata and hydathodes. Biovar 3 strain CFBP7286 was modified to produce GFP or DsRED to confirm entry points and translocation in the plant tissues (Donati et al., 2020).

The most common entry sites on leaves are stomata. Plants possess defense systems that cause the closing of stomata when molecules belonging to the pathogen are sensed. Different biovars of Psa used different molecules to overcome this defense line as coronatine produced by biovar 2 (Han et al., 2003; Vanneste, et al.,2013) or ethylene (Donati et al., 2014) that promote stomata opening. Although coronatine does not seem necessary for virulence as no strain of biovar 3, despite their high pathogenicity, own genes for its synthesis (Ferrante & Scortichini, 2010). Biovar 3 strains produces ethylene that might support the colonization of the interior of the kiwifruit by antagonizing the SA-induced plan defenses (Cellini et al., 2014).

Leaves and flowers are the primary infection sites in Kiwifruit (Donati et al., 2018; Serizawa & Ichikawa, 1993; Serizawa et al., 1989).

Contaminated pollen in field conditions represents one of the major infection pathways (Donati et al., 2018).

A limited importance of lenticel as entry sites was reported in natural conditions, although experimentally they can lead to systematic invasion of plant tissues especially from young hydrated lenticels. Roots instead do not seem to be a significative entry point for Psa cells (Donati et al., 2020).

The environmental conditions for the primary infection and for the bacterial canker progression are optimal in late winter and spring when physical damages caused by wind, rain and frost are frequent (Balestra, 2004; Serizawa et al., 1989).

In this first phase, Psa causes leaf spots between foliar veins. Wet leaves are required to connect the leaves exterior surface to the stomatal chambers providing a liquid film for the bacteria to travel into to the spongy mesophyll. If humidity exceeds 80% leaf spots can form bacterial exudates, starting a spring leaf cycle (Donati et al., 2020). A flower cycle can develop in this season too, caused by infected pollen (Donati et al., 2018). Both the flower and leaf colonization and infection may cause systemic infection during spring and consequently possible secondary symptoms during the following autumn.

During summer there is a latency in the disease progression and in symptoms occurrence mainly due to the rise in temperature, when the average temperature increases over 22 °C. Additionally the symptoms decreases when the leaves are wet below 4 h per day for more than 3 days. In Italy these conditions are met in late June (Donati et al., 2020).

In autumn a systematic bacteria spread through the apoplast follows causing the death of the infected plant (Spinelli et al., 2010). In this season leaves and fruit abscission scars and pruning cuts are the main entry points for the epiphytic pathogens. Psa colonization of leaf scars occurs even after 15 days from the natural or mechanical leaf detachment, with a partial protection from Psa entrance in the first days of detachment of the abscission layer (Donati et al., 2020). Pruning has similar effects with a colonization of the scars occurring up to one month after the cut, with a similar sensitivity for *A. chinensis* var. *deliciosa* and *A. chinensis* var. *chinensis.*

In autumn it is possible to observe secondary symptoms, as water-soaked leaf spots and exudates, following frost events (Ferrante & Scortichini, 2014).

After an asymptomatic phase in which is dormant, at the end of the winter and in the beginning of the spring Psa migrates and gives secondary internal infections, with a systemic infection of the xylem, with the rise of cankers in trunks and vines (Tyson et al. 2014).

Psa polysaccharides production and the root positive pressure that is present at the end of winter, cause an emission of exudates from pruning cuts if present and from old and new

cankers in the bark (Clearwater et al., 1990; Ichinose, et al., 2013; Mansfield et al., 2012; Von Bodman et al., 2003).

These bleeding cankers represents the primary inoculum source in spring (Kim et al., 2016). The water uptake transfers the bacteria from the root system to the buds where the pathogens can multiply with a possible failure of bud break or shoot dieback in early spring. In flower buds the phytopathogen can enter in the anthers causing the formation of infected pollen (Donati et al., 2018; Purahong et al., 2018), the main inoculum source during spring.

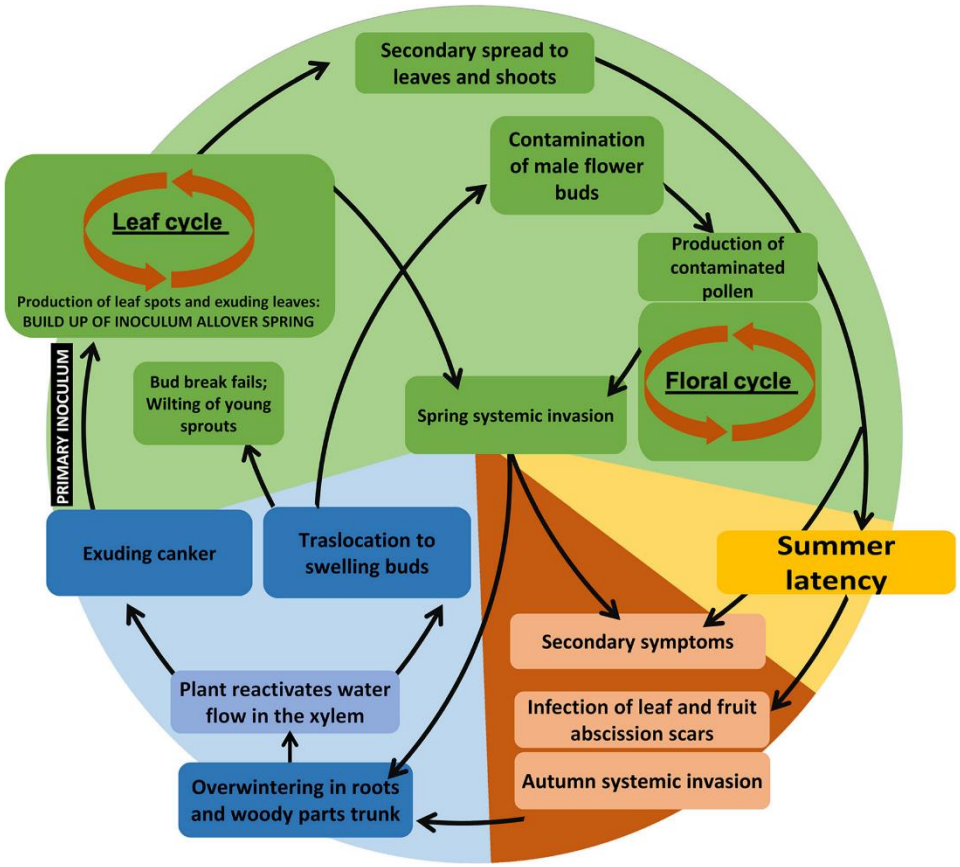

Figure 1.2: *Pseudomonas syringae* pv. *actinidia* kiwifruit bacterial canker cycle (Donati et al., 2020).

After the infection Psa bacteria migrate from the leaves to the shoots and canes through the apoplast (Donati et al., 2014; Renzi et al., 2012; Spinelli et al., 2010). The preferential pathway of migration of Psa is through the xylem where it can obstruct the xylematic vessels (Donati et al., 2020; Renzi et al., 2012). The previously cited GFP producing Psa

strain showed that Psa can colonize also the periderm, sclereids, and the pith of the plants, although the migration probably happens mainly through the xylem (Donati et al., 2020).

The migration of the phytopathogen is both basipetal and acropetal and can overcome branching nodes. Acropetal translocation can be explained by xylematic flow caused by evapotranspiration (Gao et al., 2016; Renzi et al., 2012). Xylem tyloses are formed by the plant to hinder the bacteria spread (Ferrante et al., 2012), more frequently in *A. chinensis* var. *deliciosa* than in *A. chinensis* var. *chinensis* (Renzi et al., 2012). Psa polysaccharides production can be responsible too for the apoplast migration in a phenomenon called mass flow (Ichinose et al., 2013; Mansfield et al., 2012). Another cause of translocation can be an active bacterial chemotaxis, facilitated as the infection process by a high relative humidity (Vanneste et al., 2013).

The greater number of active bacteria infecting the plants is reached in spring. There is some further activity in summer that allows the spread through multiplication in the vine xylem. The symptoms begin to express in spring/autumn that have a weather and temperatures ideal for bacteria pathogenicity. Psa has an optimum at 12-18°C, and it is inhibited by temperatures higher than 25°C preferring a cool and humid climate (Froud et al., 2015).

The phytobacteria can persist in the environment or survive through the winter in plant residues (Donati et al., 2020). Psa can be cultured again after up to 10-15 days in autoclaved soil, but up to 45 days if fine radicle particles are added to the soil. In fallen leaves and wood from pruning the Psa inoculum can persit up to 6 months. (Donati et al., 2020). The role of farmers clothes and vehicles in the spread of the pathogen seems to be negligible (Everett et al., 2012).
The epiphytic presence of Psa in surrounding plant species commonly associated with Kiwifruit orchard is infrequent. In Italy it was found mainly on *Calystegia sylvatica* and *Capsella bursa-pastoris* (Donati et al., 2020). In New Zealand Psa was found in plants used for protective belts of infected kiwifruit orchards as *Cryptomeria japonica*, *Pinus radiata* and *Casuarina cunninghamiana*, with Psa population perduring on their phyllosphere between 4 and 8 days from experimental addition. Contrasting results were gathered for Psa persistence in water, maybe for the presence of the bacteria in small concentrations below the detection limits (Donati et al., 2020). Both in planta and in the exterior environment Psa was demonstrated to live as biofilm, with the colonies of bacteria embedded in matrix (Renzi et al., 2012).

1.5 *Pseudomonas syringae* pv. *phaseolicola* (Pph)

P. syringae pv. *phaseolicola* (Pph) which is also known as *P. savastanoi* pv. *phaseolicola*, causes bean halo blight, one of the most economically relevant seed-borne disease in beans. It was isolated for the first time as *Phytomonas medicaginis* variant *phaseolicola*

(Burkholder, 1926), but in 1943 it was renamed as *Pseudomonas medicaginis* variant *phaseolicola* (Dowson, 1943) and finally in 1978 it was inserted in the species complex of *P*. *syringae* acquiring its current denomination, *Pseudomonas syringae* pathovar *phaseolicola* (Young et al.,1978). It is present in temperate areas and in tropical regions only above medium altitudes.
It can infect other legume species, in particular all the members of *Phaseoleae* excluding only *Desmodium* spp. and *Pisum sativum*. It is prevalent worldwide and cause economic losses mainly in developing countries (Taylor et al., 1996).

Pph is a Gram-negative, aerobic, motile, rod-shaped bacteria, with a diameter of 0.7-1.2 µm and a length of 1.5 µm and at least one polar flagellum. It is oxidase negative, arginine dihydrolase negative, levan positive and causes a hypersensitive reaction on tobacco (Arnold et al., 2011). In the bean plant apoplast it showed to prefer to metabolize malate, glucose and glutamate in comparison with other apoplast components as GABA and citrate (O'Leary et al., 2016). It is classified in Genomospecies 2 (Marcelletti & Scortichini, 2014) and in Phylogroup 3 (Berge et al., 2014), a group containing soybean (*P.syringae* pv. *glycinea*) and woody plants (*Pseudomonas savastanoi* pv. *savastanoi* and *P. syringae* pv. *aesculi* and *mori*) pathogens. It is considered a super model for plant-pathogen molecular interaction, and was used to better understand the evolution of host specificity (Arnold et al., 2011). Whole genome sequencing of Pph strain 1448A (Joardar et al., 2005) and the sequences of two strains representing race 5 and 8 (Cooper & Yang, 2021) are available. There is a gene-for-gene interaction between the effectors genes 'avirulence' Avr of the pathogen and the R proteins of the plant and depending on the Avr genes Pph like other *P.s*. pathovar can be subdivided in races (Taylor et al., 1996). Nine different races were identified for Pph, of which 1, 2, 5, 6 and 7 are diffuse worldwide and race 6 is the most prevalent (Taylor et al., 1996).

1.5.1 Pph infection cycle

The main way for the pathogen to spread are rain splash and irrigation water and the optimal environmental conditions for disease initiation are when a cool (less than 25°C) moist weather occurs.

Pph is able to persist both within and as an epiphyte of dry bean seed becoming active after germination (Burkholder, 1930).

It enters the host though wounds, stomata and hydathodes. Its development cycle (from contamination to symptom appearance) is quick and can last less than 7 days in optimal conditions. The pathogen causes water-soaked lesions in leaves, stems or petioles and pods. In leaves at a temperature below 23 °C then become quickly surrounded by greenish-yellow haloes, a symptom distinguishable from the narrow yellow band caused by the

common bacterial blight (*Xanthomonas axonopodis* pv. *phaseoli*) (Figure 1.4). These symptoms are more visible in mild temperatures conditions and when a large amount of inoculum is available. As the infection progresses the yellowing spread through the plant (Figure 1.3) the clogging of xylem caused by the bacteria and defensive substances produced by the plant can cause the plant death in two to four weeks (Arnold et al., 2011; Webster et al., 1983).

Figure 1.3: *Pseudomonas syringae* pv. *phaseolicola* systemic symptoms on a bean plant.

Seeds can be infected too and can show no symptoms or buttery-yellow or wrinkle patches on their surface. Infected seedlings display stunting, distortion of growth and general chlorosis. Even a low degree of presence on seed surface, in the correct weather conditions can lead to severe epidemics (Webster et al., 1983). The bacteria can also infect several weeds, providing a reservoir from which a new infection can emerge (Fernández-Sanz, et L., 2016).

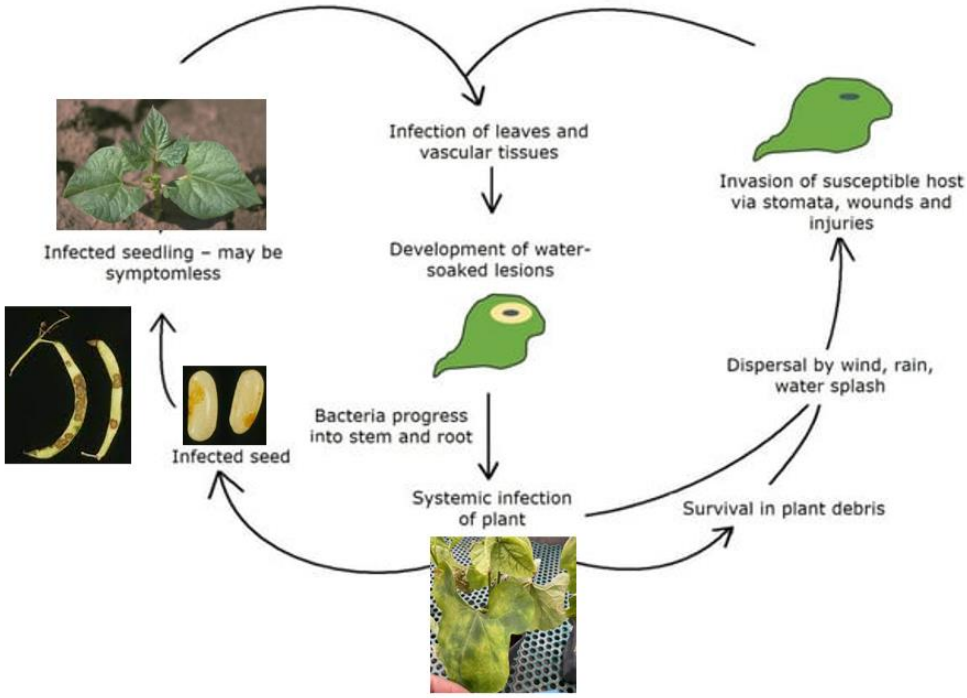

Figure 1.4: *Pseudomonas syringae* pv. *phaseolicola general* cycle in legumes.

1.6 Psa and Pph Control

1.6.1 Pseudomonas syringae pv. *actinidiae*

1.6.1.1 Chemical Control

The control of Psa relies now mainly on preventative chemical control through spraying of copper derivatives as copper sulfate and copper oxychloride and antibiotics as streptomycin (Koh, et al., 2001).

Both these solutions although arises problem linked to their phytotoxicity on leaves and stalks to residual on the protected plants and to the high possibility of resistance emergence in Psa. Streptomycin, the second antibiotic discovered by humankind, is classified as an aminoglycoside antibiotic originally used to control tuberculosis. Its action is the binding of the 16S rRNA on the 30s subunit of the bacterial ribosome and the subsequent inactivation of translation and death of the target (Mingeot-Leclercq, et al., 1999). Resistance in Psa was detected following prolonged use of streptomycin (Nakajima

et al., 1995). In Europe, an effective prevention relies only on copper derivatives products (Balestra, 2004; Collina et al., 2016; Scortichini, 2016) as the use of antibiotic for agricultural protection purposes is not allowed. However, these products were proven to damage the environment and some strains of Psa developed resistance to copper consequently to intensive copper treatments (Petriccione et al., 2017). However, there are some studies on developing nanoparticles-based copper products, to diminish the concentration of the metal used to reach the same protection from the bacteria (Ren et al., 2022). The European Commission is taking action to gradually restrict the copper derivatives in agriculture (Commission Regulation [EC], 2008. 396/2005/EC, 149/2008/EC).

1.6.1.2 Agricultural practices

Agricultural practices can be optimized to limit the spread of Psa. Pruning was demonstrated to easily spread the pathogen in the orchard, mainly inter-row. So, it should be performed when the pathogen is least active, in winter (Mauri et al., 2016). Root drip irrigation (in field, not experimentally) showed to spread the pathogen (Mauri et al., 2016). Wind and rain splashes are known to be the main pathway for the Psa bacteria to spread (Froud et al., 2015; Serizawa & Ichikawa, 1993). Plastic covers decrease the disease incidence (Black et al., 2014). Frost events, with cycles of freeze-thaw damage the plant surface (Ferrante & Scortichini, 2014). Flowers are between the main entry points (Donati et al., 2018) so certified pollen from Psa-free orchard should be used. The bacteria have been found in guts of pollinating and pathogen insects, but perduring for a brief period of time suggesting to exclude a long-range and long-term vectoring through insects (Cellini et al., 2019; Donati et al., 2017; Pattemore et al., 2014). The information to prevent the rise and spread of a Psa biovar 3 infection in kiwifruit orchard were diffused in an effective way to New Zealand farmers on the internet page https://kvh.org.nz/growers/psa-v-risk-compass.

1.6.1.3 Resistant Cultivars Breeding

Numerous breeding programs were conducted to screen varieties resistant to Psa. Wang described a method to search for Psa resistance or tolerance through an *in vitro* bioassay on canes of 18 *Actinidia* genotypes. The resistance was reached by a quick formation of callus on wounds and the sprouting of new buds (Wang et al., 2019). The morphological features associated with cultivars more sensitive to Psa were a greater branch lenticel density and a greater length and density of stomata (Miao et al., 2005). It seems that Psa resistance is mediated through the salicylic acid (SA) signaling pathway, as seedling treated with acibenzolar-S-methyl (ASM) showed a decreased incidence of the disease, opposite to seed treated with methyl jasmonate that showed an increased incidence (Reglinski et al., 2013). Kiwifruit varieties tolerance to Psa differences may be also linked to a different production and regulation of phytohormones and consequently of the plant primary metabolism (Da Silva et al., 2022).

1.6.1.4 Bacteria as Biological Control Agents

Phyllosphere is the term used to describe the above ground surface of a plant, especially related to its role as an habitat for microorganisms (Lindow & Brandl, 2003). The role of the phyllosphere microbiome is comparable with skin microbiome, as both represents the first defense line against environmental pathogens for the organism. In both cases a dysbiosis is often linked as a cause and/or an effect of a disease (Kembel et al., 2014; Koskella et L., 2017; Turner et al., 2013). On a greater scale phyllosphere microbiome can affect the relationship of the plant with herbivores also modulating the tritrophic relationship between plants, herbivore insects and parasitoids (Cusumano et al., 2022). Bacterial biocontrol agents (BCAs) can act as competitors, and inhibit the pathogen growth through the secretion of antimicrobial or pathogen signaling interfering molecules (Völksch & May, 2001).

Other bacteria are able to induce resistance in plants and promote the plant growth (Ottesen et al., 2013; Ryu et al., 2003). The use of small consortia of bacterial species was also considered to counteract the plant pathogens, exploiting their synergistic action (Kim et al., 2011; Sarma et al., 2015).

Psa presence on kiwifruit phyllosphere, in quantities sufficient to induce the disease has a significative influence on the surface microbiome of kiwifruit plants, especially female ones, inducing a reduction in the dominant genera found in healthy plants. Bacteria belonging to these genera can be considered for their antagonistic action against Psa or as enhancers of plant defense (Aitana, et al., 2021; Purahong et al., 2018). Following this research path, kiwifruit phyllosphere and rhizosphere were screened for bacterial strains against Psa, selecting three strains, one of *Streptomyces racemochromogenes*, one of *S. parvolus* and one of *Streptomyces* sp. (Kim et al.,, 2019); *Bacillus subtilis*, *Bacillus amyloliquefaciens* were tested in general as biocontrol agents (Biondi et al., 2012; Reva et al., 2004) and *Pseudomonas fluorescens*, *Bacillus subtilis*, *Bacillus amyloliquefaciens* and *Lactobacillus plantarum* were specifically tested against Psa (Collina et al., 2016; Daranas et al., 2019). A similar study took to the isolation of two *Pseudomonas fluorescens* strains able to reduce the growth of Psa (Donati et al., 2017).
But the BCAs have to be chosen with care as the pathobiome concept should be taken into account: namely that every pathogen can have an association with other host associated microorganisms that enhance its virulence or weaken the plant defense systems (Vayssier-Taussat et al., 2014). As examples Psa was found in syndemic association with *P.s.* pv. *syringae* and *P. viridiflava*, suggesting a possible pathogenic consortium (Purahong et al., 2018) and *Pseudomonas syringae* pv. *syringae* (Pss) can cause ice nucleation opening entry points for other pathogens as Psa (Lindow et al., 1978).

1.6.1.5 Elicitors of Plant Defense

Psa produces several effectors, as HopF2 and AvrRPM1 known to inhibit the action of RIN4 (Wilton et al., 2010), a protein important for the defense against bacterial phytopathogens.

RIN4 expression seems to be positively affected by Acibenzolar-S-methyl (ASM), a functional analogue of salicylic acid, together with Phenylalanine Ammonia lyase (PAL) an enzyme crucial for the production of defensive compounds called phytoalexins (Conrath, 2009). BION® 50 WG (Syngenta) a commercial formulation with 50% of ASM is currently used against Psa (Cellini et al., 2014; Reglinski et al., 2013; Valente et al., 2014). The use of *Aerobasidium pullulans* and the elicitor of defense acibenzolar-S-methyl showed a synergistic action of the two biocontrol method against Psa biovar 3 strains (de Jong et al., 2019). Chitosan and hairpin were tested also against Psa (Corsi et al., 2017; Dong, et al., 1999; Ferrante & Scortichini, 2010; Reglinski et al., 2011). Chitosan is a linear aminopolysaccharide obtained from shrimp shells and it is soluble below pH 6.5 due to an amino group on C-2 of the monomer becoming positively charged. It works as an elicitor of plant defenses, but this is not its only mechanism of action (Linden et al., 2000). Its antimicrobial properties are linked to its cationic status and to a low degree of acetylation. The mechanism of action can be linked to the interaction with the negatively charged bacteria membranes and/or interaction with bacteria DNA (Badawy & Rabea, 2011). Nevertheless, is necessary to take account of the possible loss in fruit production and/or fruit quality, caused by the relocation of the plant resources to defense following the use of elicitors (Cipollini & Heil, 2010).

1.6.1.6 Other Bioactive Molecules

Biological derived molecules have been considered also to contrast Psa as Imidazole alkaloids (Ma et al., 2022), isocoumarins derived from kiwifruit endophytic fungus *Paraphaeosphaeria sporulosa* (Chen, et al., 2022) and antimicrobic peptides (AMPs) (Cameron, et al., 2014; Mariz-Ponte et al., 2021). There are then several examples of terpenes studied as possible control means. Two monoterpenes, geraniol and citronellol showed similar inhibitory effects on *Erwinia amylovora* and Psa with geraniol being more effective than citronellol (Bauer et al., 2003; Scortichini & Rossi, 1991). Two terpenoids produced by the fungus *Bipolaris* sp are effective against Psa. (Feng et al.). It is necessary to take into account the a limited phytotoxicity of monoterpenes was observed for geraniol towards tomato (Chitwood, 2002). Additionally, inhibitors of Psa levansucrase are currently being developed (Luti et al., 2021).

1.6.2 Pseudomonas syringae pv. *phaseolicola*

1.6.2.1 Agricultural practices

The agronomic practices recommended to contrast Pph disease insurgence and persistence in field are crop rotation (Taylor et al., 1996), the use of pathogen-free seeds and the removal of diseased reservoir plants from the field (Arnold et al., 2011; OECD, 2016) Molecular diagnostic methods to detect Pph on mungbean (*Vigna radiata*) seeds as SYBR assay and hydrolysis probe techniques showed promising results (Noble et al., 2022).

1.6.2.2 Chemical Control

A certain degree of control of the Psa infection is reached through the use of copper formulations as Bordeaux mixture, copper sulfate, cupric hydroxide and copper oxychloride (Saettler et al., 1981), though this is only a preventive solution, avoiding the ingress of pathogens from the wounds (Arnold et al., 2011). These solutions show, as already mentioned for Psa, problems linked to phytotoxicity, residual on plant products and emergence of resistance in the treated populations of bacteria. Pph was found to use stationary-phase persistence to survive streptomycin treatment (Patel et al., 2021).

1.6.2.3 Resistant Cultivars Breeding

Resistance to Pph was found only in cultivars of *P. vulgaris* (OECD, 2016; Yaish et al., 2006). The resistant cultivars to halo blight obtained by breeding resulted inadequate in maintaining a high yield and quality of the fruit, without the application of other agricultural practices and disease free seeds (Singh & Schwartz, 2010). CRISPR-Cas approach for improving the resistance of common bean is considered difficult since regeneration form non-meristem containing tissues is difficult, limiting stable transformation of *P. vulgaris* (Mukeshimana et al., 2013).

1.6.2.4 Bacteria as Biological Control Agents

The microbial population is important in preventing and regulating pathogens action against the plant as mentioned in the previous paragraphs on Psa biocontrol methods. 131 endophytes bacteria of common bean were tested for growth promoting or Pph antagonistic action. Thirty plant growth-promoting bacteria were selected. Belonging to different genera of which the most represented were *Bacillus*, *Pseudomonas* and *Rhizobium*. The most effective in inhibiting Pph growth in vitro was *Pseudomonas gessardii,* that probably competes with the pathogens through the production of large amounts of extracellular siderophores (Duman & Soylu, 2019).

1.6.2.5 Elicitors of Plant Defense

Acibenzolar-S-methyl used against *P. syringae* pv. *tomato* (Louws et al., 2001). Pretreatment with analogs of salicylic acid (BABA or INA) in *P. vulgaris* gave an increased resistance against Pph caused by epigenetic modification, in an example of defense priming (Martínez-Aguilar et al., 2016). In vitro application of salicylic acid has a detrimental effect on Pph, diminishing its production of alginate that is necessary for its pathogenicity (Cooper, 2022).

1.7 Bacteriophages

The etymology of the world bacteriophages alone can explain the main activity of these viruses, which is to “devour” bacteria. Bacteriophages are viruses that target with high

specificity their bacterial host. Their number is hardly conceivable, being estimated of at least ten viruses every single bacterial cell, for a total of at least 10^{31} phages present on the Earth surface, in every niche where bacteria can be found (Wommack & Colwell, 2000).

One of the first reports of phage activity cited was for a long time a 1896 paper from Ernst Hankin in which an antimicrobial activity of water from Gange and Jumna rivers against *Vibrio cholerae* was measured (Hankin, 1896). However, this effect was not likely to be caused by phages, because the solution causing lysis retained this ability after heating in sealed tubes and the number of phage necessary to reproduce the same decrease of *Vibrio* population are not likely to be found in river water (Abedon et al., 2011). Gamaleya reported in 1898 of a lytic activity on *Bacillus anthracis* of a filtered lysate of the same bacteria. Interestingly the lysate acted specifically against *B*. *anthracis*, allowing other saprophytes bacteria to grow freely in it. At the time there was no concept of a non-cellular microbiological entity capable of parasitic replication, so the phenomenon was linked to a biochemical agent toxic to the bacteria; today we can suppose this was the first written report of bacteriophages in action (Bardell, 1982).

The official discovery of phages independently occurred in two papers in 1915 (Twort, 1915) and 1917 (d'Herelle, 1917). Both of them registered the presence of a filterable and transmissible lytic agent. Twort (1995) reckoned that the lytic principle was of enzymatic nature and d'Herelle hypothesized it was viral, naming the bacteria viruses for the first time as bacteriophages. Thirty years later d'Herelle hypothesis was confirmed.

Phages thus play a significant role in maintaining microbial diversity and regulating bacterial populations in various ecosystems (Czajkowski, et al., 2019) modulating the dynamics of free-living population of bacteria (Bouvier & Del Giorgio, 2007; Rodriguez-Valera et al., 2009; Schwalbach et al., 2004). However, their importance extends beyond controlling bacterial populations. Phages are also key players in nutrient recycling in aquatic systems, as they release nutrients from bacterial cells when they lyse them, making them available for other organisms to use and contributing to element geochemical cycles. Even large scale biogeochemical cycles, including those heavily influencing CO_2, atmospheric accumulation, and consequently climate change, are influenced by phages lysis of bacteria on the surface of the seas (Suttle, 2007; Weinbauer, 2004).

1.7.1 Bacteriophages structure and genome

Bacteriophages are composed of a protein capsid that encloses genetic material, which can be either DNA or RNA. The capsid is made up of repeating protein subunits that assemble to form a polyhedral or filamentous structure. Some bacteriophages also have additional structures, such as a tail or tail fibers that they use to attach to and infect their bacterial host. Bacteriophages exhibit a remarkable diversity in their size, shape, and structure. Some phages have a simple, icosahedral capsid that is symmetrical and geometrically

regular, while others have complex, multicomponent structures. For example, T4 phages have an elongated, hexagonal head that contains the genetic material and a contractile tail that is used to puncture the bacterial cell wall and inject the viral genome. In contrast, filamentous phages have a long, thin, and flexible structure. In some cases, the capsid is surrounded by an envelope that contains additional viral proteins and lipids. This envelope can help the bacteriophage evade the host immune system and facilitate its entry into the host cell. The tail of a bacteriophage is another important structural feature that allows the virus to recognize and attach to its host bacteria. The tail is composed of a tube-like structure that is made up of multiple protein subunits. At the base of the tail, there is a complex of proteins that acts as a molecular motor, which helps the virus inject its genetic material into the host cell. Some bacteriophages also have tail fibers that can bind to specific receptors on the surface of the host cell, allowing the virus to target particular bacterial species (Harper et al., 2019).

Phage genomes can be classified into several different types based on their genetic material. Most phages have double-stranded DNA (dsDNA) genomes, although some have single-stranded DNA (ssDNA) or RNA genomes. The size and complexity of phage genomes can also vary widely, with some containing just a few dozen genes and others containing hundreds of genes. The genes encoded in phage genomes are involved in different aspects of the viral life cycle, including replication, transcription, translation, and virion assembly. The organization of phage genomes is also diverse, with different phages having different genome architectures. Some phages have linear genomes, while others have circular genomes. Some phages have genomes that are segmented into multiple pieces, while others have single, contiguous genomes. The genes within phage genomes are arranged in different ways, with some phages having a "head-to-tail" arrangement, in which genes are organized in a linear fashion, while others have a more complex organization. No common sequences as bacteria 16S rRNA or fungi 18S/ITS were identified in bacteriophages, so it is not possible to easily identify phages only from their genetic content in a culture-independent way. On the contrary for a reliable identification, phages must be cultured, sequenced and their morphology observed through electron microscopy

Phage genomes also contain a variety of unique features that enable phages to rapidly adapt to changing environments and to infect different host bacteria. For example, phages often have genes encoding enzymes that modify the bacterial cell wall or other host structures, allowing the phage to more efficiently infect the host cell.

The structural diversity of bacteriophages reflects their evolutionary adaptations to different host environments and modes of infection. Phages can follow two different life cycles when they infect a host bacterium: the lytic cycle and the lysogenic cycle (Figure 1.5). In the lytic cycle, the phage infects the host cell, replicates its genome, assembles new phage particles, and then lyses the host cell, releasing the progeny phages into the surrounding environment. The lytic cycle is a rapid and efficient method of phage

replication, and can result in the death of the host cell in a matter of minutes to hours. In contrast, the lysogenic cycle involves integration of the phage genome into the host cell chromosome, where it is replicated along with the host DNA during cell division. The integrated phage genome is called a prophage, and it is passed on to daughter cells each time the host cell divides. Under certain conditions, such as exposure to stress or DNA damage, the prophage can be induced to excise from the host chromosome and enter the lytic cycle, leading to the production of new phage particles and lysis of the host cell. The lysogenic cycle allows phages to persist within a host population without immediately causing cell death, and can also lead to the transfer of genetic material between different bacterial strains, which can have important evolutionary consequences. It is possible also to have pseudolisogeny, a phenomenon in which a temperate bacteriophage appears to integrate into the host bacterium's genome as a prophage, but actually exists as an episome that can replicate independently. This process is mediated by a repressor protein that can switch between binding to the integrated prophage and the extrachromosomal episome forms of the phage. Pseudolisogeny is thought to provide a selective advantage to the phage, allowing it to maintain a persistent presence in the host population while avoiding immune detection or lysogenic induction (Harper et al., 2019) (Benler & Koonin, 2020).

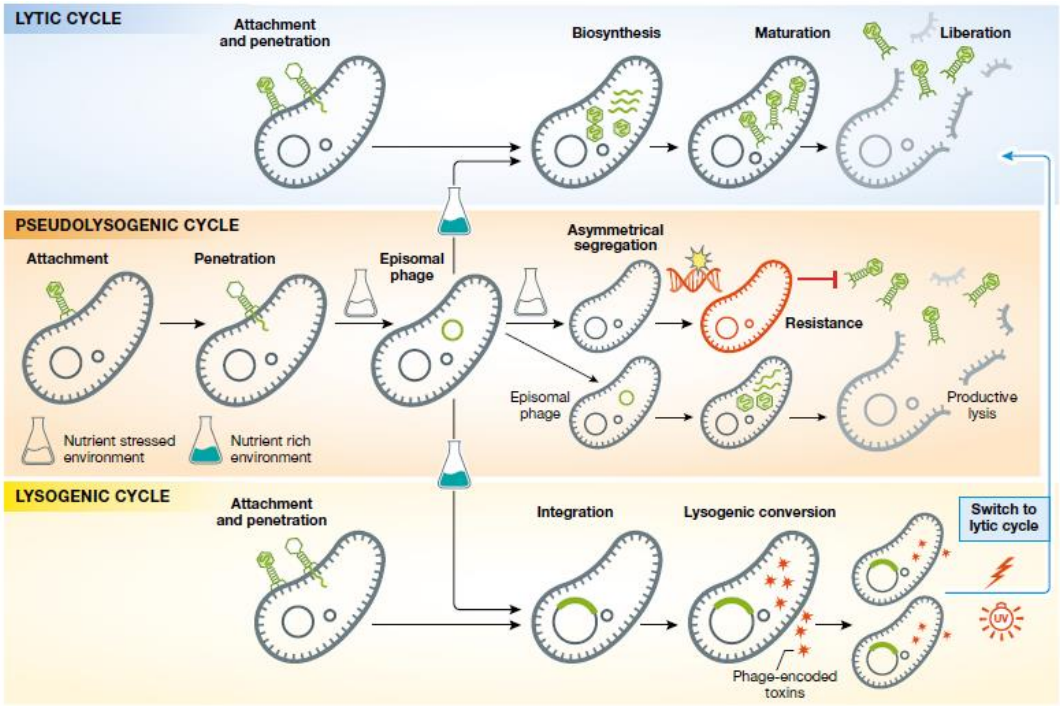

Figure 1.5: Bacteriophages infection cycles (Venturini, et al., 2022).

Bacteria and phages engage in complex co-adaptation dynamics, where bacteria try to minimize their susceptibility to phage infection, and phages strive to retain or regain it. Phages have usually a limited host range due to the high degree of specialization required to counteract the numerous bacteria defense systems. The most common adaptive response to phage predation is the alteration of cell surface phage receptors, which can be achieved through modification, masking, or synthesis of competitive inhibitors. Bacterial susceptibility to phages can be modulated by horizontal exchange of receptors or genetic modification of cell surface structures targeted by phages. However, bacterial adaptations come at a fitness cost, which can increase bacterial vulnerability to both the immune system and/or antibiotics. The use of phages to clear bacterial infections in vivo has resulted in the emergence of phage-resistant mutants that are less virulent and more susceptible to antibiotics. Phages may counter-evolve to regain their infectivity by modification of their own host attachment receptors. The use of cocktails of multiple phages acting in synergy has been shown to broaden the target range and minimize the occurrence of phage resistance (Venturini et al., 2022).

Defense systems in bacteria can be divided in innate and adaptive immune systems Another classification divides the defense mechanism by the main method to inhibit, stop or make useless the action of the bacteriophages. The mechanisms can cause the degradation of phage nucleic-acids, the inhibition of DNA and RNA synthesis or the programmed cell death (PCD) of the infected cell (abortive infection). Some systems can have different way to inactivate the bacteriophages such as type III CRISPR-Cas that can cause both degradation of phage genome and abortive infection (Rostøl & Marraffini, 2019).

The defense method linked to the physical breaking of the nucleic acids of the phages for a long time were mainly identified with the systems of Restriction-modification of any nucleic acids recognized as foreign (an innate system). More targeted defenses in this category, were discovered later, such as the bacterial Argonaute system (pAgo), hypothesized to work through DNA interference (Ryazansky et al., 2018) and CRISPR Cas (an adaptive system). There is a complex relationship between bacteriophages and bacterial CRISPR-Cas adaptive immune systems. There are several mechanisms by which phages can escape CRISPR-Cas defenses, including the evolution of phage-encoded anti-CRISPR proteins that can inhibit the bacterial CRISPR-Cas machinery (Malone et al., 2021).

A more drastic way to prevent the spread of the phages in a bacteria population is an induced cellular death of an infected cell, called abortive infection that can be achieved through different paths. One of the most studied one is the Toxin-antitoxin system (TA): a toxin causes the programmed cell death (PCD) or dormancy of the host bacterium and it is

always expressed; an antitoxin is capable to neutralize the action of the toxin through inhibition of the expression and of the action of the toxin. At the moment of the infection the antitoxin action stops allowing the action of the toxin. Other abortive infection path is linked to CRISPR Cas III defense mechanism (Chopin, et al., 2005).

In *Escherichia coli* pangenomes recently 21 new possible defence mechanisms were found indicating that there are many other defence mechanisms from phages we do not know. In fact, the *in silico* method normally used to detect the resistant strains are bound to exclude the resistance mechanisms not clustering in defence islands, but associated to mobile genetic elements spread through the bacteria genomes (Vassallo et al., 2022). Looking more in general at interactions between phages and bacteria can lead to the discoveries of new approaches to counteract bacteria (Wan et al., 2021).

1.7.2 Phage endolysins

There are two main classes of bacteriophage-encoded enzymes that can be useful against antibiotic resistant bacteria, endolysins and bacteriocins. The endolysins are active only against Gram positive bacteria, in which they can reach easily the peptidoglycan layer while phage tail-like bacteriocins can be active against both Gram negative and Gram-positive bacteria (Harper et al., 2019; Scholl, 2017). Lysin structure can be described as modular with a cell binding domain (CBD) and an enzymatically active domain (EAD) modules in Jumbophages; in other phages lysins have a globular structure, with only one module with both the functions of attaching bacterial cell wall and cut the chemical link in the cell wall (Harper et al., 2019). Lysins can be classified as endolysins or Virion Associated Peptidoglycan hydrolases (VAPGHs). Lysins can be modified to be able to lyse also Gram negative bacteria and were previously studied to treat streptococcal diseases (Gutiérrez & Briers, 2021; Linde et al., 2021)

Besides using whole phages, phage lysins are also a potential approach in the innovative antibacterial campaign of phage therapy (Kaur et al, 2021). Lysins are a class of phage borne hydrolytic enzymes that act on the bacterial cell wall and hydrolyze the peptidoglycan layer (Schmelcher et al., 2012; Love et al., 2020). They are responsible for i) introducing the phage genomic DNA into the bacterial cell and ii) the final lysis of the bacterial cell allowing the release of progeny phages from the host. Lysins, being proteins with enzymatic activity, face similar challenges parent phages do, including the issue of stability and the retention of their lytic potential.
As a biotechnological application, their fusion with Outer Membrane Permeabilizing peptides (OMPs) gives molecules called Artylisins, capable to induce lysis in Gram – bacteria from the exterior, contrasting with their original function, a peptidoglycan layer lysis from

the interior passing through pores in the internal membrane formed by phage encoded holins (Harper et al., 2019).

1.7.3 Phage training or evolution in vitro

It is possible to "train" the phages to make them more efficient in lysing bacteria exposing them repeatedly to the target strain (Borges, 2021). Borin in 2021 after 1 month of phage training of bacteriophage lambda obtained a new trained lambda phage capable to reach a greater reduction in the number of *E. coli* and a slower emergence of resistant strains (Borin et al., 2021). In this case the results were obtained as a consequence of the development of the ability to recognize a second receptor by the lambda phage. The resistance to the attachment to this second receptor required mutations in a set of genes and was costly in term of bacterial fitness. It is interesting to notice that the trained lambda phage continued to evolve and counteradapt to the resistance strategies of the bacteria even after the training. It seemed that the priming with the exposition to the bacteria helped it to adapt more easily that the untrained phage to further mutations of the bacteria. One block of gene useful for the improved action of the trained phage was demonstrated to originally belong to an *E. coli* inactive prophage. This highlights the potential resources every bacterium has in its active and inactive prophages, following recombination with the infecting phages.

Another case of recombination of two parental genotypes originated a more effective phage against *Listeria monocytogenes* after a briefer training of 60h (Peters et al., 2020). Phage training can be useful to use phage synergistically with antibiotic (Chan et al., 2018), but it must be checked that the phages do not increase the antibiotic resistance of bacteria as it was reported by Burmeister (Burmeister et al., 2020).

1.7.4 Phage therapy

Phage therapy is a promising alternative to traditional antibiotics and pesticides that uses bacteriophages as biocontrol agents to treat bacterial infections in various fields including veterinary, medicine, and agriculture. Phage have to be considered not only as possible antibacterial agents but also as antivirulence agents as in many cases the resistance developed from the bacteria to counteract the phage infection come with a trade off in fitness and virulence toward their host (Shen & Loessner, 2021). Overall, phage therapy is a promising approach to treating bacterial infections in various fields, with the potential to reduce the use of traditional antibiotics and combat antibiotic resistance (Rob Lavigne & Loessner, 2021).

1.7.4.1 Clinic and veterinary

In veterinary medicine, phage therapy has been explored as a treatment for bacterial infections in livestock and pets. Phages can be used to target specific bacteria, reducing the use of broad-spectrum antibiotics and limiting the development of antibiotic resistance (Harper et al., 2019). Studies on phage therapy in veterinary focused mainly on zoonoses and the most economically relevant diseases (as mastitis, affecting milk quality and safety), while the studies on pets are still few. (Loponte et al., 2021). Bacteriophages of *Pseudomonas aeruginosa*, an agent of otitis in dogs, and *Pseudomonas plecoglossicida*, a fish pathogen, were studied for possible phage theraby approaches to the diseases caused by the bacteria (Wright et al., 2009). (Kawato et al., 2015; Park & Nakai, 2003; Park, et al., 2000). In human medicine, phage therapy has been studied as a potential treatment for a range of bacterial infections, including those caused by antibiotic-resistant bacteria such as MRSA. While research is ongoing, phage therapy has shown promise in treating infections that are difficult to treat with traditional antibiotics (Kortright et al., 2019; Venturini et al., 2022). There are challenges shared between these two fields as phage inactivation by the acidic pH of the stomach, patient antibodies phage neutralization and development of phage resistance by the target bacteria.

1.7.4.2 Agriculture

In agriculture, phage therapy has been explored as a method of controlling bacterial infections in crops and livestock. By targeting specific bacteria, phages can help reduce the use of antibiotics in agriculture and limit the spread of antibiotic-resistant bacteria.

In Europe a stringent regulation of phytopharmaceutical products is enforced (EU Directive 2009/128/EC) (van Lenteren et al., 2018) and it is encouraged the development of organic farming through the formation of a new legislative framework (Regulation (EU) N° 354/2014 on organic agriculture) also in the framework of the 2030 Sustainability Development Goals (SDGs) as goal 12 (responsible production and consumption) and goal 15 (protection of terrestrial ecosystem).

In this context the use of bacteriophages isolated in the same regions of the pathogens, opposed to the use of copper derivatives would be favorable. Studies on phyllosphere viruses were conducted in the past, but focusing only on eukaryotic viruses (Alcalá-Briseño, et al., 2020; Fonseca et al., 2018). Nowadays there are numerous examples of isolation of phages of phytopathogens directly form the plant surface, or phyllosphere. Bacteriophages were found to be able to influence which was the dominant taxa on plants surface on brief timescales on tomato plants (Morella et al., 2018).

Among the phyllosphere microbes found in a metagenomic study on wheat phyllosphere *Pseudomonadaceae* and *Xhantomonadaceae* viruses were the most represented (Forero-Junco et al., 2022).

The deployment of phage-based products in agriculture would have numerous advantages, such a high specificity of action against the target bacteria (Loc-Carrillo & Abedon, 2011), a relatively low cost of production (Jones et al., 2007), the ability self-limiting their number one time that the host bacteria is not present anymore in the environment (Vu & Oh, 2020), and absence of residues of the biocontrol product on the vegetables surface (Harper et al., 2019; Svircev et al., 2018).

On the other hand, different practical obstacles are present in the development of an effective phage product, able to lyse the target bacteria not only in vitro, but also in greenhouse and field conditions. A method to reduce infectivity losses during the delivery and storage phases of the product has to be implemented (Svircev et al., 2018).

Among the possible drawbacks of implementing phage therapy, it is paramount to take into account the possible spread of antibiotic resistance or virulence factors through horizontal gene transfer (HGT), namely though transduction (González-Villalobos & Balcázar, 2022). An example can be represented by phage morons, phage genes not useful for the phage replication, that may be useful for the bacteria fitness or virulence. These genes play an important role for *Pseudomonas aeruginosa* (Tsao et al., 2018) and more generally for prokaryotes (Taylor et al., 2019). Thus, it is important to check the deployed phage genomes for absence of similar genes. Finally, the phages are generally sensitive to abiotic stresses, as UV radiation and desiccation, reducing their period of activity on the plants surface, and requiring specific formulates with protectants to persist more.

Recently, an increasing number of phages active against relevant phytophatogens has been isolated and tested as possible biocontrol agents e.g. *Xylella fastidiosa*, agent of olive quick decline syndrome and grape Pierce's disease (J. Chen & Civerolo, 2008; Clavijo-Coppens et al., 2021; Das et al., 2015; Domingo-Calap et al., 2021). These phages seem to be transmissible between individuals of the pathogen vector, glassy winged sharpshooters (Bhowmick et al., 2016).

Different kind of applications were tested for phage products. In several studies on *Ralstonia solanacearum* phage-based biocontrol in which plants roots were treated adding the phage solutions to the soil at high concentrations (X. Wang et al., 2019; Bae et al., 2012; Álvarez et al., 2019; Bhunchoth et al., 2015; Fujiwara et al., 2011). Kimmelshue used seed coatings of phages combined with protective polymers to prevent infection from *Clavibacter michiganensis* subsp. *nebraskensis* in corn (Kimmelshue et al., 2019). In a study to use a phage to control *Xanthomonas euvescicatoria*, agent of pepper bacterial spot, phages were applied with a handheld sprayer and showed synergic action if used together with copper-hydroxide (Gašić et al., 2018). To prevent a quick insurgence of resistant bacteria in the pathogens population it is important to use mix of phages, called phage cocktail, preferably with each phage deployed recognizing different receptors on the target bacteria surface. A Phage cocktails was used for example in a biocontrol study against *P.s.*

pv. *porri,* submerging the plants in a solution containing phages before planting them in field (Rombouts et al., 2016; Holtappels et al., 2020) The Omnilytics company has recently had its product -Agriphage- solutions containing phage cocktails, accepted by the Washington State Department of Agriculture as a certified organic bacteriocide. The product has different version acting against several plant diseases (*Xanthomonas campestris* pv. *vescicatoria*, *Xanthomonas citri* pv. *citri*, *Pseudomonas syringae* pv. *tomato* and *Clavibacter michiganensis* subsp. *michiganensis*). Some products are designed to act in woody plants against fire blight caused by *Erwinia amylovora* in apple and pear tree, and citrus canker caused by *Xanthomonas citri* subsp. *citri*. These products must be applied daily in greenhouse and 1-2 times per week in the field, not mixed with copper-based products but compatible with some fungicides, fertilizers and insecticides. The product should be added last to the tank with a dilution of about 1 to 400. Probably its formulation defends the phages from UV radiation because it can be applied also during daytime. Spraying phages one hour prior to inoculation of *Clavibacter michiganensis* subsp. *michiganensis* was used to protect tomatoes from bacterial canker (Ingram & Lu, 2009).

The deployment of phages has also been investigated also for post-harvest protection of food products. The efficacy of phage formulations in these cases varies in relation to different food matrixes and physical and chemical conditions of storage, although in many studies a reduction of at least two orders of magnitude of the target bacterial population was achieved (Hertwig et al., 2013; Stefan et a., 2013; Vikram et al., 2021).

1.8 Aim of the research and structure of thesis

Taking in account the present situation of increasing antibiotic resistance and need to decrease the copper residues on crop, phage therapy can be a valid alternative control method for the pathovar of *Pseudomonas syringae* Psa and Pph. The bacteriophages would be isolated from soil in the proximity of kiwifruit canker or halo blight diseased plants and so highly specific for Psa and Pph, diminishing the risk of being active against other beneficial bacteria on the phyllosphere.

The main aims of this PhD were to identify and characterize phages able to effectively lyse Psa and Pph bacteria and to start to test their use as biocontrol methods in greenhouse and field conditions on bean and kiwifruit plants. These two aims are associated with the first two chapters.

In the third chapter we describe the beginning of a different biocontrol approach, linked to the ability of phages to control and regulate the microbiome of phytopathogenic insects, and ultimately the insect fitness.

2 Phages Isolation and Characterization

The main content of this chapter was published as:

Martino, G., Holtappels, D., Vallino, M., Chiapello, M., Turina, M., Lavigne, R., M. Ciuffo, M. (2021). Molecular Characterization and Taxonomic Assignment of Three Phage Isolates from a Collection Infecting *Pseudomonas syringae* pv. *actinidiae* and *P. syringae* pv. *phaseolicola* from Northern Italy. Viruses, 13(10), 2083.

2.1 Abstract

Bacterial kiwifruit vine disease (*Pseudomonas syringae* pv. *actinidiae*, Psa) and halo blight of bean (P. *syringae* pv. *phaseolicola*, Pph) are routinely treated with copper, leading to environmental pollution and bacterial copper resistance. An alternative sustainable control method could be based on bacteriophages, as phage biocontrol offers high specificity and does not result in the spread of toxic residues into the environment or the food chain. In this research, specific phages suitable for further development of phage-based biocontrol strategies effective against Psa and Pph were isolated and characterized. In total, sixteen lytic Pph phage isolates and seven lytic Psa phage isolates were collected from soil in Piedmont and Veneto in northern Italy. Genome characterization of fifteen selected phages revealed that the isolated Pph phages were highly similar and could be considered as isolates of a novel species, whereas the isolated Psa phages grouped into four distinct clades, two of which represent putative novel species. No lysogeny-, virulence- or toxin-related genes were found in four phages, making them suitable for potential biocontrol purposes. A partial biological characterization including a host range analysis was performed on a representative subset of these isolates. This analysis was a prerequisite to assess their efficacy in greenhouse and in field trials, using different delivery strategies.

2.2 Introduction

The *Pseudomonas syringae* pathovar group is considered one of the ten most important phytobacteria, having a high scientific and economic importance (Mansfield et al., 2012). Within this species complex, *P. syringae* pv. *actinidiae* (Psa) is one of the most prevalent bacterial agents causing diseases in kiwifruit orchards. Psa can infect both *Actinidia chinensis* var. *deliciosa* and *A. chinensis* var. *chinensis* and is widely spread in Italy and New Zealand, the two major production areas worldwide (Donati et al., 2020). Psa penetrates the plant through wounds caused by frost, wind and rain, and natural openings such as stomata and hydathodes, causing primary external infections. In this first phase, it causes interveinal leaf spots. After an asymptomatic phase in which the bacteria are dormant, at the end of winter and in the beginning of spring, it multiplies again and migrates with a systemic infection of the xylem resulting in secondary internal infections. This secondary infection is characterized by the appearance of cankers in trunks and vines (Donati et al., 2020). In spring and summer, the bacteria actively multiply and invade the vine xylem,

which they use as a highway to spread throughout the plant. The symptoms are particularly visible in spring and autumn because of its mild temperature and high humidity conditions which are ideal for bacterial pathogenicity (Donati et al., 2020; Froud et al., 2015). *P. syringae* pv. *phaseolicola* (Pph), by contrast, which is also known as *P. savastanoi* pv. *phaseolicola*, causes bean halo blight, an economically relevant seed-borne disease in beans. It causes water-soaked lesions surrounded by halos in leaves, stems and pods in the common bean, *Phaseolus vulgaris*, and different species and cultivar of beans worldwide (Arnold et al., 2011; Taylor et al., 1996). The bacteria can also infect several weeds, providing a reservoir from which a new infection can emerge (Fernández-Sanz et al., 2016). For both diseases, the main defense strategy used in Europe is an integrated pest management (IPM) approach based on good agricultural practices, resistant crops and copper treatments. However, efficacy of IPM can be hindered by the emergence of new bacterial strains (Taylor et al., 1996), and varieties resistant to the most prevalent Pph race 6 are not available (Terán et al., 2009). Moreover, copper treatments are only preventive and were proven to be harmful for kiwifruits and for the environment, and their intensive use is responsible for the selection of copper resistant strains (Colombi et al., 2017; Svircev et al., 2018). Therefore, bacteriophage-based biocontrol should be studied as a sustainable alternative. Phages are bacterial viruses and are advantageous in that they are very specific and do not leave harmful residues on the crop that would impair human and environmental health (Svircev et al., 2018). In recent years, the research on phages to tackle phytopathogens is increasing and has been recently reviewed (Rabiey et al., 2020). Regarding the *P. syringae* species complex, phages have been characterized against *P. syringae* pathovars *porri* (Rombouts et al., 2016), *aesculi* (James et al., 2020) and *morsprunorum* (Pinto et al., 2014; Rabiey et al., 2020). Several studies have described phages that could potentially be used to control Psa (Di Lallo et al., 2014; Flores et al., 2020; Frampton et al., 2014; Frampton et al., 2015; Ni et al., 2020; Pinheiro et al., 2020; Yin et al., 2019; Yu et al., 2016) and Pph (Eman & Afaf, 2014; Sistrom et al., 2015; Vidaver et al., 1973). This study reports the isolation and characterization of two Psa phages, with isolates psageA1 and psageB1 as representatives of two newly defined species, and a group of Pph phages, with pphageB1 as representative of a third new phage species. Some of these phages have been selected as potential biocontrol candidates for a safe and efficient prevention or treatment of kiwifruit canker and bean halo blight, respectively.

2.3 Results

2.3.1 Bacteria Isolation and Characterization

Pph and Psa bacteria were successfully isolated from symptomatic leaves of bean plants and from symptomatic leaves and bark samples of kiwifruit plants in Piedmont, respectively. A total of 22 Psa strains, 10 Pph strains and nine strains of different *P. syringae* nonpathogenic to kiwifruit and bean (Table 2.4) were also considered. The PCR analysis

performed with specific primers confirmed they were *P. syringae* belonging to the pathovar *actinidiae* or *phaseolicola*. The Illumina sequencing of ten strains (bioproject PRJNA952184) confirmed the pathovar of 8 Psa and Pph strains, while UB246 was reclassified as *Pseudomonas quasicaspiana* and PSS as *Pseudomonas syringae* pv. *syringae*.

2.3.2 Phage Isolation and Morphology

Between 2018 and 2019, sixteen Pph and seven Psa phage isolates were obtained from soil collected from bean fields or kiwifruit orchards, respectively (Table 2.2). The phages were isolated by testing their ability to lyse Psa strain K7#8 or Pph strain Cuneo #6_18 (Table 2.4). No phages could be isolated from irrigation water or from plant symptomatic tissues. The phages isolated in the kiwifruit orchards displayed a variety in plaque size and morphology on the bacterial lawns. Conversely, all the phage isolates active against Pph strains caused similar plaques, clear and 5 mm in diameter, as described in Table 2.2. PsageK4e was isolated in the same area of psageK4, but from soil collected one year after the first sampling, and showed a similar plaque morphology.

TEM observations were performed on all the Psa phages and on some of the Pph phage isolates. These observations displayed capsids composed of icosahedral heads linked to tail structures, thus indicating their putative association to the *Caudoviricetes* virus class, following the previous morphological method of classification. This positioning was confirmed later through molecular analysis. PsageK4, psageK4e, and psageA1 had a typical myovirus morphology, with TEM images revealing sheathed contractile tails. psageA1 had an isodiametric head of 72 nm diameter (SE = 0.3 nm; n = 129) and a contractile tail of 125 nm length (SE = 0.8 nm; n = 101). Three isolated siphovirus-like phages (psageB1, psageK9 and psageB2) were characterized by their long flexible tail. PsageB1 had a head of 78 nm diameter (SE = 0.4 nm; n = 83) and a flexible non-contractile tail of 176 nm length (SE = 2.2 nm; n = 74). All phages isolated in bean fields showed an icosahedral head and a short, stubby tail. PphageB1 phage had an isodiametric head with a diameter of 54 nm (SE = 0.4 nm; n = 84); (Figure 2.1).

2.3.3 Phage Sequencing and Annotation

For groups of phages able to lyse the same subset of bacteria, and isolated from the same area, some representatives were chosen (15 total isolates) to extract and sequence their genomic DNA. The phages subjected to whole-genome sequencing contained double-stranded DNA genomes with lengths ranging from 41.7 kb to 112 kb and a GC content ranging from 48.79% to 60.44%. In Table 2.3, the number of proteins encoded on the genomes of the sequenced phages are shown and were labelled as hypothetical proteins, ORFans (ORFs without sequence homologs in other known genomes), or proteins associated with a predicted function. Due to the methodology used for library synthesis associated with sequencing (Nextera Flex), the physical termini of our isolates were not able to be detected through bioinformatic methods. Thus, the sequences termini were arbitrarily based on the termini of the phages most similar in the NCBI database. Furthermore, to infer the type of genomic ends and packaging strategy, we followed the

method of Merrill (Merrill et al., 2016), and built a phylogenetic tree using the large terminases of psagaeA1, psageB1 and pphageB1, and the large terminases sequences of phages whose packaging systems and physical ends were experimentally determined (Figure 2.S1). PsageA1 terminase was located with terminases of phages with 50 Cos ends, psageB1 with phages with phages with 30 Cos ends and pphageB1 with phages that have termini with short direct terminal repeats (DTRs). PsageA1, psageB1 and pphageB1 may share these packaging strategies. None of the phages showed evidence of toxins or bacterial virulence proteins encoded in their genomes. Proteins related to lysogeny were only found in psageB2. The online artificial intelligence platform PhageAI (Tynecki et al., 2020) agreed with our analysis, predicting a temperate lifestyle for psageB2 and a lytic lifestyle for all the other phages. Following the sequencing results the 15 isolates were divided into 5 groups (in Table 2.3 the characteristics of one representative for each group are displayed) based on the similarity of their sequences, and the molecular characteristic of each group is discussed below.

2.3.3.1 Genomic characteristics of pphageB1

The eight sequenced phages active against Pph (pphageB1, pphageB2_1, pphageT1_2, pphageT2_1, pphageBV2, pphageBV4, pphage BV7_1 and pphageBV7_2) showed an almost complete identical sequence at the nucleotide level and therefore phage pphageB1 was arbitrarily chosen as the type sequence. PphageB1 sequence showed 73.89% similarity with *P*. *fluorescens* SBW25 phage phi-2 (NC_013638) but with a query cover of only 3%. Phi-2 was still used as the basis to assemble and orient the pphageB1 genome. The most similar phage to pphageB1 is MR18 with a sequence identity of 88.65% (query cover 51%). Nevertheless, the highly identical Pph phage isolates may be considered as representatives of a novel phage species (Turner et al., 2021). The pphageB1 genome sequence was assembled in one contig using 181,767 reads. The genome of pphageB1 was 41,714 bp long, with a GC content of 56.6% (Table 2.3). The pphageB1_1 genome codes for 52 open reading frames (ORFs), 25 of which encodes proteins with a predicted function. No integrases were found to be encoded on the pphageB1 genome, suggesting a lytic lifestyle. A clear functional organization was noticed between two regions in the genome, the first associated with DNA metabolism (DNA replication, repair and recombination) and the second with morphogenesis genes. The small and large subunits of the terminase (pphageB1_44, pphageB1_45) involved in the packaging of the DNA and one protein associated with lysis (pphageB1_47) were located in the same region near the cluster of structural protein associated genes. No tRNA sequences were predicted in the pphageB1 genome. Notably, one of the structural proteins (pphageB1_39) had a C-terminal lysozyme fold having a putative double function: capsid formation and bacterial lysis. In Figure 2.2A, the pphageB1 genome organization is compared with the sequence of phage MR18. The figure clearly displays the high level of synteny between the two phages, with a similar organization of clusters linked to the DNA processing and to the phage morphogenesis and lysis, although they have a lower grade of similarity in the regions associated with morphogenesis of the two genomes. PphageB1 has a holin encoding CDS (pphageB1_27) at the relative position where MR18 has a phosphodiesterase (PssvBMR18_gp31). The

pphageB1 RNA polymerase(pphageB1_29) maintains its relative position, but with little similarity. The small and large subunits of the terminase (pphageB1_44, pphageB1_45), lysozyme (pphageB1_47) and Rz-protein (pphageB1_49) CDSs are in the same region. MR18 has an additional putative SGNA/GDSL protein (PssvBMR18_gp53) compared with pphageB1. Regarding the other eight Pph phage isolates, four shared 100% similarity with a query coverage of 99% without detectable SNPs (pphageBV2, pphageBV4, pphageB1 and pphageBV71). Regarding the remaining four Pph phages, following a variant calling analysis through snippy software, the SNPs that differentiate pphageB1 frompphageB21, pphageT12, pphageT21, and pphageBV72 phages, were identified (supplementary Tables 2S1–S4). PphageB2_1 had a majority of synonymous variants (119) and 28 missense variants. Only synonymous mutations were found in the morphology-associated protein named "unclassified head protein" (pphageB1_38) and in the phage terminase subunits (pphageB1_44, pphageB1_45). The missense SNPs were located in a limited number of ORFs associated with (I) structural functions (predicted phage tail tubular protein A pphageB1_36, predicted phage tail tubular protein B pphageB1_37), (II) DNA metabolism (two phage exonucleases pphageB1_23 and pphageB1_25), (III) lysis (a predicted phage lysozyme pphageB1_47 and a peptidoglycan lytic exotransglycosilase pphageB1_40), and (IV) in five ORFs coding for hypothetical proteins. PphageT21 compared with pphageB1 had 110 synonymous variants mostly in structural proteins and in the DNA polymerase coding sequence; 28 missense variants were found in protein associated with morphology, DNA metabolism and lysis and in six hypothetical proteins. PphageT12 had 680 synonymous changes and 67 missense mutations, with the majority of the missense SNPs concentrating in the lysis proteins and in the phage tail fibers (pphageB1_41, pphageB1_42). PphageBV72 had 69 synonymous variations and 14 missense changes with a distribution in proteins similar to the other Pph phages SNPs compared with pphageB1 genome; additionally, there was a missense mutation in the DNA ligase protein sequence (pphageB1_16).

2.3.3.2 Genomic characteristics of psageB1

PsageB1 showed 83.6% identity along 72% of the genome of *P. syringae* pv. *avii* phage nickie (NC_042091.1) (Figure 2.2B), isolated from wastewater. A global alignment performed with EMBOSS Stretcher revealed an identity of 72%. This was below the identity threshold to distinguish phages at the species level (95%). Therefore, psageB1 may be considered a representative of a novel species of phages infecting Psa. The phage had a genome of 112,269 bp with a 56.47% GC content and contained 161 ORFs of which the majority of encoded proteins were classified as hypothetical proteins (105) and ORFans (16). Only one fourth of the ORFs were associated to proteins with a predicted function (40) (Table 2.3). Four tRNA sequences were found in psageB1, organized in a small cluster. As shown in Figure 2.2, the genome organization is similar to phage nickie, with a region associated to morphogenesis genes, followed by a cluster of genes linked to lytic activity (holin psageB1_039, lysozyme R psageB1_040, two GDSL-like lipases psageB1_034, psageB1_038 and a particle-associated lyase psageB1_035) and a series of genes linked to DNA processing (Figure 2.2B). In the arbitrarily assigned terminal part of the sequence, both phages were annotated with a long series of short hypothetical proteins that shared little

identity between the two phages. Both phages had a similar large terminase (psageB1_012_) in the same genomic region. Nickie had an additional GDSL-like lipase (CNR34_00036) next to the holin ORF shared with psageB1 (psageB1_039). PsageB1 had an ORF associated with the recombinase A (recA) (psageB1_066) and two ORFs associated with recombination related exonucleases (psageB1_069, psageB1_070). It seems that recA-related genes are used in replication in *Siphoviridae* (Murphy, 2016) and *Myoviridae* (Calendar, 2012) members.

2.3.3.3 Genomic characteristics of psageA1

Phages psageA1 and psageA2 shared 100% identity at the nucleotide level. The psageA1 and psageA2 sequence showed partial similarity (74.28% identity with 10% query cover) with the lytic *P. syringae* pv. *avii* phage ventosus (HMG018930). These phages may be considered as representatives of a new species active against Psa following ICTV guidelines. The total length of the psageA1 genome was 98,780 bp and it had a 48.79% GC content. Annotation (Figure 2.2C) found 176 different ORFs, 51 of which encoded a predicted function. The remaining ORFs were associated with hypothetical proteins (76) and ORFans (16) (Table 2.3). The genome organization was similar, although with very limited sequence similarity to the organization of the *Otagovirus* genus (R. Frampton et al., 2014) with a tRNA cluster followed by the large terminase protein (psageA1_065), a region with the capsid, tail and baseplate structural components (psageA1_066, psageA1_067, psageA1_069, psageA1_070, psageA1_072, psageA1_074, psageA1_075, psageA1_078, psageA1_080, psageA1_083, psageA1_084), followed by a lysin (psageA1_092) and a region with all the proteins used for DNA replication. In psageA1 there were 14 different sequences coding for tRNAs. Additionally, psageA1 seemed to have a tRNA-specific adenosine deaminase (psageA1_042) (Figure 2.2C).

2.3.3.4 Genomic characteristics of psageB2 and psageK9

PsageB2 and psageK9 pairwise alignment showed high identity (99.5%). This sequence showed an identity of 99.95% along 97% of its sequence with the *P. syringae* pv. *actinidiae* phage phiPsa1 (Di Lallo et al., 2014) (KJ507100) (Figure 2.2E). This identity was greater than 95%, thus psageB2 cannot be considered as a new phage species, but it was an isolate of the phiPsa1 species (Turner et al., 2021). The psageB2 dsDNA genome was 50 kb long, with a GC content of 58.51%. Only 26 of the 77 identified ORFs had a predicted function assigned for their product, and the majority of the rest of ORFs were annotated as hypothetical proteins (47) and ORFans (4). No tRNA sequence was found in psageB2 genome by tRNAscan-SE (Table 2.3). The genome organization was the same as phiPsa1 with a clear distinction of regions assigned to morphogenesis followed by an endolysin ORF and DNA replication- and modification-related ORFs followed by one single ORF associated to the large terminase. The sequence of both psageK9 and psageB2 had a CDS of an integrase (psageB2_018c) and of a cI repressor (psageB2_043c) that identified them as lysogenic

phages, as was confirmed for phiPsa1. Furthermore, two recombinase genes were annotated, NinB and NinG (psageB2_054 and psageB2_056).

2.3.3.5 Genomic characteristics of psageK4, psageK4e and psageK4v

Phage isolates psageK4, psageK4e and psageK4v had a 99% identity between each other. The psageK4 sequence had a 96.84% identity with 97% coverage of the sequence of the Psa phage phiPsa267 (R. Frampton et al., 2014) (MT670417.1) (Figure 2.2D). The psageK4 assembly gave a sequence of 98,440 bp with a GC percentage of 60.44%. Among its numerous annotated ORFs (179), the majority were classified as hypothetical proteins (112) and ORFans (16), and only 51 ORFs had a specific function assigned following the annotation pipeline (Table 2.3). Eighteen tRNAs were organized for the main part in a cluster positioned similarly to psageA1. A psageK4 and psageK4e genomes variant calling analysis (Supplementary Materials Table 2.S5) revealed the presence of 836 synonymous SNPs prevalently on structural proteins and 159 missense SNPs on structural protein also but on the terminase (psageK4_064), DNA polymerase(psageK4_115), and phosphoesterase (psageK4_129), in addition to many hypothetical proteins associated with ORFs. A BLASTn comparison of the two genomes (Figure 2.2D) revealed the presence of an additional ORFan in psageK4e between the ORFs similar to psageK4_102 and psageK4_103, and the absence of two ORFans present in psageK4 (psageK4_164 and psage_138). PsageK4 and psageK4e had the same genome organization of phages of the genus *Otagovirus*. This structure, despite the limited similarity shared, was similar to that previously described for psageA1 as displayed comparing Figure 2.2C, 2.2D.

2.3.4 Phages Host Ranges

Ten of the fifteen sequenced phages were selected to be tested for their ability and efficiency to lyse with an EOP assay the strains of Pph and Psa present in the collection. The selection of phages for this assay was based on having at least one phage representative for each of the five groups identified through sequencing and to account for the diversity within these groups. As shown in Table 2.1, pphageB1 was able to lyse every strain of its target bacteria, but was ineffective in producing plaques on any Psa strain. The isolates with genomes highly similar to pphageB1, pphageB21, pphageBV72, pphageT12 and pphageT21 also showed a similar host range. Conversely, some of the phages isolated from kiwi orchards showed the ability to lyse several Pph isolates in addition to their ability to lyse many if not all of the collected Psa strains. The psageK4e isolate was the most effective against both *P. syringae* pathovars in the collection. Notably, psageK4 isolate could lyse all the Psa and Pph strains in the collection but displayed low efficiency in the case of Pph strains. Psagek4e had a similar host range but was also able to effectively infect Pph strains. PsageA1 and psageB2 were not efficient or not able at all to lyse Pph strains. To expand the

possibility of a cocktail to use in phage therapy application, we tested the specificity of another phage collection we had access to (Rabiey et al., 2020) on our Psa and Pph bacterial strains: only one of the phages, MR8, a phage similar to pphageB1, was able to efficiently infect the strains in the collection (Table 2.1). MR8 was able to infect both the pathovars of *P. syringae*, but had a greater EOP on the Pph strains. Phages MR1 and MR2 had 90% identity with the phage PPPL-1 (NC_028661), capable to lyse Psa, but could not lyse any of our collection Psa strains (not shown). All phages showed a reduced activity against the *P. syringae* nonpathogenic strains tested. Despite this, psageB1 was able to lyse three nonpathogenic strains efficiently.

2.3.5 Phages Resistance to Abiotic Stresses

A representative for further assays was selected for each of the five groups (cladelike) described above, excluding the group with predicted lysogenic properties which are not of immediate exploitation for phage therapy for plant diseases. Nevertheless, temperate phages could be used as biocontrol agents with different approaches described previously (Monteiro et al., 2019), and we do not exclude finding an application in biocontrol for psageB2 and psageK9 in the future. Figure 2.3 displays the ability of pphageB1, psageK4, psageA1 and psageB1 to conserve infectivity after being exposed to three abiotic stresses: pH, temperature and UV-C irradiation. After 18 h of exposition to different pH environments, phages showed a similar behavior, keeping their activity stable between pH 4 and 10 with the exception of psageB1 that reduced its titer to 99% at pH 10 compared with pH 4. All of phages rapidly decreased in their capacity to lyse at the most acidic pH tested, pH 2 (Figure 2.3A). Regarding exposure to heat stress, all tested phages showed a comparable titer when exposed to 4 ℃, 26 ℃ and 37 °C for 1 h (Figure 2.3B). However, at 55 ℃, no viable phage particles could be detected for the phages psageB1 and pphageB1. At the same temperature, the psageK4 virus titer remained stable after one hour, and psageA1 showed a reduced activity, but not a complete inactivation (Figure 2.3B). The irradiation with UV-C caused a constant decrease in the number of infectious phages counted after exposure, already visible after 10 min. In the majority of cases, a complete inactivation of the phage particles was observed after two hours. Notably, one of the phages tested, pphageB1, showed the ability to lyse its target bacteria even after 3 h of exposure (Figure 2.3C).

2.3.6 Phylogenetic Analysis

The three phage representatives of new species (pphageB1, psageA1 and psageB1) were classified in the *Caudoviricetes* class following our phylogenetic analysis. The phylogenetic trees built comparing the major capsid protein (MCP) (Figure 2.4A) and RNA polymerase (Figure 2.S3) of pphageB1 revealed that this virus is likely belonging to the *Autographiviridae* family and *Krylovirinae* subfamily. *Autographiviridae* in the past was a

group included in the *Podoviridae* family, because of similar capsid morphology. PphageB1 seems to cluster together with the clade 3 of phages outlined by Rabiey et al. (2020) from which we used MR5 as a representative. PphageB1 and MR5 seem to be not similar enough to share a genus but are likely to be located in the same subfamily. Two phylogenetic trees based on MCP (Figure 2.S3) and DNA ligase of psageA1 (Figure 2.4B) identify the phage as an unclassified myovirus positioned near the genus of phiPsa267, the genera *Otagovirus* and *Pakpunavirus*. The phylogenetic tree comparing the MCP of psageB1 (Figure 2.4C) with the closest phages present in databases, locates the phage in the *Nickievirus* genus and suggests the phage as being a member of a new species of this genus.

2.3.7 Phage Delivery

2.3.7.1 In vitro and Greenhouse bioassays on Pph Phaseolus vulgaris pathosystem

A preliminary pathogenicity test resulted in the selection of the most virulent strains, Pph #9, Pph #13 and Pph#14 among the Chinese strains and Pph #6_18 among the Piedmontese strains. These strains were used for the greenhouse bioassays assessing the effect of surface sprayed phages on bean plants. The plants treated with pphageB1 1 hour prior to Pph inoculation a month after showed significatively less symptoms, expressed by lower average disease index, than untreated inoculated plants and plants treated at the same time of the inoculation. Application of phages 1h post inoculum of bacteria was tried in preliminary experiments, but the outcomes after 30 days were not different from the infected control (Figure 2.5, Figure 2.6 and Figure 2.7).

2.3.7.2 Carrier Bacteria Method

Phages are extremely specific so it is necessary to select bacteria similar to the host as a carrier, to increase the possibility to find a phage able to infect both microorganisms. PsageB1 showed the most interesting results being able to produce clear plaques in three nonpathogenic strains and turbid plaques in USA052. It can indicate a temperate life style associated with that particular strain. Interestingly psageB1 is a phage able to infect both Psa and Pph strains in our collection, so it can be tested to be associated with carrier bacteria for contrasting both diseases in our study. PsageB1 has a critical decrease in its concentration after an exposition of 1 hour to UV-C radiation and it is completely degraded in 2 hours. The protection from a nonpathogenic strain could have a great influence on the survival rate of the phage in greenhouse and field applications. SZ131 and USA052 are part of the same clade (Diallo et al., 2012). The EOP analysis reveals that only one phage, psageB1, between the tested is able to lyse some of the nonpathogenic strains. This is promising, knowing that psageB1 is able to lyse both Psa and Pph strains. The greater efficiency of psageB1 in lysing the bacteria was observed against the strains UB210 and UB246. The results of the two experiments regarding the persistence of the phages on the bean leaves surface are showed in table 2.4, table 2.5 and in figure 2.8. The phage particles lose quickly their ability to lyse if applied alone. In the second experiment (table 2.5, figure

2.8B), it was not even possible to detect active phages 1 hour after application. Conversely, the phages previously mixed with a growing culture of UB210 or UB246 showed greater numbers of infecting particles 1 hour after the application and one day after the application. We noticed a greater number of phages with the combination of psageB1 with UB210 strain in both the repetitions of the experiment. Real time PCR data (not shown) were also collected for every sample, but they revealed to be not useful to predict the real activity of the virus particles, as it was able to detect psageB1 DNA until the third or fourth days in the two experiments. At this time the phages were not able anymore of cause bacterial infection, so the presence of the DNA was not predictive of the presence of infectious viral particles.

2.4 Material and methods

2.4.1 Bacterial Isolation and characterization

The Psa collection was composed of 22 Psa strains isolated from infected *Actinidia* spp. in the Piedmont and Veneto regions of northern Italy. Seven Psa strains were collected from symptomatic leaves of *Actinidia deliciosa* and bark tissues sampled in the field from the 2018 growing season in Cuneo province (Piedmont). The Psa collection was further expanded with sixteen additional strains pathogenic for *Actinidia deliciosa* and *Actinidia chinensis* from the Phytosanitary Inspection Services of Piedmont and Veneto regions (Table 2.4). For Pph, ten strains were gathered from infected bean plants from Piedmont and China between 2015 and 2018. Additionally, two isolates of Pph were received from the Phytosanitary Inspection Service of Piedmont (Table 2.4).

Included in the biological assays were some *P. syringae* strains that are nonpathogenic to kiwifruit and bean. One strain of *P. syringae* pv. *syringae* causing disease in apricot, was kindly donated by the University of Milan, and eight P. *syringae* nonpathogenic strains, whose lack of pathogenicity is caused by the absence of a functioning Type 3 Secretion System, were provided by the French National Research Institute for Agriculture, Food and the Environment (INRAe) (Diallo et al., 2012; Morris et al., 2010). Bacterial colonies were identified or confirmed as Psa or Pph pathovars using specific PCR primers as previously described (Audy et al., 1996; Gallelli et al., 2011; Koh & Nou, 2002). The amplified fragments of Psa and Pph were cloned in pGEM-Teasy (Promega), transformed in competent *Escherichia coli* DH5 cells, and grown in Lysogeny Broth (LB) at 37 C°. The sequences of the amplified fragments were analyzed through Sanger sequencing to confirm species and pathovars (BioFab Laboratories, Rome, Italy). Strains were maintained in glycerol at -80°C (15% glycerol). Bacteria were routinely cultured in solid King's Broth (KB) plates (1.5% of agarose) or in low-salt LB medium (LB_{LS}) (0.5 g NaCl). Solid LB_{LS} (1.5% agar) and soft LB_{LS} (0.6% agar) were used to grow bacterial strains and perform plaque assays.

Ten bacteria strain (Pph Cuneo #6_18, Pph #13, Psa K7#8, Psa K7#1, Psa K4#3, Psa 5847.19, Psa 5846.19, Psa 453e, PSS and USB246) were sequenced through Illumina Miseq and their

sequences were deposited at GenBank under the bioproject PRJNA952184 and will be available once processed by GenBank.

2.4.2 *Sample Preparation, Phage Isolation, Amplification and Purification*

For bacteriophage isolation, plants, soil and wastewater samples were collected near Psa- and Pph-infected plants with typical disease symptoms in Veneto and Piedmont (Table 2.2). Thirteen additional phages isolated from cherry bacterial canker (caused by P. *syringae* pv. *morsprunorum* race 1, *P*. *syringae* pv. *morsprunorum* race 2, and P. *syringae* pv. *syringae*) were added to our host range analysis (Rabiey et al., 2020). Phage buffer (10 mM Tris pH 7.5, 10 mM MgSO4, 150 mM NaCl) was used for storage, enumeration, stability assays and dilution of phages. Psa strains K7#1 and K7#8, and Pph strains Cuneo #6_17 and Cuneo #6_18, were used as bacterial host strains. The symptomatic leaf and bark samples were crushed with physiological solution (0.8% NaCl v/w) in stomacher bags and the filtrates were stored at 4 °C before plaque assays. For each soil sample, a 5 g aliquot was taken and suspended in 20 mL of filtered and deionized water. These samples were gently mixed at 4 °C overnight to release the phages from the soil particles before centrifugation (4000 rpm; 20 min). The supernatant was filtered with 0.45 m pore size membrane filters (Millipore, Sigma-Aldrich, Gillingham, UK). Next, plaque assays were performed to test the filtrates for the presence of phages using the soft-agar overlay method (Sanders, 2012). Plates were incubated at 26°C for one night to allow the formation of plaques. The plaques detected with this method were propagated in three successive single plaque isolations to obtain pure phage isolates. The amplification of the phages was performed by growing host bacteria to an optical density at 600 nm of 0.3 (approximately 10^9 CFU/mL). Then, 0.5 mL of phage buffer containing phages picked with a sterile toothpick from a plaque were added. The broth was left shaking at 180 rpm and 26 °C overnight. Obtained crude lysates were filtered through 0.22 µm membrane filters (Millipore, Sigma-Aldrich, Gillingham, UK). To concentrate the phages, the crude lysate was purified through virion precipitation with polyethylene glycol (PEG) 8000 (15%). After the addition of PEG to 35 mL of crude lysate, the mixtures were left slowly shaking at 4 °C overnight. The solution was then centrifuged at 4000 rpm (Sorvall GSA rotor, ThermoFisher, Waltham, MA, USA) for 1 h, and the resulting pellet was dissolved in 3 mL of phage buffer and titrated. The purified samples were kept with a concentration of at least 10^8 PFU/mL. For long-term storage at -80 °C, 700 µL of the amplified phage solution was mixed with 300 µL of 50% glycerol.

2.4.3 *Transmission Electron Microscopy*

A drop of 10 µL of PEG-purified phages was deposited on carbon and formvar-coated 400 mesh grids (Gilder, Grantham Lincolnshire, England) and left to adsorb for 3 min. Grids were rinsed several times with water and negatively stained with aqueous 0.5% w/v uranyl acetate; excess solution was removed with filter paper. Observations and photographs were made using a Philips CM 10 transmission electron microscope (Eindhoven, The Netherlands), operating at 60 kV. Micrograph films were developed and digitally acquired

at high resolution with a D800 Nikon camera; images were trimmed and adjusted for brightness and contrast using the GIMP 2 software (Ver.2.10.24). The pphageB1, psageA1, and psageB1 phage capsid diameter and tails length were measured using ImageJ (Ver. 1.53e) (Schneider et al., 2012).

2.4.4 Host Range Assay

Bacteriophages were originally isolated using Psa strain K7#8 and Pph strain Cuneo #6_18 as hosts. The host range of each selected phage was tested through an efficiency of plating (EOP) analysis (Abedon, 2021). Serially diluted phage lysates were applied (5 µL drops) to soft agar containing one of the bacteria strains of our collection (4 mL of melted 0.6% LB_{LS} soft-agar and 250 µL of an overnight culture of Psa or Pph). For each bacteria phage combination three different dilutions were spotted from the same phage crude lysate. The plates were incubated at 26 °C for 24 h and then the plaques were counted to obtain phage titration. For each phage, all the titration values were compared quantitatively to the titration value of the same phage infecting the strain used for its isolation.

2.4.5 Influence of pH, Temperature, and UV Radiation to Phage Viability

Phages pphageB1, psageA1, psageB1, and psageK4 were exposed to different abiotic stresses (pH, temperature and UV-C radiation) and then titrated using the reference bacterial strains described above. All these tests were performed on crude lysates after amplification in liquid bacterial cultures. For testing resistance to high temperature, phages were exposed to 26 °C, 37 °C and 55 °C for 1 h and then titrated. For testing resistance to UV-C radiation, phages were exposed to radiation from a UV-C lamp (253.7 nm with an ultraviolet output of 4.9Wat a 48 cm distance). In the pH stability assay for each phage, 100 µL of crude lysate were added to 900 µL phage buffer adjusted with NaOH or HCl to a pH of 2, 4, 6, 8 or 10 and left at room temperature for 18 h before titration. The titers of viable phages were compared with the titers of phages left in phage buffer, at pH 7.5. The graphic visualization of the stability test was obtained using the ggplot2 R package (Ginestet, 2011) and the statistical analysis was performed with the agricolae R package (De Mendiburu & Reinhard, 2015).

2.4.6 Phage Genome Sequencing, Assembly, and Annotation

Phage DNA was extracted using a chloroform-phenol extraction protocol after treatment with DNAse I and RNAse A to remove bacterial genetic material and a proteinase K treatment to break the virus capsids and release phage genomic DNA (Sambrook, Fritsch, & Maniatis, 1989). The phage's genomic DNA was sequenced in-house at KU Leuven (Laboratory of Gene Technology) in Belgium. Illumina sequencing libraries for each sample were created using the Nextera Flex DNA Library Kit. The quality of the libraries was assured using an Agilent Bioanalyzer 2100. The libraries were then sequenced with a MiniSeq Mid-Output flowcell (300 cycles; 2 x 150 bp reads). The reads were trimmed with Trimmomatic (v0.36.5) (Bolger et al., 2014). The coverage obtained for all the sequenced phages are

available in the Supplementary Materials Table 2.S6. The obtained data were assembled and annotated using PATRIC online platform (v3.6.2) (Wattam, 2016) that employed SPAdes (v3.15.2) (Bankevich et al., 2012) and Pilon (v.1.23) for assembly, and RASTtk (Brettin et al., 2015) and tRNAscan-SE (Lowe & Chan, 2016) as annotation software. Default settings were applied. The assembled genomes were compared with the NCBI databases using BLASTn. Manual functional annotation was performed by comparing PATRIC predicted ORFs against the non-redundant GenBank protein database (Kelley et al., 2015) through BLASTp (Altschul et al., 2005). To exclude the presence of bacterial virulence genes, the phage genomes were screened against VirulenceFinder 2.0 database (v 2.0.3) (accessed on 20 August 2021) (Joensen et al., 2014). Pairwise global alignment between genomes was performed through EMBOSS Stretcher (Myers & Miller, 1988). The online tool phageAI (https://phage.ai/) (accessed on 20 April 2020) (Tynecki et al., 2020) was used to predict phage lifestyles. Finally, the graphic visualization of the genomes and of their comparison was obtained with R package genoPlotR (Guy et al., 2020). The variant calling analysis of highly similar phages was performed using the tool Snippy (v.4.6.0) with default settings through the Galaxy platform (Afgan et al., 2018).

2.4.7 Phylogenetic Analysis

To define the evolutionary history of the new phage species, phylogenetic analysis was performed. To choose the protein sequences to compare, we used as reference the protein used for the closest phage taxonomic group as indicated in the International Committee on Taxonomy of viruses (ICTV) documentation (Walker et al., 2020). To generate a pphageB1 tree, the major capsid protein (MCP) and RNA polymerase (RNAPol) were used as reference genes to perform the analysis. For psageB1, only the MCP was used. Phage psageA1 was grouped and classified based on its DNA ligase and MCP. The phages chosen for each tree were those included in the established ICTV trees used as reference, supplemented with other closely related phages found by BLASTp searches and tBLASTn comparisons to the NCBI protein database (accessed on 20 August 2021). The outliers were chosen between phages of close virus families according to ICTV. The alignments were performed using MAFFT through EMBL-EBI (Madeira et al., 2019) and the trees were assembled with IQtree (Trifinopoulos et al., 2016) using a maximum-likelihood method with a bootstrap number of 1000. The trees were visualized and graphically improved using the Mega7 software (Kumar et al., 2016).

2.4.8 In vitro and Greenhouse bioassays on Pph Phaseolus vulgaris pathosystem

A pathogenicity assay was conducted to choose the strains to use in the subsequent greenhouse trials. Snap beans pods were surface sterilized with NaClO 1% and rinsed with sterile milliq water for two times. For every strain of our collection three pods were put in a petri dish with a wet sterile paper disk to maintain the humidity. Every pod was pricked with sterile toothpicks previously soaked in a 10^8 CFU/ml, 10^6 CFU/ml and 10^4 CFU/ml Pph bacteria suspensions. Every pod was then wounded with a certainly pathogenic strain as a

positive control and with *E. coli* DH5α as a negative control. For greenhouse bioassay a multiplicity of Infection (MOI) of 1, was selected after several tries, with 10^8 CFU/ml of bacteria and 10^8 PFU/ml of phage. Different inoculum techniques were tried, metal brush, carborundum and spraying.
Different humidity condition were tested. Trying to arise the relative humidity plants were partially covered with plastic containers. This method did increase the insurgence of the disease in Pph infected plants, but not in a consistent way and it was arising problem of fungal development on the plants, so it was abandoned.
Another variable we changed was the bean cultivar. We used at first *Saxa* cultivar of string beans, a cultivar with a quick development and sensitive to halo blight. Then we passed to a cultivar of dwarf borlotti beans, *Meccano*, more sensitive to the halo blight. Meccano is a dwarf cultivar, with a determinate growth (bred for less branching, shorter internodes, insensitivity to day length and greater investment in reproductive structures than in vegetative ones). Its pod production happens in a shorter more consistent period of time to ease mechanized harvest, and it is a dwarf variety. For these characteristics it is easily employed in an experimental setting.

After several tries inoculating 15 days age plants, not resulting in an insurgence of the disease in greenhouse, VC bean development stage, at 8 days of age of the plants (https://beanipm.pbgworks.org/common-bean) was the time used for inoculation. in the bioassays improving the disease progression in the positive controls.
Meccano plants, MOI of 1 and inoculum of 8 days did the trick and we had finally a good pathosystem to experiment with.

When the Halo blight was found to consistently infect the positive controls, four repetitions of the experiments were registered. The severity of the disease was registered for each plant through a disease index from 0 to 5 in which 0 describe a healthy plant and 5 a dead plant (Figure 2.6).

At the beginning were set three cases apart of negative (only water or only phage solutions applied to leaves surfaces) and positive controls (only Pph bacteria applied to leaves surface), namely the application of phages 1 h before, at the same time and 1 h after the bacteria inoculation. In the last iterations of the experiment, it was excluded the application of phages one hour after suspension as it didn't show differences from the positive controls.

The statistical analysis of the disease index data was conducted through Kruskal-Wallis test (McKight & Najab, 2010) and Wilcoxon paired test (Lam & Longnecker, 1983) through R software (Culpepper & Aguinis, 2011) that was also utilized to visualize the results through the use of ggplot2 package (Ginestet, 2011).

2.4.9 Carrier Bacteria Method

We had access to eight *Pseudomonas syringae* nonpathogenic strains described by Demba Diallo, which behavior is caused by the absence of a functioning Type 3 Secretion System (Diallo et al., 2012) sent by Dr. Chandeysson (INRA). We tested these strains (UB197, UB210, UB246, USA052, CC1504, SZ030, SZ122, SZ131) against the most promising phages active against Psa and Pph in our study (psageB1, psageB21, psageBV72, psageT12, psage T21, psageA1, psageK4, psageK4e, psageB1, psageB1 and MR8) in an efficiency of plating (EOP) analysis (Table 2.1). Serially diluted phage lysates were applied (5 µl drops) to soft agar containing one of the bacteria strains of our collection (4 mL of melted 0.6% LBLS soft-agar and 250 µl of an overnight culture of Psa or Pph). For each bacteria phage combination for different dilutions were spotted from the same phage crude lysate. The plates were incubated at 26 °C for 24 h and then the plaques were counted to obtain phage titration. For each phage, all the titration values were compared quantitatively to the titration value of the same phage infecting the strain used for its isolation. To set the greenhouse experiments we have performed some preliminary tests. These tests were useful to choose the correct mixing time between bacteria and phages (30 minutes or 1 hour) and the best solution to suspend them in (phage buffer or milliQ sterile water for phages and the LB_{LS} culture media or physiological solution 0.8% NaCl for the bacteria). We tested three different Multiplicity of Infection (MOI), 0.1, 1 and 10. We spread the solution with phages, bacteria, or the mix of the two microorganisms on the leaf surface. Furthermore, we tested the better method to retrieve the phages from the bean leaves surface. We detached foliar disks of 1.2 cm of diameter and tried three different methods to retrieve the phages: crushing the disks with ceramic beads using FastPrep24 (MP Biomedicals) instrument in 2 ml O-ring tubes containing 500 µl of a solution or shake the disks in the same amount of solution in 1.5 tubes for 30 minutes or 1 hour. We tried as solution to suspend the phages, PBS or phage buffer (10 mM Tris pH 7.5, 10 mM MgSO4, 150 mM NaCl). The phages titer was evaluated through classical double agar assay, testing the solutions obtained from the processing of the leaf disks. We concluded that the best conditions for the experiments were the following: the bacteria should be diluted in LB_{LS}, the phages in milliQ sterile water with a MOI of 0.1, the mixing step should be of 30 minutes at 26 °C and 180 rpm. The test of the foliar disks should be conducted shaking the disks in 1.5 ml tubes in 500 µl of phage buffer solution for 1h. We designed the first experiment to assess if the mix of phage and carrier bacteria would be more stable on bean leaves surface than a phage solution at the same concentration. After the treatment with psageB1 or the two mix of psageB1 with UB210 and UB246 we took disks of 1.2 cm of diameter from the leaves (three biological replica as three different plants) at day 0, 1 and 4. The disks were soaked in 500 µl phage buffer and shaken to suspend the phages on their surface. The suspension obtained in this way was the starting point for a titration though double agar assay and a Real Time analysis of the phage genome (after 3 min at 100°C to destroy capsids. For the double agar assay we used the bacterial strain Pph #9 as host. A second experiment was repeated with a similar setting but sampling the plants at days 0, 1, 2 and 3 from the treatment, to focus

our attention on the first days after the application of the phages. The statistical analysis was performed through R (Culpepper & Aguinis, 2011) and ggplot2 R package was used to producing the plot images (Ginestet, 2011).

2.5 Discussion

Bleeding canker of kiwifruit and halo blight of bean cause worldwide significant crop losses (Donati et al., 2020; McCann et al., 2017). Strategies to prevent and cure these pathologies without the use of antibiotics or copper-based pesticides are currently not available. An IPM approach that includes the use of bacteria's natural predators and parasites—specifically bacteriophages—as biological control, could be an alternative method that can be adopted to minimize chemical control. In particular, for biocontrol purposes, lytic phages are required to have a high stability in the environment. Phages have the advantages of being very specific and not leaving toxic residues on the plant. One of the most numerous Psa phage collections was gathered in New Zealand in 2014 (Frampton et al., 2014) with 258 phages active against Psa, of which 24 were observed by TEM, revealing myovirus-, podovirus- and siphovirus-like morphologies. Among these phages, myovirus phiPsa21 showed an unusually large genome and was later recognized as a jumbo phage (Wojtus et al., 2019), containing genes possibly associated with the formation of a nucleoidlike structure in the host cell. In the same year, Di Lallo (Di Lallo et al., 2014) isolated and sequenced two Psa phages: phiPSA1 and phiPSA2. While phiPSA2 displayed a good efficacy against the Psa strain tested, phiPSA1 showed a temperate lifestyle and a narrower host range. The group of Flores (Flores et al., 2020) isolated and sequenced four *Podoviridae* phages similar to phiPsa2 (Di Lallo et al., 2014): CHF1, CHF7, ChF19 and CHF21; these phages were tested alone and combined as biocontrol agents and showed a significant decrease in Psa symptoms in vitro and a decrease in the bacterial load on kiwifruit plants in a greenhouse trial. In Korea, Yu and co-authors characterized two myoviruses and three podoviruses active against Psa, which were tested for their stability to different pH and UV-B exposition but were not tested as biocontrol agents (Yu et al., 2016). Yin and collaborators in 2019 isolated 36 phages from surface water samples in the Shanghai region, using the strain of Psa biovar 3 XWY0007 as target bacteria (Yin et al., 2019). The phages were represented mainly by myovirus-like particles, with some phages similar to *Podoviridae* and *Siphoviridae* families. In summary, this shows that there is a large variety of Psa phages with a certain degree of overlapping features from different geographical locations. A much lower variety and number of Pph phages are reported in literature, with the already cited cystovirus phi6 being the first isolated Pph phage (Eman & Afaf, 2014; Sistrom et al., 2015; Vidaver et al., 1973). Later, two more phages were isolated, but they were not characterized molecularly, one with a podoviruslike morphology and one with a cystovirus morphology [24]. Phi6 was tested as a biocontrol agent against *P.s*. pv. *syringae* (Pinheiro et al., 2019) and against Psa (Pinheiro et al., 2020), with a decrease in the titer of two strains of Psa biovar 3 in vitro and with a minor effect of reduction in the bacteria number in ex planta experiments performed on excised kiwifruit

leaves. However, the efficacy of phi6 against Pph strains has not yet been assessed. The current study isolated phages from soil in the same areas of plants infected by Psa or Pph, but was not able to isolate viruses from water sources or from symptomatic tissue, indicating a possible greater stability of phages in soil as indicated by Iriarte (Iriarte et al., 2012). All the virus isolates this current study found belong to the class *Caudoviricetes*, consistent with more than 97% of all described Pseudomonas phages (Ceyssens & Lavigne, 2010). Following the 2022 update of phage taxonomy by the International Committee on Taxonomy of Viruses (ICTV), between the families quoted in this paper, only *Autographiviridae* retained the family status. *Myoviridae*, *Siphoviridae* and *Podoviridae* are no longer considered families due to their highly polyphyletic nature. Now all the genus of these former family are grouped under the class *Caudoviricetes*. No genes associated to lysogeny were found, except for psageB2. The psageK4 isolate resulted in belonging to the same species of virus phiPSA267 (Pinheiro et al., 2020) isolated in New Zealand, while psageB2 belonged to the same species as phiPSA1 (Di Lallo et al., 2014), and M13 and M15 (Rabiey et al., 2020), isolated in Italy and England, respectively. PsageB2 is temperate just like phiPSA1 and has a narrow host range compared with the other phages isolated by our group. The isolation of phage variants belonging to the same species is probably due to the global diffusion of Psa biovar 3 strains (Ferrante & Scortichini, 2015) and consequently the global presence of the viruses associated with it. The virus isolate psageK4e was collected in the same location as psageK4 one year later, and shares with it a similarity of 99%, indicating a consistence of phage population in the same field in distinct growing seasons. The two phage genomes are highly similar in the region where all the genes linked to the morphology are located, the DNA terminase and some of the ORFs linked to DNA metabolism. They are less similar in their regions with a great number of ORFs encoding hypothetical proteins. A limited number of ORFs coding for hypothetical proteins are present only in one of the two phages. Their high similarity is reflected in their capability to lyse almost the totality of Psa and Pph strains of our collection. However, the EOP of psageK4e is significantly greater than psageK4 EOP. Phage psageA1 can be considered a representative of a novel species and it may represent the only member of a new genus of *Myoviridae* with the most similar phages located in the *Otagovirus* genus. For this new genus, we propose the name 'Mantavirus' and accordingly the name 'Mantavirus psageA10 for the species including our isolates psageA1 and psageA2. Phage psageB1 can be described as a representative of a new species of Siphoviridae that can be situated within the *Nickievirus* genus. Thus, we propose the binomial name 'Nickievirus psageB1' for this species. Its genome codes for a recombinase, RecA, but this is probably not linked to a temperate lifestyle or transduction, but to DNA replication as in other phages (Murphy, 2016); in fact, a temperate behavior was not observed in our host range. This protein can also have a role, such as in other siphoviruses, in the evolution through recombination of the phage (Hofstatter et al., 2016; Kupczok et al., 2018). Based on these results, PphageB1 in combination with the *P. syringae* nonpathogenic strains SZ131, UB210 and UB246 can be used for future experiments in a carrier bacteria approach (Harper et al., 2019) to

sustain the population of one of the phage or both on the phyllosphere of kiwifruit and beans in a possible biocontrol approach. Pph is an endemic pathogen in Piedmont and was isolated in Italy in 1962 (Ercolani & Crosse, 1966). All Pph phage isolates of Piedmont and Veneto were associated through sequencing to the same novel virus species. The isolation in different places of almost identical phages in the same species may be linked to a homogeneous population of Pph in northern Italy, which could be race 6, the most prevalent worldwide (Taylor et al., 1996). The Pph phages variant call analysis revealed that the majority of changes were synonymous mutations, the main part of which were located on structural genes whose sequence is bound to the stability of the capsid, which are highly sensitive to even small changes (Dion et al., 2020). Consistently, the main part of the DNA metabolism associated genes is not subject to variation. The missense mutations are located mainly on the phage tail fiber, and on the proteins of the lysis cassette suggesting differences in their host range in comparison with pphageB1. These mutation hotspots may be crucial for the Pph phages to continuously adapt to their bacterial host in a process of coevolution. The variation occurred mainly between the phages isolated in Piedmont, with a minor diversity between the Piedmont phages and the Veneto phages and inside the group of Veneto phages. SNPs in very similar phages were reported to be linked in differences in stability to abiotic stresses and lysis time (Liu et al., 2014), so these phages, although very similar, can be used to design phage cocktails. Concerning the pphageB1 sequence, both its high genome sequence similarity to existing phages and its genome organization, support its assignment to the *Autographiviridae* family in the *Krylovirinae* subfamily. Its genome sequence is not similar enough to any phage in the genera now described within *Krylovirinae*, so we propose this isolate with the pphageB21, pphageBV72, pphageT12 and pphageT12, as representatives of a new genus called 'Ceppovirus', containing only one species, with the proposed binomial name 'Ceppovirus pphageB1'. Like the other members of this family, pphageB1 encodes for a single-subunit DNA-directed RNA polymerase (pphageB1_29), placed in proximity of the cluster of DNA processing genes (Lavigne et al., 2003). Interestingly, one of the structural proteins (pphageB1_39) has a lysozyme C-terminal domain that can be linked to bacterial lysis, even if the target bacteria is Gram-negative (Masschalck et al., 2001). This enzyme is likely linked to the lysis of biofilm polymer or to expose the phage receptor on the bacteria surface degrading the peptidoglycan. PphageB1 has a similar genome organization in comparison with phage phiPSA17 (Frampton et al., 2015) and the *P. syringae* phages Bertil, Misse and Strit (Jørgensen et al., 2020). PphageB1 sequence has no strong homologies to other phages in literature, and shows the highest identity with *P*. *morsprunorum* phage MR18. Furthermore, pphageB1 shares a limited similarity with the P. fluorescens phage phi-2: pphageB1 phage should be tested in the future for the capability to lyse *P*. *fluorescens* strains indicated by Frampton (Frampton et al., 2014; Frampton et al., 2015) since it could be a possible carrier bacterium for biocontrol. A carrier strain would protect the phages from UV radiation and increase the phage number during the application. A great number of tRNA sequences in phages is often associated with a lytic lifestyle and a greater host

range because of the higher adaptive potential to different host codon usages and to different composition of the bases in genomes that can be partially indicated by the GC content (Bailly-Bechet et al., 2007; Yoshikawa et al., 2018). Our isolate psageA1 has a GC content (48%) much lower than Psa (58%) (Fujikawa & Sawada, 2019) and the presence of 14 tRNA sequences in psageA1 could partially explain its wide host range in our Psa and Pph collection. Conversely, psageB2 (GC content of 58%), psageB1 (GC content of 56%) and pphageB1 (GC content of 56%) have a more similar GC content to the Pph GC percentage (60%) (Palleroni) and this is consistent with the presence of only four tRNA in psageB1 and of no tRNA in psageB2 and pphageB1. Bacteriophage biocontrol in agriculture to control phytobacterial diseases faces several challenges such as scarce persistence in the plant phyllosphere, high diversity of the target and high probability of resistance development (Svircev et al., 2018). Possible solutions are the use of protective formulations, development of phage propagating bacterial strains and adapting timing and frequency of application (Balogh, et al., 2010). The isolated phages performed well in vitro under the tested stress conditions. These experiments may be indicative of their stability to stress occurring in the open field, but confirmatory experiments in field conditions are required. Phages psageK4, psageA1, psageB1 and pphageB1 resist for one hour temperature ranges normally found in the field on the leaf surface, so they should be applied at dawn to avoid the effects of the temperature and UV radiation, and increase their persistence on the phyllosphere. Most phages are resistant to a pH from 5 to 8 (Kutter & Sulakvelidze, 2004); our phages were only inactivated at pH 2, but their infectivity was not affected by an 18 h exposure to pH from 4 to 10. This may have an important role for their possible application on kiwifruit vines through trunk injection as the pH in the xylem lies around 5. Additionally, the phages we collected would not be affected by the pH of the majority of formulants, that are not highly acidic (Kutter & Sulakvelidze, 2004). Phage cocktail persistence in the open field could be improved with specific formulations (Svircev et al., 2018) and their action can be increased in synergy with the addition with other compounds such as carvacrol (Ni et al., 2020) and garlic extract (Eman & Afaf, 2014). Additionally, the phages we isolated can be a useful source of endolysins as an alternative Psa and Pph biocontrol method (Ni et al., 2021); the vast number of functionally uncharacterized ORFs they encode could contribute to further control approaches once their role is elucidated, urging a vast effort to assign function to the unprecedented proteomic diversity harbored by phages (Adriaenssens et al., 2020; Dion et al., 2020; Fernández-Ruiz, Coutinho, & Rodriguez-Valera, 2018). As reported previously in literature (Munoz-Adalia et al., 2018; Vidaver et al., 1973) UV exposure is detrimental to most phages. In our assays, the majority of the phage collection indeed showed sensitivity to UV light. However, the phage pphageB1 has a greater resistance to this treatment, increasing its possible persistence on the phyllosphere of plants in a biocontrol setting. This is important in relation of the high amount of UV radiation the plants' surface is exposed to in kiwifruit orchards. Host range analysis showed a versatility of all the Psa phage isolates that were able to lyse many of the Pph strains of our collection. Conversely, Pph phages were not capable to lyse any of the Psa strains. Thus,

the Psa phages that we isolated may recognize receptors shared by the *P.s*. species complex phylogroup of Psa (PG1) and Pph (PG3) (Dillon et al., 2019). To better elucidate the nature of these receptors, adsorption analysis on both bacterial phytopathogens will be necessary. It is possible that the bacteria belonging to pathovar *actinidiae* and *phaseolicola* also share the replication and translation bacterial machinery involved in a successful phage infection. The *P*. *syringae* pv. *morsprunorum* and *syringae* phage MR8 (Rabiey et al., 2020) was able to lyse several Psa strains and one Pph strain, making it a suitable candidate to be inserted in a future cocktail designed against both phytobacteria subjects of this study. P. *syringae* pv. *morsprunorum* race 1 is located in the same phylogroup of the *P.s* species complex of Psa (PG1), and *P*. *syringae* pv. *morsprunorum* race 2 in the same phylogroup as Pph (PG3), supporting the hypothesis of shared susceptibility determinants between these two phylogroups. The isolated phages will be tested in different combinations or cocktails allowing a broader host range and a possible synergy between phage actions (Schmerer, Molineux, & Bull, 2014). Psa phages have been reported to infect other *P*. *syringae* pathovars such as *morsprunorum* (Smith, Zamze, & Hignett, 1994) and other *Pseudomonas* species such as *P*. *fluorescens* (Kutter & Sulakvelidze, 2004). The phages we isolated can be active against both Psa and Pph similarly to the phages isolated by Yin (Yin et al., 2019), broadening the possibility to design a cocktail against these phytobacteria. Therefore, they could potentially be useful to design cocktails against other phytobacteria in the *P*. *syringae* species complex.

2.6 Author contributions

Conceptualization, M.C. (Marina Ciuffo), M.T. and R.L.; methodology, G.M., J.W. and D.H.; validation, G.M. and M.C. (Marco Chiapello); genome sequencing investigation and annotation, J.W., D.H. and G.M.; data curation, M.C. (Marco Chiapello); writing—original draft preparation, G.M.; writing—review and editing, M.T., M.C. (Marina Ciuffo), J.W., D.H. and R.L.; visualization at electron microscope, M.V.; supervision, M.C. (Marina Ciuffo); funding acquisition M.T. and M.C. (Marina Ciuffo) All authors have read and agreed to the published version of the manuscript.

2.7 Figures and Tables

Table 2.1 *Pseudomonas syringae* pv. *actinidiae* and pv. *phaseolicola* strains properties and their phage sensitivity profiles. The key to phage Efficiency of plating (EOP) is shown at the right end of the table. Red colour indicates an EOP comparable to the one measured in the isolation strain (K7#8 for psageA1, psageK4, psageK4e, psageB1 and psage B2; Pph Cuneo #6_18 for the pphageB1, pphageB21, pphageBV72, pphageT12 and pphageT21; Pph Cuneo #6_18 arbitrarily chosen as reference for MR8). The other colours represent different levels of EOP with darker colours indicating a greater efficiency in their lytic activity. "-"symbols represent cases for which we have not observed plaques at any concentration of the crude lysate. * Variety *deliciosa*; $ Phytosanitary Inspection Service.

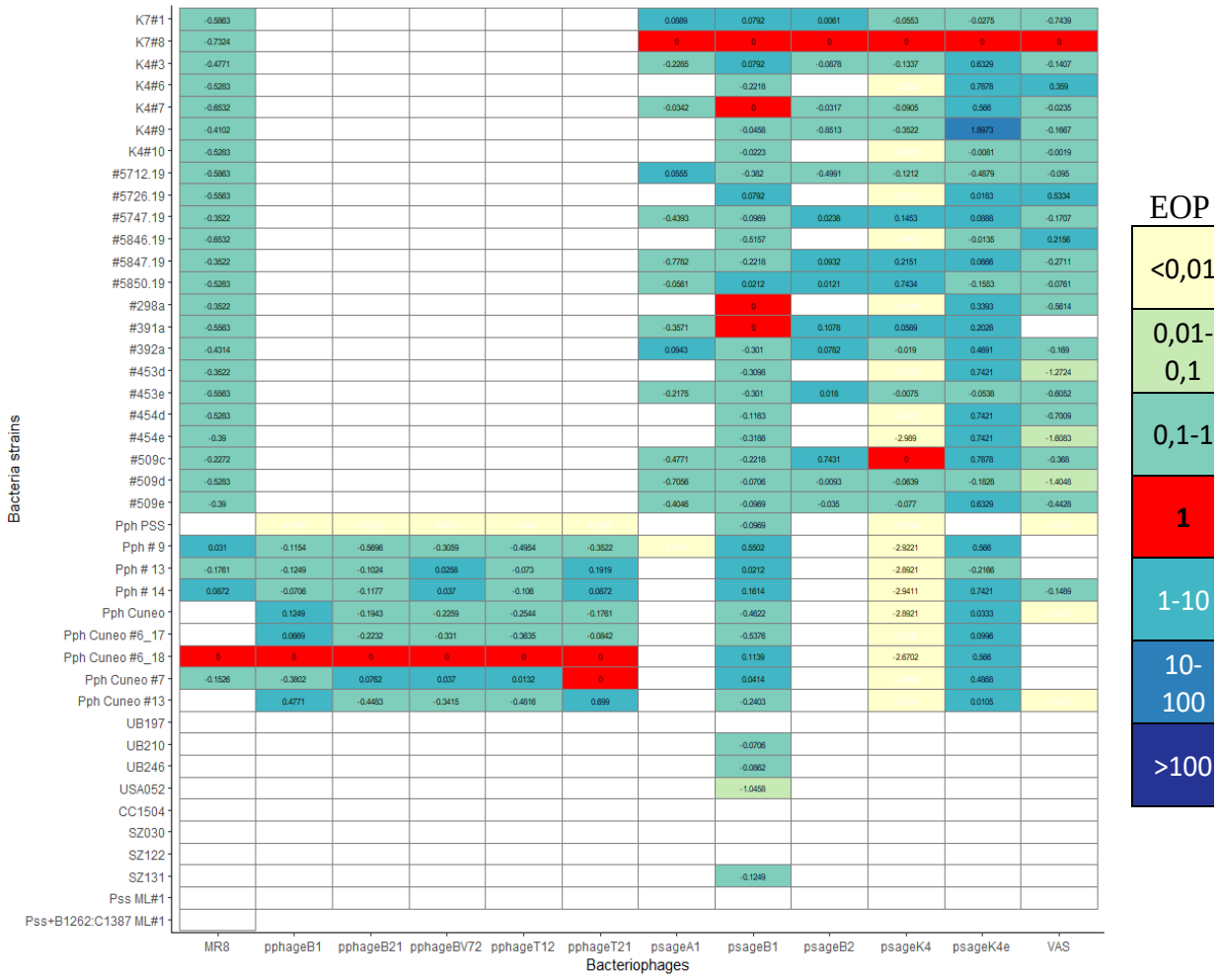

Table 2.2. Summary of the main features of phages isolated in this study. The classification of the phages is based on phylogenetic trees analysis we have performed (Figure 4)

Phage name	Source	Origin [a]	Field Species and Cultivar	Source	Region	Year	Plaque morphology (LB_{LS} 0.6%) [b]	Classification [c]
psageK4	Soil	Manta (CN)	*Actinidia chinensis* var. *deliciosa*	Agrion	Piedmont	2018	Clear, 1 mm	*Caudoviricites* (former *Myoviridae* morphology)
psageK4e	Soil	Manta (CN)	*Actinidia chinensis* var. *deliciosa*	Agrion	Piedmont	2019	Clear, 1 mm	*Caudoviricites* (former *Myoviridae* morphology)
psageK4v	Soil	Vassalli (CN)	*Actinidia chinensis* var. *deliciosa*	Agrion	Piedmont	2021	Clear, 1 mm	*Caudoviricites* (former *Myoviridae* morphology)
psageA1	Soil	Manta (CN)	*Actinidia chinensis* var. *deliciosa*	Agrion	Piedmont	2018	Clear, 1-2 mm	*Caudoviricites* (former *Myoviridae* morphology)
psageA2	Soil	Manta (CN)	*Actinidia chinensis* var. *deliciosa*	Agrion	Piedmont	2018	Clear, 1-2 mm	*Caudoviricites* (former *Myoviridae* morphology)
psageB1	Soil	Manta (CN)	*Actinidia chinensis* var. *deliciosa*	Agrion	Piedmont	2018	Clear, 2 mm	*Caudoviricites* (former *Siphoviridae* morphology)
psageB2	Soil	Manta (CN)	*Actinidia chinensis* var. *deliciosa*	Agrion	Piedmont	2018	Clear or turbid , 2mm	*Caudoviricites* (former *Siphoviridae* morphology)
psageK9	Soil	Borgo d'Ale (VC)	*Actinidia chinensis* var. *deliciosa*	IPSP	Piedmont	2019	clear or turbid 2mm	*Caudoviricites* (former *Siphoviridae* morphology)
pphageB1	Soil	Boves (CN)	*Phaseolus vulgaris* cv. *Billò*	Agrion	Piedmont	2018	Clear, 5 mm	*Autographiviridae*
pphageB12	Soil	Boves (CN)	*Phaseolus vulgaris* cv. *Billò*	Agrion	Piedmont	2018	Clear, 5 mm	*Autographiviridae*
pphageB13	Soil	Boves (CN)	*Phaseolus vulgaris* cv. *Billò*	Agrion	Piedmont	2018	Clear, 5 mm	*Autographiviridae*
pphageB21	Soil	Boves (CN)	*Phaseolus vulgaris* cv. *Billò*	Agrion	Piedmont	2018	Clear, 5 mm	*Autographiviridae*
pphageB51	Soil	Boves (CN)	*Phaseolus vulgaris* cv. *Billò*	Agrion	Piedmont	2018	Clear, 5 mm	*Autographiviridae*
pphageB101	Soil	Boves (CN)	*Phaseolus vulgaris* cv. *Billò*	Agrion	Piedmont	2018	Clear, 5 mm	*Autographiviridae*
pphageT11	Soil	Tetti Pesio (CN)	*Phaseolus vulgaris* cv. *Borlotto nano*	Agrion	Piedmont	2018	Clear, 5 mm	*Autographiviridae*
pphageT12	Soil	Tetti Pesio (CN)	*Phaseolus vulgaris* cv. *Borlotto nano*	Agrion	Piedmont	2018	Clear, 5 mm	*Autographiviridae*
pphageT13	Soil	Tetti Pesio (CN)	*Phaseolus vulgaris* cv. *Borlotto nano*	Agrion	Piedmont	2018	Clear, 5 mm	*Autographiviridae*
pphageT21	Soil	Tetti Pesio (CN)	*Phaseolus vulgaris* cv. *Borlotto nano*	Agrion	Piedmont	2018	Clear, 5 mm	*Autographiviridae*
pphageT22	Soil	Tetti Pesio (CN)	*Phaseolus vulgaris* cv. *Borlotto nano*	Agrion	Piedmont	2018	Clear, 5 mm	*Autographiviridae*
pphageT23	Soil	Tetti Pesio (CN)	*Phaseolus vulgaris* cv. *Borlotto nano*	Agrion	Piedmont	2018	Clear, 5 mm	*Autographiviridae*
pphageBV2	Soil	Verona (VR)	*Phaseolus vulgaris* cv. *Spagnolet (Lamon)*	Phytosanitary Inspection Service	Veneto	2019	Clear, 5 mm	*Autographiviridae*
pphageBV4	Soil	Verona (VR)	*Phaseolus vulgaris* cv. *Spagnolet (Lamon)*	Phytosanitary Inspection Service	Veneto	2019	Clear, 5 mm	*Autographiviridae*
pphageBV71	Soil	Verona (VR)	*Phaseolus vulgaris* cv. *Canalino (Lamon)*	Phytosanitary Inspection Service	Veneto	2019	Clear, 5 mm	*Autographiviridae*
pphageBV72	Soil	Verona (VR)	*Phaseolus vulgaris* cv. *Canalino (Lamon)*	Phytosanitary Inspection Service	Veneto	2019	Clear, 5 mm	*Autographiviridae*

[a] The letters in brackets indicate the province. CN stands for Cuneo, VC for Vercelli and VR for Verona

[b] For Psa strains we used as reference strain for this assay K7#8 and for Pph, strain Pph Cuneo #6_18

[c] The classification in the last column of the table was either through high identity with taxonomically classified phages already present in the database for the 15 phages that were sequenced in their whole genome. For the other 8, identical TEM observed morphology was confirmed with specific primers designed on the sequenced isolates.

Table 2.3. Summary of the characteristic of the genomes of selected phages.

Phage name	Accession number	Bacterial host	Genome length	GC content (%)	ORFs	Hypothetical proteins	proteins with predicted function	ORFans	tRNAs
psageA1	MT740307	Psa K7 #8	98,780 bp	48.79%	176	76	51	49	14
psageB1	MT354569	Psa K7 #8	112,269 bp	56.47%	161	105	40	16	4
pphageB1	MT354570	Pph Cuneo #6_18	41,714 bp	56.63%	52	23	25	4	0
psageK4	MZ348426	Psa K7 #8	98,440 bp	60.44%	179	112	51	16	18
psageB2	MZ348425	Psa K7 #8	50,739 bp	58.51%	77	47	26	4	0

Table 2.4. Summary of the characteristic of the bacteria strain used in this research.

Identification	Origin	Geographical Origin	Source	Bacterial strains	Year
P.s. pv. *actinidiae*	*Actinidia chinensis* var. *deliciosa*	Piedmont	Agrion	K7#1	2019
P.s. pv. *actinidiae*	*Actinidia chinensis* var. *deliciosa*	Piedmont	Agrion	K7#8	2019
P.s. pv. *actinidiae*	*Actinidia chinensis* var. *deliciosa*	Piedmont	Agrion	K4#3	2018
P.s. pv. *actinidiae*	*Actinidia chinensis* var. *deliciosa*	Piedmont	Agrion	K4#6	2018
P.s. pv. *actinidiae*	*Actinidia chinensis* var. *deliciosa*	Piedmont	Agrion	K4#7	2018
P.s. pv. *actinidiae*	*Actinidia chinensis* var. *deliciosa*	Piedmont	Agrion	K4#9	2018
P.s. pv. *actinidiae*	*Actinidia chinensis* var. *deliciosa*	Piedmont	Agrion	K4#10	2018
P.s. pv. *actinidiae*	*Actinidia chinensis* var. *deliciosa*	Veneto	Phytosanitary Inspection Service	#5712.19	2019
P.s. pv. *actinidiae*	*Actinidia chinensis* var. *deliciosa*	Veneto	Phytosanitary Inspection Service	#5726.19	2019
P.s. pv. *actinidiae*	*Actinidia chinensis* var. *chinensis*	Veneto	Phytosanitary Inspection Service	#5747.19	2019
P.s. pv. *actinidiae*	*Actinidia chinensis* var. *deliciosa*	Veneto	Phytosanitary Inspection Service	#5846.19	2019
P.s. pv. *actinidiae*	*Actinidia chinensis* var. *deliciosa*	Veneto	Phytosanitary Inspection Service	#5847.19	2019
P.s. pv. *actinidiae*	*Actinidia chinensis* var. *deliciosa*	Veneto	Phytosanitary Inspection Service	#5850.19	2019
P.s. pv. *actinidiae*	*Actinidia chinensis* var. *deliciosa*	Piedmont	Phytosanitary Inspection Service	#298a	2019
P.s. pv. *actinidiae*	*Actinidia chinensis* var. *deliciosa*	Piedmont	Phytosanitary Inspection Service	#391a	2018
P.s. pv. *actinidiae*	*Actinidia chinensis* var. *deliciosa*	Piedmont	Phytosanitary Inspection Service	#392a	2018
P.s. pv. *actinidiae*	*Actinidia chinensis* var. *deliciosa*	Piedmont	Phytosanitary Inspection Service	#453d	2016
P.s. pv. *actinidiae*	*Actinidia chinensis* var. *deliciosa*	Piedmont	Phytosanitary Inspection Service	#453e	2016

Identification	Origin	Geographical Origin	Source	Bacterial strains	Year
P.s. pv. *actinidiae*	*Actinidia chinensis* var. *deliciosa*	Piedmont	Phytosanitary Inspection Service	#454d	2018
P.s. pv. *actinidiae*	*Actinidia chinensis* var. *deliciosa*	Piedmont	Phytosanitary Inspection Service	#454e	2018
P.s. pv. *actinidiae*	*Actinidia chinensis* var. *deliciosa*	Piedmont	Phytosanitary Inspection Service	#509c	2018
P.s. pv. *actinidiae*	*Actinidia chinensis* var. *deliciosa*	Piedmont	Phytosanitary Inspection Service	#509d	2018
P.s. pv. *actinidiae*	*Actinidia chinensis* var. *deliciosa*	Piedmont	Phytosanitary Inspection Service	#509e	2018
P.s. pv. *phaseolicola*	*Phaseolus vulgaris*	Piedmont	Phytosanitary Inspection Service	Pph PSS	2015
P.s. pv. *phaseolicola*	*Phaseolus vulgaris*	China	Private company	Pph # 9	2015
P.s. pv. *phaseolicola*	*Phaseolus vulgaris*	China	Private company	Pph # 13	2015
P.s. pv. *phaseolicola*	*Phaseolus vulgaris*	China	Private company	Pph # 14	2015
P.s. pv. *phaseolicola*	*Phaseolus vulgaris*	Piedmont	IPSP	Pph Cuneo	2016
P.s. pv. *phaseolicola*	*Phaseolus vulgaris*	Piedmont	Agrion	Pph Cuneo #6_17	2017
P.s. pv. *phaseolicola*	*Phaseolus vulgaris*	Piedmont	Agrion	Pph Cuneo #6_18	2018
P.s. pv. *phaseolicola*	*Phaseolus vulgaris*	Piedmont	Agrion	Pph Cuneo #7	2018
P.s. pv. *phaseolicola*	*Phaseolus vulgaris*	Piedmont	Agrion	Pph Cuneo #13	2017

Figure 2.1. Plaque morphology and electron microscopy images of the three phages representing putative new species: (**A**) pphageB1 capsid has an icosahedric head with a short tail and clear fibers, typical for a podovirus morphology; (**B**) psageA1 has an icosahedral head and a putative contractile tail typical for the myovirus morphology; (**C**) psageB1 shows a long and flexible non-contractile tail linked to an icosahedral head, a typical siphovirus morphology.

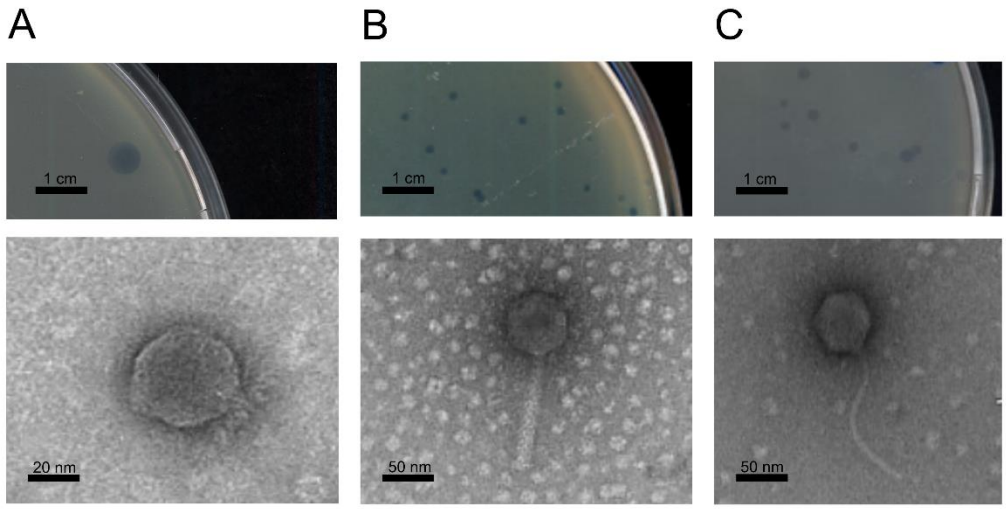

Figure 2.2. Genome organization of pphageB1 phage compared with MR18 (**A**), psageB1 compared with nickie (**B**), psageA1 (**C**), psageK4 compared with psageK4e and phiPsa267 (**D**), and psageB2 compared with phiPsa1 (**E**). The arrows indicate annotated ORFs; and the asterisks, annotated tRNA sequences. Yellow arrows indicate ORFs associated with structural proteins, blue DNA- and metabolism-associated ORF, red ORFs that encode for lysis associated proteins, and purple ORFs homologues to terminases. The intensity of the color between two compared sequences indicates percentages of BLASTn similarity.

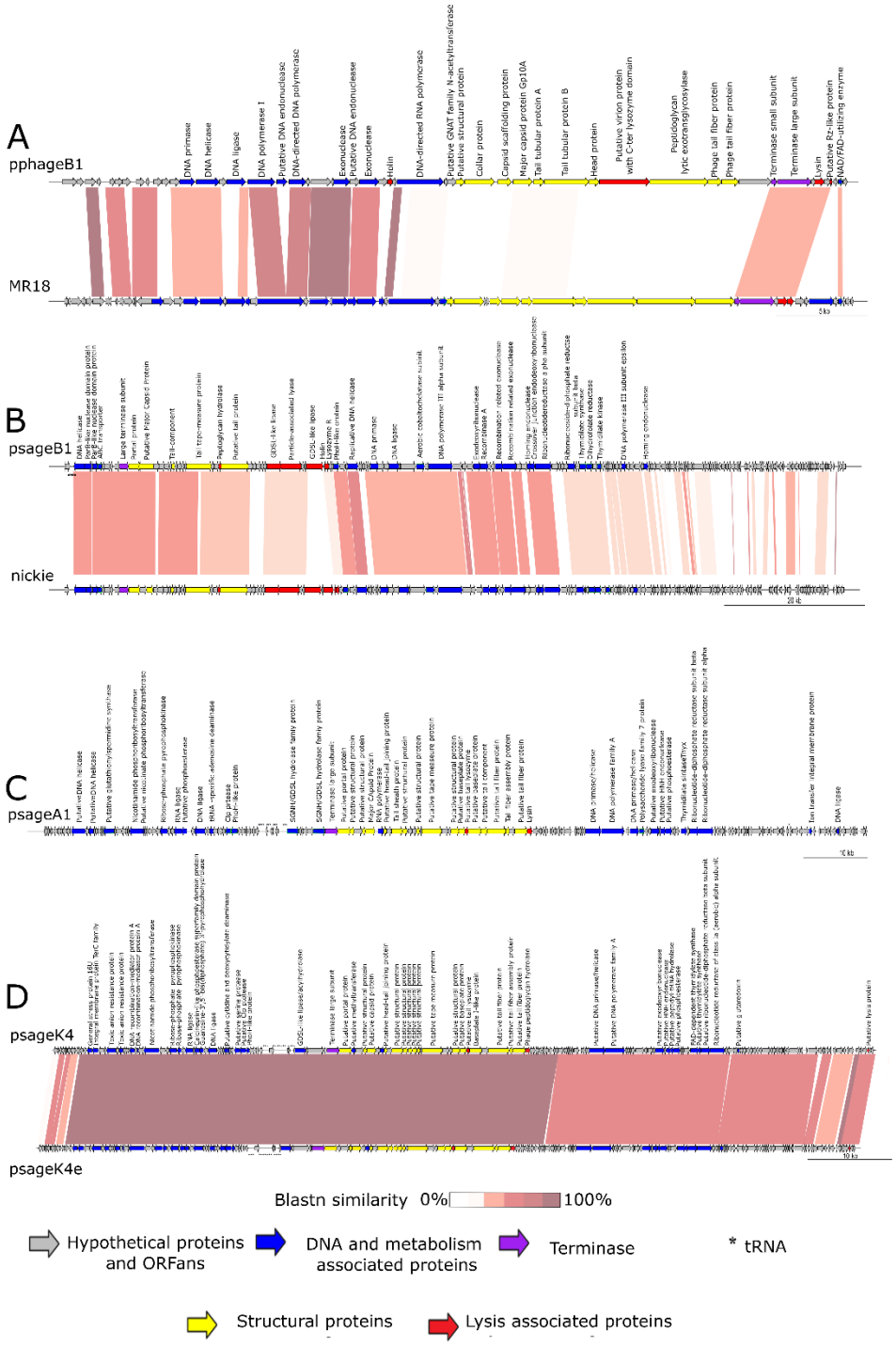
A
pphageB1
MR18
DNA primase
DNA helicase
DNA ligase
DNA polymerase I
Putative DNA endonuclease
DNA-directed DNA polymerase
Exonuclease
Putative DNA endonuclease
Exonuclease
Holiin
DNA-directed RNA polymerase
Putative GNAT family N-acetyltransferase
Putative structural protein
Collar protein
Capsid scaffolding protein
Major capsid protein Gp10A
Tail tubular protein A
Tail tubular protein B
Head protein
Putative virion protein with C-ter lysozyme domain
Peptidoglycan lytic endoglycosylase
Phage tail fiber protein
Phage tail fiber protein
Terminase small subunit
Terminase large subunit
Lysin
Putative Rz-like protein
NAD/FAD-utilizing enzyme
5 kb
B
psageB1
nickie
20 kb
C
psageA1
10 kb
D
psageK4
psageK4e
10 kb
Blastn similarity 0%
100%
Hypothetical proteins and ORFans
DNA and metabolism associated proteins
Terminase
* tRNA
Structural proteins
Lysis associated proteins

Figure 2.3. The charts show the viability of pphageB1, psageK4, psageB1 and psageA1 phages under exposure to different pHs (**A**), or temperatures (**B**), for one hour, and to different times of UV-C irradiation (**C**). The number of replicates for every condition is four, and the error bars indicate the standard error. The statistical significance was calculated through the agricolae R package and consists of ANOVA (ANOVA p-values are shown under every plot) and Kruskal–Wallis
analysis (significant differences indicated by letters over the bars). Different lower-case letters above each bar plot represent statistically different values.

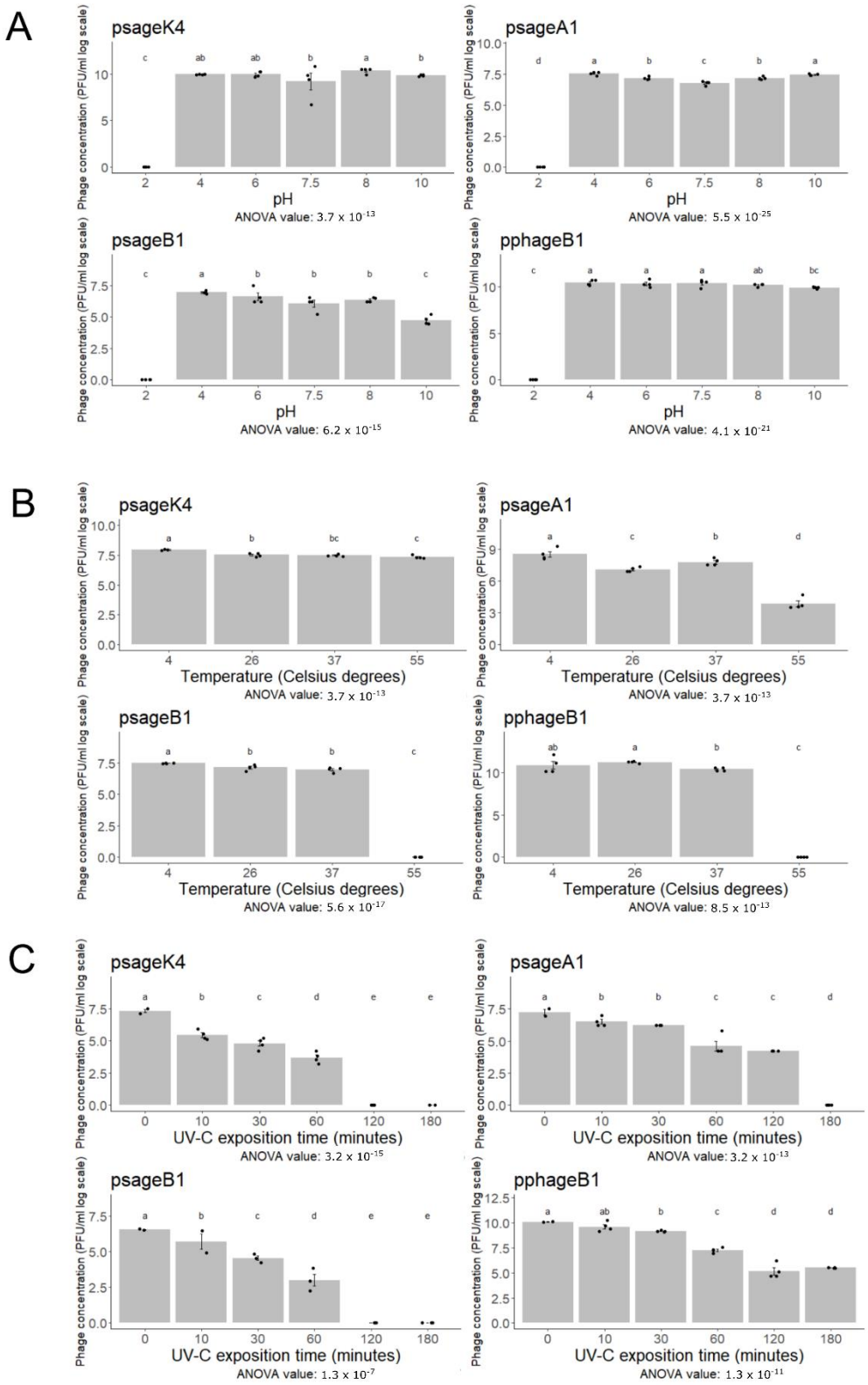
A
psageK4
psageA1
psageB1
pphageB1
Phage concentration (PFU/ml log scale)
pH
ANOVA value: 3.7 x 10-13
ANOVA value: 5.5 x 10-25
ANOVA value: 6.2 x 10-15
ANOVA value: 4.1 x 10-21
B
Temperature (Celsius degrees)
ANOVA value: 3.7 x 10-13
ANOVA value: 3.7 x 10-13
ANOVA value: 5.6 x 10-17
ANOVA value: 8.5 x 10-13
C
UV-C exposition time (minutes)
ANOVA value: 3.2 x 10-15
ANOVA value: 3.2 x 10-13
ANOVA value: 1.3 x 10-7
ANOVA value: 1.3 x 10-11

Figure 2.4. Phylogenetic analysis of a selected number of Major Capsid Protein (MCP) sequences similar to the MCP of pphageB1 phage (**A**), of a selected number of DNA ligases similar to the DNA ligase of psageA1, psageK4 and psageK4e phages (**B**), and of a selected number of MCP similar to the psageB1 MCP (**C**). The Escherichia virus T7 MCP and DNA ligase were used as an outgroup for psageB1 and psageA1. The N4 phage MCP sequence was used as an outgroup for pphageB1 tree. The maximum likelihood methodology was used to obtain the best tree. After comparisons, the chosen best model of substitution was WAG+G4 for the pphageB1 and psageB1 trees and Blosum62+G4 for the psageA1 tree. Consensus trees were constructed from 1000 bootstrap trees. PphageB1, psageA1 and psageB1 are indicated in bold characters. At the nodes, the bootstrap values, expressed in percentages

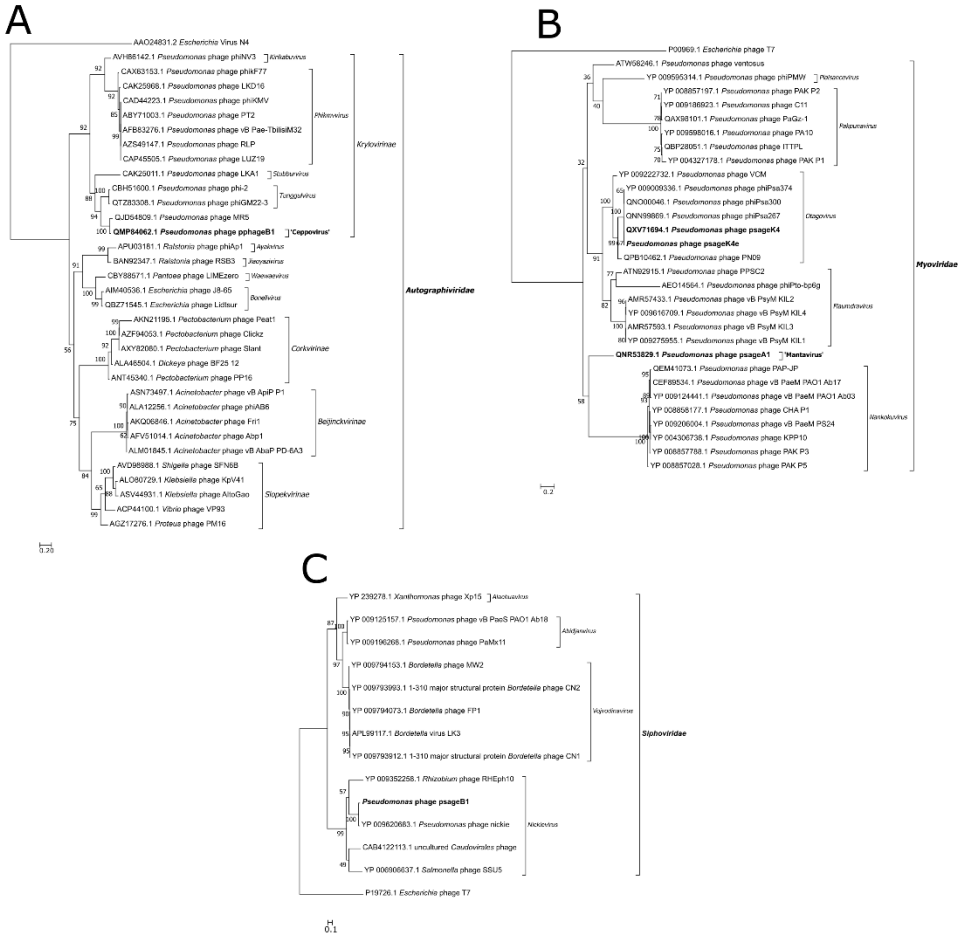

Figure 2.S1. phylogenetic analysis of the terminases of pphageB1, psageA1 and psageB.

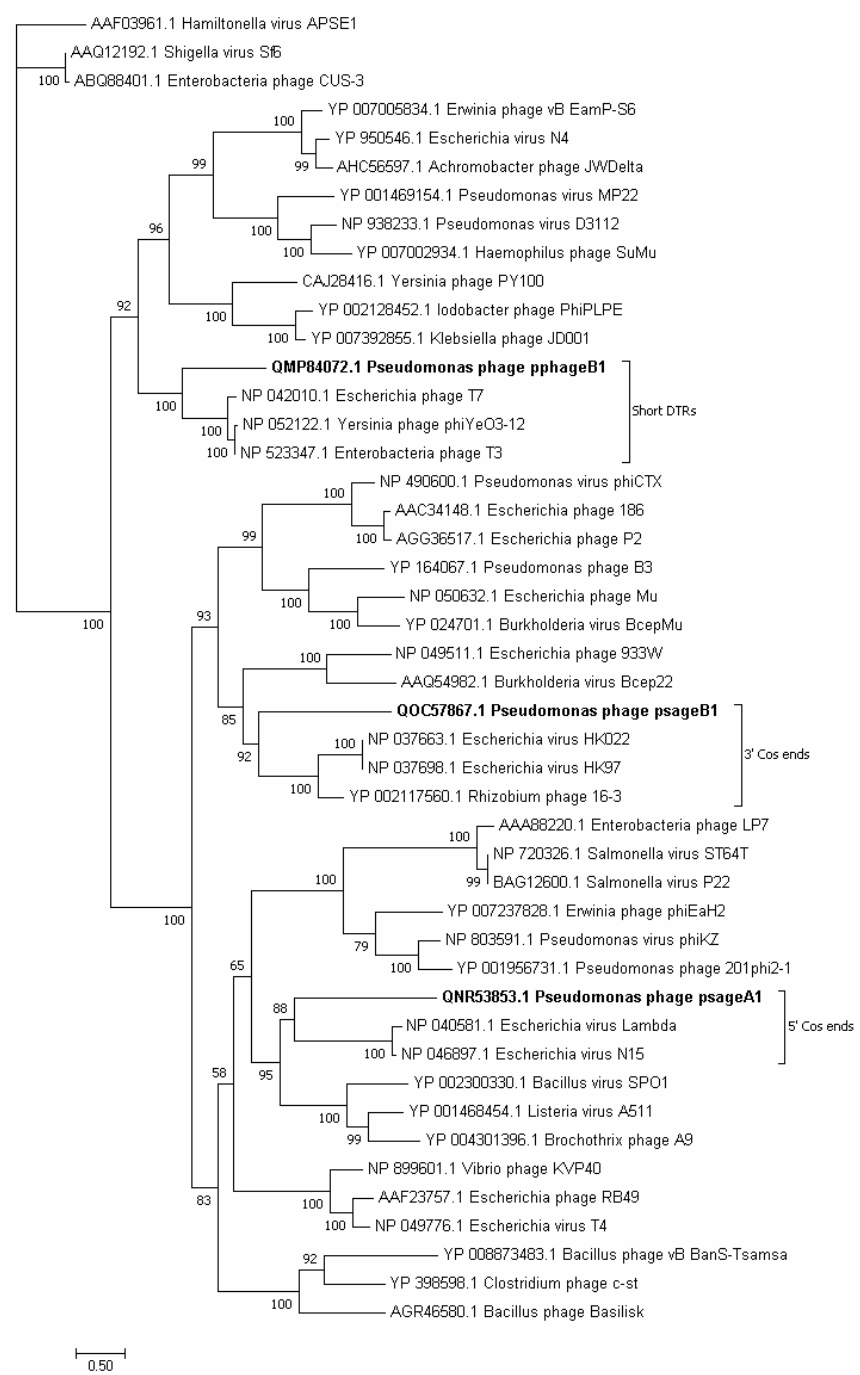

Figure 2.S2. Phylogenetic analysis of a selected number of RNA Polymerase (RNAP) sequences similar to the RNAP of pphageB1 phage.

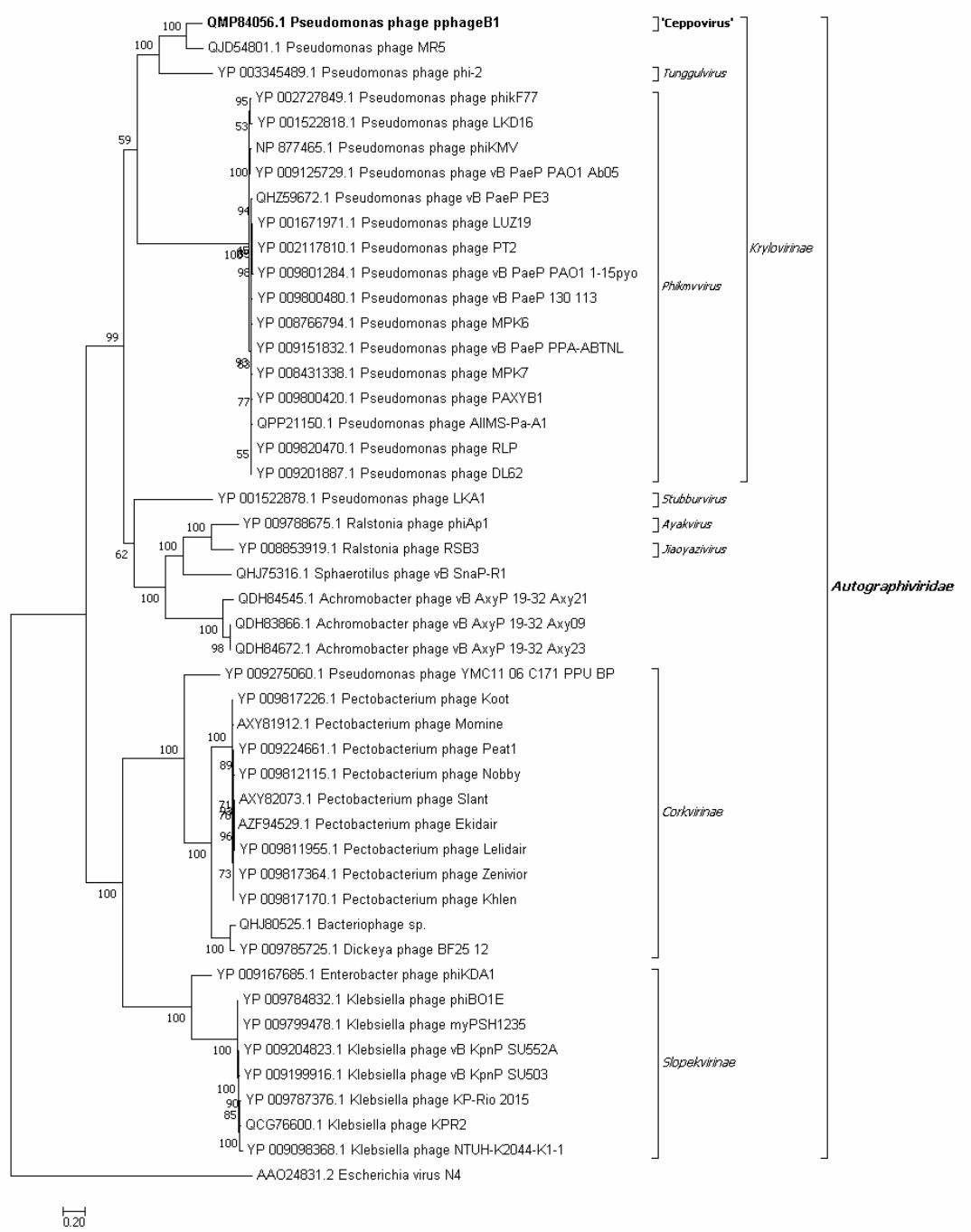

Figure 2.S3. Phylogenetic analysis of a selected number of Major Capsid Protein (MCP) sequences similar to the MCP of pphageA1 phage.

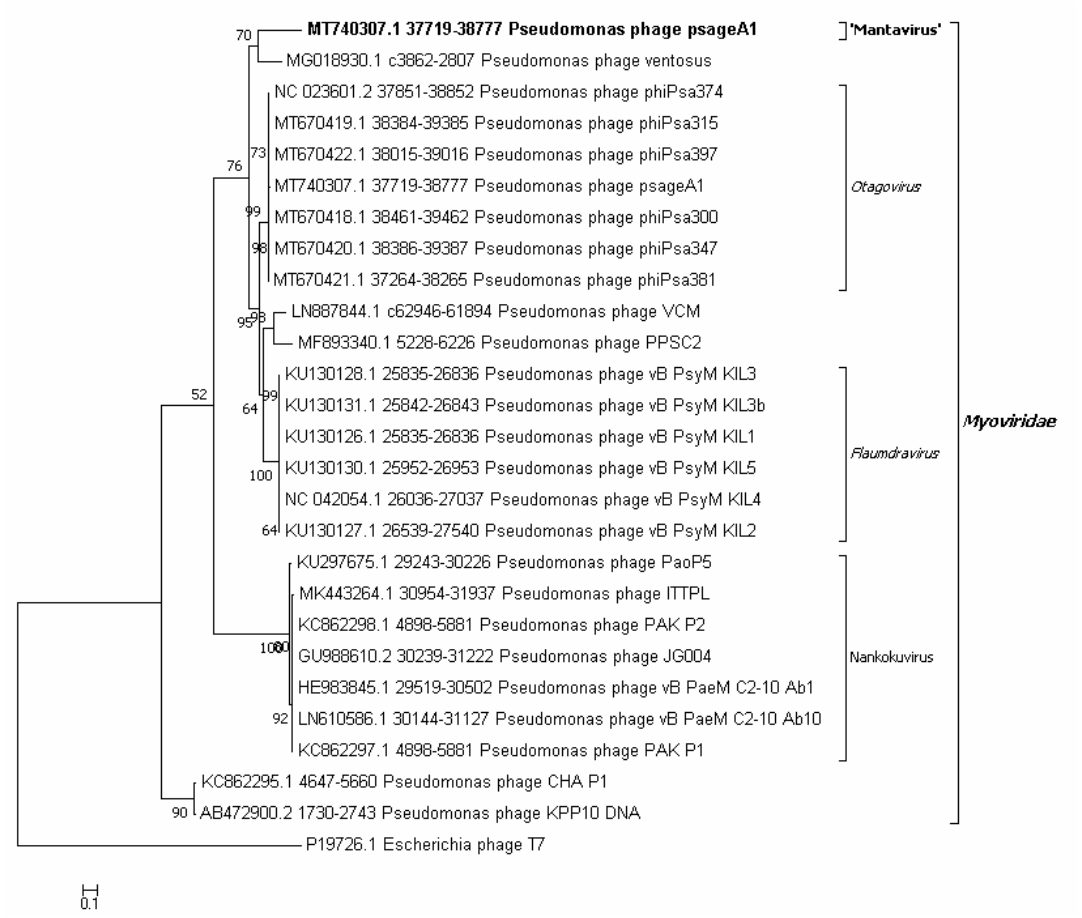

Figure 2.5: photo of the fourth repetition of bioassay on bean plants. The results of the experiment, measured as disease index after 1 month are showed in figure 2.6.

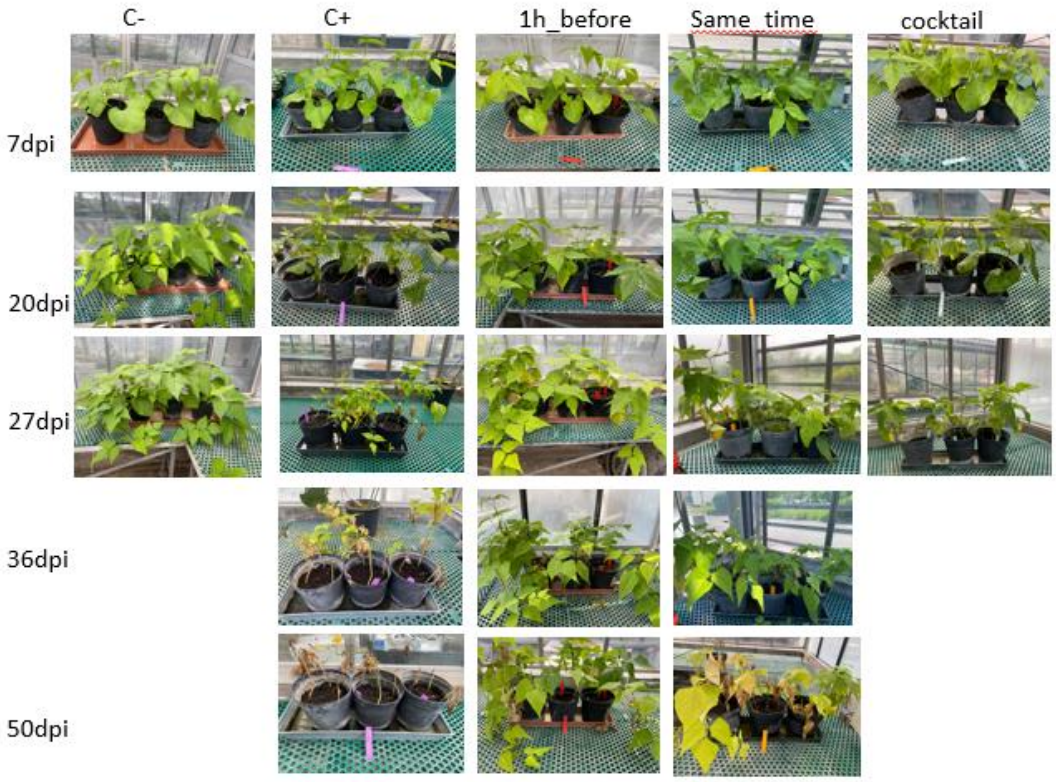

Figure 2.6: Severity index of halo blight on bean plants (0: Healthy plant, 1: Local symptoms, 2: Local and mild systemic symptoms, 3: Local and severe systemic symptoms, 4: severely damaged plant, 5: deceased plant).

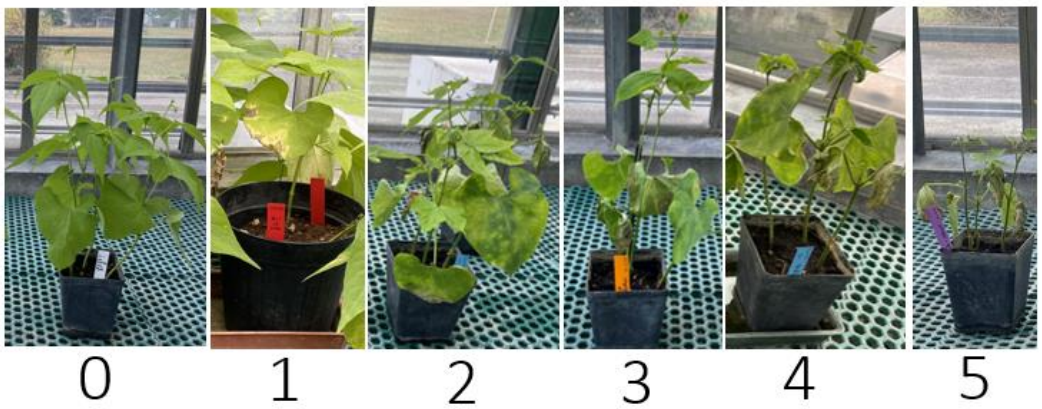

Figure 2.7: scatter plot of the severity of halo blight after 1 month from inoculation in test.

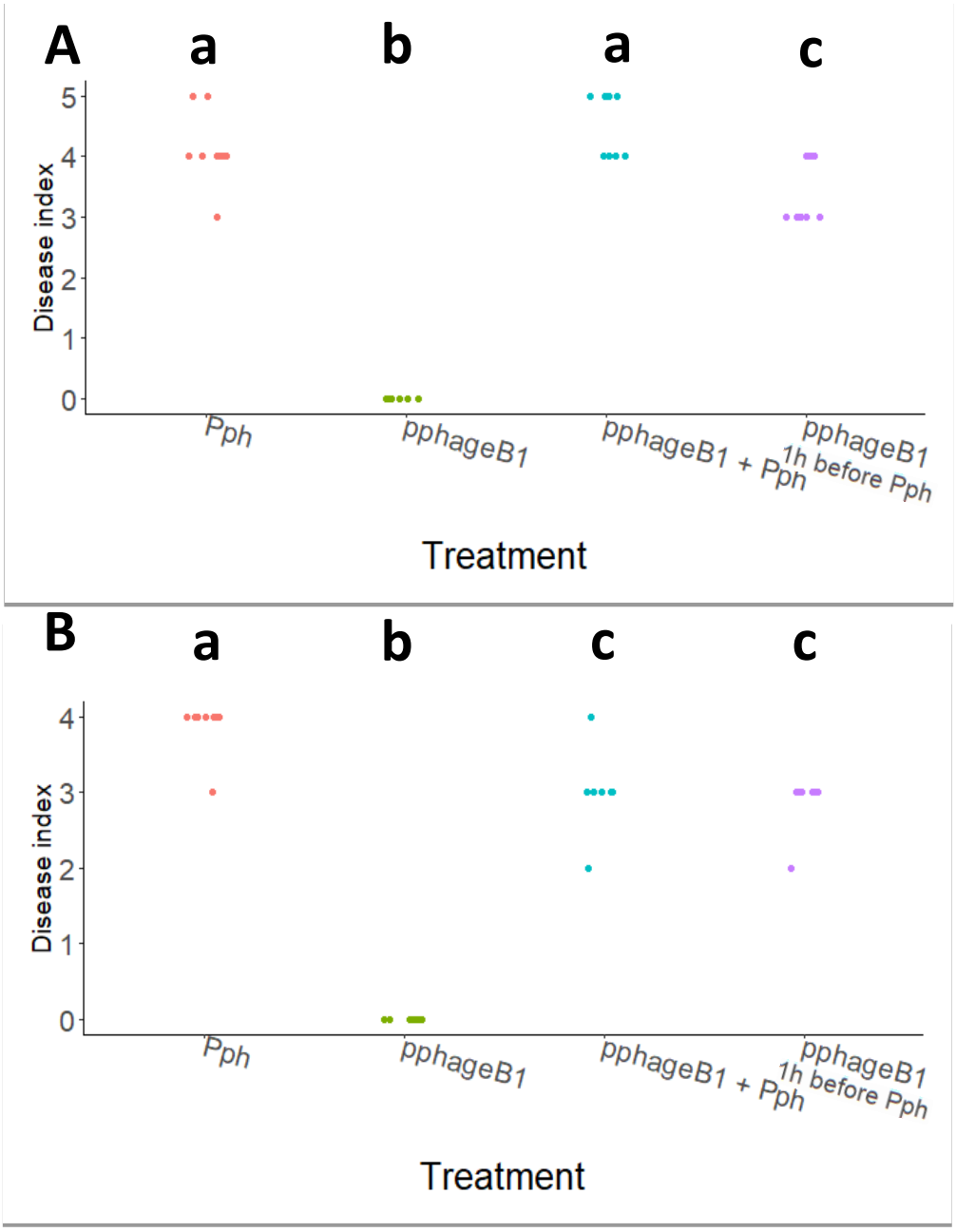

Figure 2.8: bar plot of the first repetition of the persistence of psageB1 on phyllosphere with or without a carrier bacterium (table 2.4) (**A**); bar plot of the second repetition of the persistence of psageB1 on phyllosphere with or without a carrier bacterium (table 2.5) (**B**).

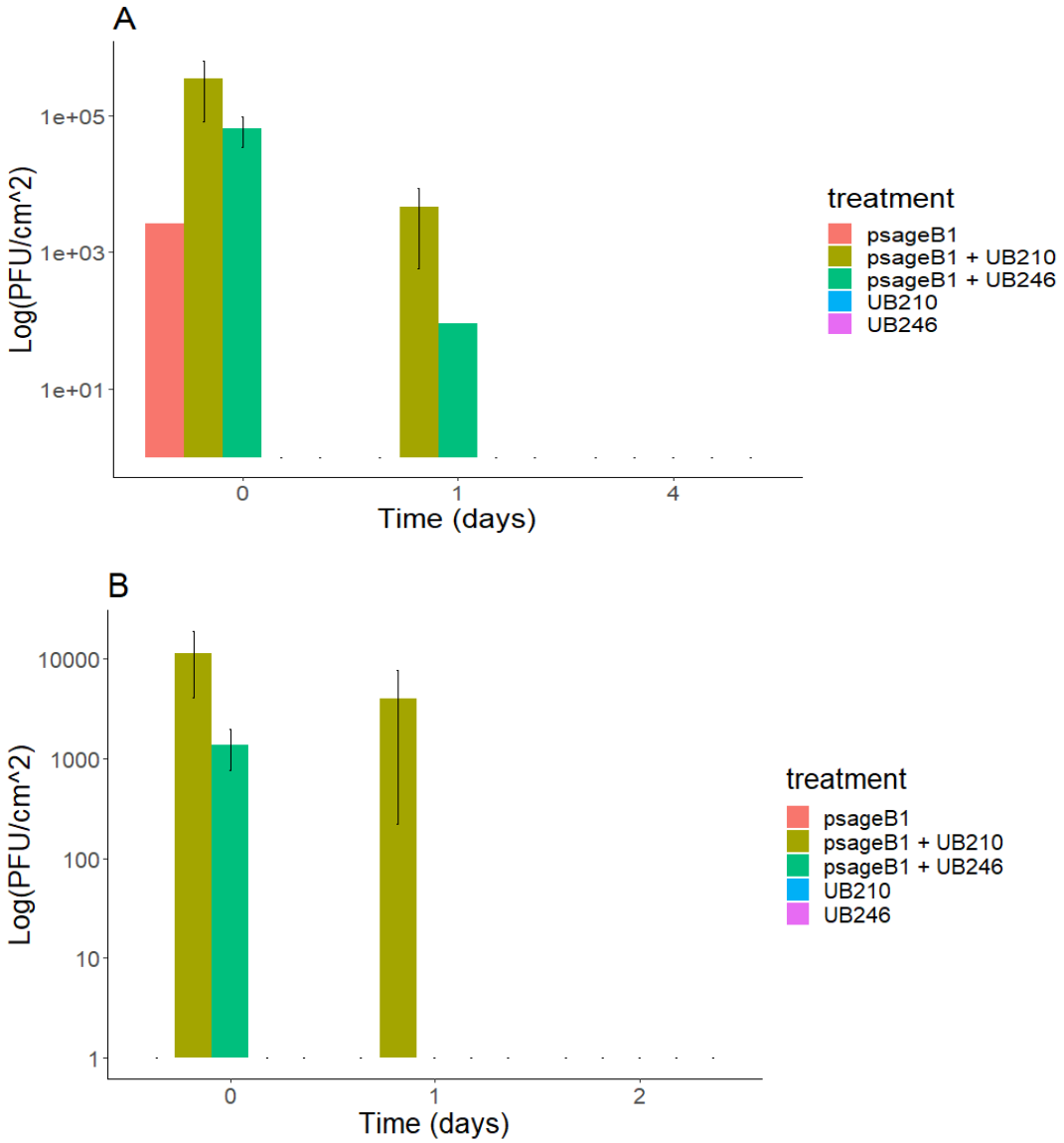

untreated plants (Pph), plants treated with phage pphageB1 at the same time of Pph inoculation (pphageB1 + Pph) and 1 hour before the Pph inoculation (pphageB1 1h before Pph), and as negative control plants only treated with the phage (pphageB1) in two repetitions of the experiment (**A**) and (**B**). Severity was associated to a diseased index (0: Healthy plant, 1: Local symptoms, 2: Local and mild systemic symptoms, 3: Local and severe systemic symptoms, 4: severely damaged plant, 5: deceased plant). The statistical significance of the data was tested through Kruskall-Wallis test and Wilcoxon paired

Time (days)	*Phage concentration (PFU /cm^2)*				
	psageB1	*psageB1 + UB210*	*psageB1 + UB246*	*UB246*	*UB210*
0	*2650*	*885000*	*46000*	*0*	*0*
0	*NA*	*79600*	*23000*	*0*	*0*
0	*NA*	*79600*	*124000*	*0*	*0*
1	*0*	*265*	*89*	*0*	*0*
1	*0*	*885*	*NA*	*0*	*0*
1	*0*	*12400*	*NA*	*0*	*0*
4	*0*	*0*	*0*	*0*	*0*
4	*0*	*0*	*0*	*0*	*0*
4	*0*	*0*	*0*	*0*	*0*

Table 2.4: concentration of active viral particles of psageB1 on bean leaf surface. Every case was repeated on three different plants. The leaves were treated with psageB1, mixes of psageB1 and UB210 or UB246 *Pseudomonas syringae* nonpathogenic strains and with liquid cultures of UB210 or UB246 as negative control. Results of the first repetition of the experiment.

Time (days)	Phage concentration (PFU /cm^2)

	psageB1	psageB1 + UB210	psageB1 + UB246	UB246	UB210
0	0	25700	2123	0	0
0	0	796	NA	0	0
0	0	7960	619	0	0
1	0	442	0	0	0
1	0	11500	0	0	0
1	0	0	0	0	0
2	0	0	0	0	0
2	0	0	0	0	0
2	0	0	0	0	0
3	0	0	0	0	0
3	0	0	0	0	0
3	0	0	0	0	0

Table 2.5: concentration of active viral particles of psageB1 on bean leaf surface. Every case was repeated on three different plants. The leaves were treated with psageB1, mixes of psageB1 and UB210 or UB246 *Pseudomonas syringae* nonpathogenic strains and with liquid cultures of UB210 or UB246 as negative control. Results of the second repetition of the experiment.

Supplementary material

The following are available online at https://www.mdpi.com/article/10.3390/v13102083/s1, Figure S1: phylogenetic analysis of the terminases of pphageB1, psageA1 and psageB1; Figure S2: phylogenetic analysis of pphageB1 RNA polymerase; Figure S3: phylogenetic analysis of psageA1 MCP; Table S1: variant calling analysis between the genomes of pphageB1 and pphageB2_1; Table S2: variant calling analysis between the genomes of pphageB1 and pphageBV7_2; Table S3: variant calling analysis between the genomes of pphageB1 and pphageT1_2; Table S4: variant calling analysis between the genomes of pphageB1 and pphageT2_1; Table S5: variant calling analysis between the genomes of pphageK4 and pphageK4e; Table S6: coverage values of the sequenced phage genomes.

3 PHAGES TO CONTROL INSECT POPULATIONS

The main content of this chapter was published as:

Vallino, M., Rossi, M., Ottati, S., Martino, G., Galetto, L., Marzachì, C., & Abbà, S. (2021). Bacteriophage-host association in the phytoplasma insect vector *Euscelidius variegatus*. Pathogens, 10(5), 612.

3.1 Abstract

Insect vectors transmit viruses and bacteria that can cause severe diseases in plants and economic losses due to a decrease in crop production. Insect vectors, like all other organisms, are colonized by a community of various microorganisms, which can influence their physiology, ecology, evolution, and also their competence as vectors. The important ecological meaning of bacteriophages in various ecosystems and their role in shaping microbial communities has emerged in the past decade. However, only a few phages have been described so far in insect microbiomes. The leafhopper *Euscelidius variegatus* is a laboratory vector of the phytoplasma-causing Flavescence dorée, a severe grapevine disease that threatens viticulture in Europe. Here, the presence of a temperate bacteriophage in *E. variegatus* (named *Euscelidius variegatus* phage 1, EVP-1) was revealed through both insect transcriptome analyses and electron microscopic observations. The bacterial host was isolated in axenic culture and identified as the bacterial endosymbiont of *E. variegatus* (BEV), recently assigned to the genus '*Candidatus* Symbiopectobacterium'. BEV harbors multiple prophages that become active in culture, suggesting that different environments can trigger different mechanisms, finely regulating the interactions among phages. Understanding the complex relationships within insect vector microbiomes may help revealing possible microbe influences on pathogen transmission, and it is a crucial step toward innovative sustainable strategies for disease management in agriculture.

3.2 Introduction

Like all other organisms, insects harbor a rich, dynamic, and interactive community of microorganisms, collectively known as the microbiome, which comprises not only living members (microbiota), but also elements considered as not living organisms (viruses, plasmids, prions, viroids, and free DNA) and a whole spectrum of molecules produced by the microorganisms (Berg et al., 2020). Both microbiome composition and its modification influence insect ecology, physiology, evolution, and behavior through genetic and metabolic interactions. In many cases, survival of insects depends on their microbiome composition (Gurung et al.,2019). For these reasons, both pest control and insect protection may take advantage by deciphering the relationships between insects and their

microbiome as well as among microbiome components (Qadri et al., 2020). In the past decade, many studies have been devoted to characterizing the microbiome of insects, essentially through next-generation sequencing approaches. Even though bacteria, fungi, protozoa, and viruses may be associated with their insect host permanently or transiently, the vast majority of these works have focused on bacterial communities (Gurung etal., 2019; Ishii et al., 2013). However, more recently, the study of insect virome (inclusive of viruses that infect eukaryotic cells, bacteriophages that infect bacteria, viruses that infect archaea, and virus-derived genetic elements within host chromosomes) is gaining more attention (Leigh et al., 2018; Ng et al., 2011; Ottati et al., 2020; Shi et al., 2016; Varghese & Rij, 2018; Zhang et al., 2018). Bacteriophages (phages) are the most abundant organisms in the biosphere (Clokieet al., 2011). Interest in studying phages has recently increased in medicine because of their ability to shape the composition and diversity of the human gut microbiome (Guerin et al., 2018; Sutton & Hill, 2019), in control of disbyotic disorders and their possible use as an alternative to antibiotics (phage therapy) (D'Accolti et al., 2021; Gurney et al., 2020), and in ecology because of the important role they play in different ecosystems (Czajkowski et al., 2019; Obeng et al., 2016). Nevertheless, only a minimal part of phage biodiversity has been described (Czajkowski et al., 2019; Hatfull & Hendrix, 2011). In the case of insect microbiomes, few phages have been identified, and their impact on insect biology is still poorly understood. The arthropod endosymbionts *Spiroplasma* spp., '*Candidatus* Hamiltonella defensa', and *Wolbachia* spp. are known to host bacteriophages (Cohen et al., 1987; Masui et al., 2001; Van Der Wilk et al., 1999). The best characterized insect-bacteria-phage association is the tripartite interaction among the pea aphid *Acyrthosiphon pisum*, the insect endosymbiont *Hamiltonella defensa*, and its bacteriophage named APSE-1 (Van Der Wilk et al., 1999). Aphids carrying APSE-1 are more resistant against parasitoid attacks compared to aphids without this phage, thanks to eukaryote-targeted toxins encoded by the phage genome (Degnan & Moran, 2008; Degnan et al., 2009). The symbiosis system comprising eukaryotic hosts, bacterium *Wolbachia*, and bacteriophages WO is widely spread through nearly half of the known arthropod species (Miao et al., 2020). WO has received heightened interest because of its ability to mediate horizontal transfer of Wolbachia bacterial genes [26] and its possible involvement in the cytoplasmic incompatibility in insect hosts induced by Wolbachia (LePage et al., 2017; Shropshire et al., 2018). Since their discovery and despite their ecological relevance, these cases remain the only characterized bacteriophage-endosymbiont interactions described in insects. Here, we report the identification of bacteriophages in the phytoplasma insect vector *Euscelidius variegatus* Kirschbaum. Phytoplasmas are plant pathogenic bacteria transmitted by insects that can cause severe loss in agriculture. The leafhopper *E. variegatus* (*Cicadellidae*: *Deltocephalinae*) is a multivoltine and polyphagous species, widespread in Europe and North America. E. variegatus is a natural vector of '*Candidatus* Phytoplasma asteris' (chrysanthemum yellows strain) and a laboratory vector of the Flavescence dorée phytoplasma [reviewed in (Health et al., 2016)], and it is used as a model system to study phytoplasma-vector interactions because of the difficulties in rearing the

monovoltine natural vector *Scaphoideus titanus*. Insecticide treatments are the main control strategy to contain disease spread by insect vectors (Tomkins et al., 2018). Recent findings proved that the microbiome can interfere with the vector ability to acquire and transmit pathogens directly or indirectly (Gonella et al., 2019; Ishii et al., 2013; Trivedi et al., 2016; Weiss & Aksoy, 2011). Gong et al. (Gong et al., 2020) showed that the artificial association of the insect vector *Nilaparvata lugens* with a *Wolbachia* bacterial strain from another leafhopper species makes the insect unable to transmit a severe viral disease of rice. This work demonstrates that manipulating insect microbiome is a viable strategy for changing insect traits and that a better knowledge of insect microbiome is the basis for new plant pest control strategies. In this work, the presence of a temperate bacteriophage in *E. variegatus* (named *Euscelidius variegatus* phage 1, EVP-1) was revealed through both insect transcriptome analyses and microscopic observations. The bacterial host was isolated in pure culture and identified as the bacterial endosymbiont of E. variegatus (BEV), which has been recently assigned to the genus '*Candidatus* Symbiopectobacterium' (Martinson et al., 2020). Actually, BEV harbors multiple prophages that become active in culture, suggesting that different environments can trigger different mechanisms that finely regulate the within-host interactions among phages. Moreover, our results demonstrate that identifying expressed phage sequences in transcriptomic data can be a new and valuable approach to detect and study bacteriophages.

3.3 Results

3.3.1 Bacteriophage-Like Particles in Euscelidius variegatus

During the electron microscope observation of a partial viral purification obtained from a *Euscelidius variegatus* Torino (EvaTO) population (Abba et al., 2017), aimed at revealing insect virus particles, bacteriophage-like particles were serendipitously observed. Those phages had head-and-tail morphology typical of the viral class *Caudoviricetes* and in particular of the former family *Siphoviridae*; they had a prolate (elongated) oval head 132 nm long (SE = 0.7 nm; n = 48) and 59 nm wide (SE = 0.3 nm; n = 48) and a flexuous thin non contractile tail 179 nm long (SE = 4.4 nm; n = 16) (Figure 3.1a). Frequently, heads and tails appeared detached (not shown).

3.3.2 Selection of Expressed Bacteriophages Sequences

In an effort to identify the siphovirus-like phage observed by TEM, RNA extracted from EvaTO adults was used to construct two cDNA libraries. The two datasets were then merged and depleted of reads matching to the insect transcriptome in order to generate a *de novo* metatranscriptome assembly of *E. variegatus* microbiome. A blastx analysis of the assembled sequences revealed the presence of 12 expressed sequences that were identified as hallmark bacteriophage structural genes, i.e., major capsid, minor capsid, baseplate, major tail, minor tail portal, tail fiber, tail sheath, collar and head-tail joining proteins. After a further annotation with the ViPTree server (Nishimura et al., 2017), 5 out of 12 sequences appeared to be polycistronic mRNAs (Table 3.1), i.e., they encoded at least

two putative proteins. The selected transcripts included three different complete major capsid/head proteins, suggesting that the selected expressed sequences belonged to at least three different phages thereafter referred to as EVP-1 (*Euscelidius variegatus* phage 1, associated with MW965291 ORF3), EVP-2 (associated with MW965292) and EVP-3 (associated with MW965289 ORF2).

3.3.3 Phylogenetic Analysis of the Identified Major Capsid Proteins

The deduced amino acid sequences of the three major capsid proteins were aligned to the first hit retrieved by blastx against the NCBI nr database and the first ten hits identified by blastp against the NCBI RefSeq protein limited to the taxon "Viruses (taxid:10239)". We considered for the analysis only complete major capsid proteins from phages assigned to one of the *Caudoviricetes* families recognized by the International Committee on Taxonomy of Viruses (ICTV). The phylogenetic analysis (Figure 3.2) showed that EVP-1 was part of a completely separate cluster from the one that included the other two identified major capsid proteins. Such a cluster was formed only by major capsid proteins from members of the former family *Siphoviridae*. The other cluster was far more heterogeneous, including members of both the former families *Siphoviridae* and *Myoviridae*. EVP-2 and a protein identified in *Serratia marcescens* (best blastx hit) formed a separate branch that diverged from a clade including both siphoviruses and myoviruses. Finally, EVP-3 formed a strongly supported clade (100% bootstrap value) with major capsid proteins from '*Candidatus* Symbiopectobacterium sp.' Dall1.0 and from a member of the former family *Myoviridae*.

3.3.4 Detection and Prevalence of the Three Phages

Specific primers designed on the three genes (Table 3.2), coding for the identified major capsid proteins, were used on DNA extracted from insect whole bodies and a partial viral purification. All the three primer pairs produced amplicons of the expected size and sequence from 20 individuals randomly selected from the EvaTO population (data not shown). By contrast, only primers designed on EVP-1 major capsid protein gave an amplification product from the DNA extracted from viral particles (Figure 3.1b). Therefore, we could reasonably associate the phage observed by TEM to EVP-1.

3.3.5 Isolation of EVP-1 Bacterial Host

In an attempt to identify the EVP-1 bacterial host, EvaTO hemolymph was cultivated on chocolate agar and purple agar plates, yielding several colonies (Figure 5.S1). Few colonies appeared after one/three days of incubation and showed a fast growth. After 7-10 days, many other whitish small colonies (almost forming a layer) appeared; they looked all similar and grew slowly (Figure 3.S1a,b). The fast growing (1C-3C, 5C-7C, 1P, 2P) and some of the slow growing (4C, 8-15C, 3-5P) colonies were isolated and sub-cultivated on both chocolate and purple agar, irrespective of their original selection medium. Ten out of the 20 isolated colonies were positive to the PCR amplification with EVP-1 primers (Figure 5.S1b). All the fast-growing colonies were negative; almost all the slow growing colonies (except 10C and 11C) were positive and they were considered as EVP-1 bacterial host. The growth of EVP-1

positive colonies on chocolate and purple agar was scanty, with low viability. Attempts at subculturing these colonies on Tryptic soy agar (TSA) resulted in faster growth, with similar viability (about two weeks). Three colonies were selected and maintained on TSA for further investigations: 4C, 12C and 14C. At each subculture step, the presence of EVP-1 was checked by PCR with EvaTOphage1 primers (not shown). The 16S ribosomal sequences of the three colonies were 100% identical to each other and 99% identical (95% query coverage) to the one isolated from the "Bacterial parasite of *Euscelidius variegatus*" [BEV, Genbank accession number: Z14096 (Campbell & Purcell, 1993)] (Figure 3.S2), which has been recently named Candidatus *Symbiopectobacterium* (Martinson et al., 2020). Based on this result, primers BEV3/BEV4 (Galetto et al., 2009), specifically designed on the BEV 16S ribosomal sequence, were used hereinafter. In particular, they were used to exclude the presence of bacterial host DNA after DNA extractions from viral particles (Figure 3.1b). Previous literature has reported that BEV can colonize multiple insect host organs, including the midgut (Cheung & Purcell, 1993; Purcell, Steiner, Mégraud, & Bové, 1986), PCR and RT-PCR experiments on *E. variegatus* dissected guts not only confirmed the presence of EVP-1 but also revealed that the phage was transcriptionally active in this tissue (Figure 3.3a). In addition, TEM observations of negatively stained crude extract from guts demonstrated the presence of siphovirus-like particles similar to those observed in the viral purification of the whole insect (Figure 3.3b).

3.3.6 Multiple Phages in EVP-1 Host

According to a preliminary survey of BEV genome size and content (Degnan et al., 2011), there was evidence for an extrachromosomal element that could represent a prophage and 65 partial coding sequences that could be ascribed to phages. A blastn analysis against all the BEV sequences submitted to the GenBank Trace Archive revealed that 11 out of 12 putative phage transcripts identified in this work found a hit with percentages of identity > 88% but with low percentage of query coverage (average coverage < 41%) (Table 3.S1). Such result could be explained by the fact that some deposited sequences are shorter than the identified transcripts and all of them contain ambiguous nucleotides (Ns), which in the case of gn1 | ti | 2292005461 represented more than 50% of its length. Nevertheless, those results suggested that most of the identified sequences could be assigned to phages that have BEV as their bacterial host. A colony PCR confirmed that EVP-2 and EVP-3 were also likely to be associated with BEV (Figure 3.4e). Electron microscopy observation of negative-stained bacteria from TSA cultured revealed rods from 2.1 to 5.3 µm long (with a mean value of 3.1 µm, n=60), from 0.60 to 0.79 wide (with a mean value of 0.68 µm, n = 60), without flagella and sometimes curved (Figure 3.4a). In the proximity of bacterial cells, some bacteriophage particles were noted; some were siphovirus-like and similar to those observed in the insect extract (Figure 3.4c). Moreover, and unexpectedly, myovirus-like (Figure 3.4b) and podovirus-like (Figure 3.4d) particles were also present. In particular, the number of podovirus-like particles were approximately 100-times higher than the number of siphovirus- and myovirus-like ones (Figure 3.5). The bacterial colony was subjected to an

enrichment of viral particles and a DNase treatment prior to DNA extraction to ensure the purification of encapsidated DNA only. Given the different phage morphologies observed by TEM, the three phage primer pairs were used in PCR. Amplicons of the expected size were obtained with specific primers for EVP-1 and EVP-3, whereas a faint band was observed with EVP-2 primers (Figure 3.4e). BEV primers failed to amplify bacterial DNA, so we could exclude the presence of contaminating phage DNA integrated into the host chromosome. PCR results confirmed that the siphovirus-like phage observed by TEM was EVP-1 and suggested that the myovirus-like particles could be associated with EVP-3.

3.4 Discussion

Phage "omics" studies are represented mostly by metagenomic shotgun analysis applied to a wide range of environments and locations, from uncultured marine samples (Breitbart et al., 2002; Paez-Espino et al., 2016; Roux et al., 2016) to human gut microbiome (Dutilh et al., 2014; Guerin et al., 2018; Manrique et al., 2016; Paez-Espino et al., 2016; Yutin et al., 2018). Differential filtrations and density-dependent gradient centrifugations are the usual enrichment steps taken to concentrate viral DNA and limit bacterial constituents and other contaminants before sequencing.
While metagenomics is the most rapid and efficient approach used to describe the overwhelming diversity of phages, transcriptomics has been generally used to investigate the transcriptional response of bacteria isolated in pure cultures upon phage infection (Mojardín & Salas, 2016; Sacher et al., 2018; Zhao et al., 2016). Only a few untargeted metatranscriptomic studies, which explored, which explored mainly soil microbial communities, reported the discovery of novel RNA phages (Krishnamurthy et al., 2016; Starr et al.,, 2019) and phage-related mRNA sequences (Jacquiod et al., 2018; Neri et al., 2022; Sieradzki et al., 2019).

Metatranscriptomics has here been integrated wih classical microbiological and microscopy techniques to identify a DNA tailed-phage and its bacterial host within the microbiome of a phytoplasma insect vector. To this end, we re-analyzed two RNA-seq libraries that were originally constructed without any prior phage enrichment step to explore *E. variegatus* transcriptome (Galetto et al., 2018). *De novo* identification of phage sequences can be an extremely challenging task, especially from a background of genes expressed by the insect host and all the active microorganisms that constitute its microbiome. Nevertheless, the stringent selection of phage-hallmark genes resulted in a reliable identification of the observed phage. Such a bioinformatic approach was clearly a non-exhaustive way to retrieve all the expressed phage sequences in the libraries. Some were probably overlooked due to the lack of similarity with known phage sequences (the so-called "dark matter") and/or the wrongful identification as bacterial genes in public databases. The absence of a biomarker gene among DNA phages and the polyphyletic origin of most viral lineages poses a hindrance for identifying all the putative phages. In any

case, the characterization of the whole *E. variegatus* phageome was beyond the scope of this work, and the chosen approach proved effective in the detection of the transcribed phage genes associated with the observed phage particles. Although RNA-seq data provided information about the active fraction of phages within the insect microbiome, they were not sufficient to apply the new computational approaches developed to predict phage-host relationships (Boeckaerts et al., 2021; Edwards et al., 2016). Therefore, classical microbiological techniques were applied for the unambiguous phage-host identification. All the bacterial hosts of the phages identified by the BLAST analyses belonged to the order *Endobacterales*, so it was reasonable to hypothesize that bacteria of the same order could be part of the *E. variegatus* microbiome and hosted the identified phages. Only two cultivable bacterial endosymbionts, BEV [*Endobacterales* (Purcell et al., 1986)] and *Asaia* sp. [*Rhodospirillales* (Gonella et al., 2019; Gonella et al., 2018)], are known to be facultatively associated with *E. variegatus*. Because comprehensive studies of the bacterial fraction of its microbiome had never been undertaken, we did not have any a priori knowledge about either the possibility of isolation in axenic culture of the other endosymbionts or the most suitable media for their cultivation. The chosen growth media, usually adopted to identify enteric bacteria or to isolate fastidious bacteria, were effective in isolating the EVP-1 host. Interestingly, the EVP-1 host was shown to be the already known *E. variegatus* endosymbiont BEV, i.e., '*Candidatus* Symbiopectobacterium'. Moreover, colony-PCR proved that BEV was also the host of the other two identified major capsid protein-coding genes. Interestingly, the best blastx hits of the EVP-3 major capsid protein was the one identified in '*Candidatus* Symbiopectobacterium sp.' Dall1.0 during a metagenomic study of *Diachasma alloeum*, a parasitoid of the apple maggot *Rhagoletis pomonella* (Tvedte et al., 2019). Such result further supported the proposal made by Martinson et al. (Gonella et al., 2019) that the genus '*Candidatus* Symbiopectobacterium' represents a monophyletic group of invertebrate host-associated microbes. With the huge production of whole genome sequencing data, it is known that most bacterial genomes carry multiple prophages, a phenomenon called polylysogeny (Argov et al., 2019): however, inferred prophage sequences do not always correspond to active temperate phages (Williamson et al., 2008). The association of multiple active phages to BEV was confirmed by electron microscope observation and PCR reactions on the bacterial colonies. The intense phage lytic activity observed in vitro may explain the low viability of the bacterium in culture. It is likely that, after a few days in pure culture, most bacterial cells undergo phage lysis as it is shown by the the massive production of podovirus-like particles. By contrast, neither viral particles nor transcripts that could be associated with podoviruses were identified in the insect microbiome. This may indicate that these are in the prophage status in the insect environment, while they switch to the lytic phase in plate culture condition. A transcript coding for a myovirus-like major capsid protein was retrieved during the RNA-seq analysis, even if myovirus-like particles were not observed in the viral partial purification obtained from the whole insect. Hence, we can suppose either that the phage is present at very low concentration in the insect body (below the detection limit) or that

the particles were, for some reason, destroyed during the purification process. Nevertheless, on the one hand. Some regulation mechanisms should operate in the insect to prevent the podovirus-like phage from producing the same massive release of viral particles observed in pure culture, which could potentially cause the lysis of the whole bacterial population. On the other hand, the growth of the BEV population within the insect could be kept under control by the action of EVP-1 and, maybe, EVP-3. It is known that temperate phages have an important role in shaping microbial diversity and community structure; in fact, not only do they alter the biology of their hosts (i.e., regulating gene expression, introducing novel functions), but they also influence the surrounding hosts and non-host bacterial cells (i.e., entering the lytic cycle and killing susceptible bacteria, liberating intracellular contents used as nutrients by neighboring cells)(Burns et al., 2015; Howard-Varona et al., 2017). Moreover, bacteriophages-bacteria interactions are considered by Refardt (Refardt, 2011) as an ideal system for studying the competitive interactions within hosts. In particular, he considered the competition among phages in the same host, which is still an unexplored area in phage ecological research, and showed that multiple infection in *Escherichia coli* often resulted in a decreased lytic productivity. At present, we do not know whether BEV active phages can influence the lysogenic status of the other prophages or whether they can infect other insect bacterial endosymbionts. These two phenomena deserve to be elucidated in view of using this system as a model both for among-hosts competition studies and for developing microbiome-based and in particular phage-based new plant pest control strategies. In fact, unravelling the microbiome of insect vectors and understanding the complex relationships within its components may help to reveal possible microbe influences on pathogen transmission, and it is a crucial step toward an innovative sustainable strategy for disease management in agriculture.

3.5 Materials and Methods

3.5.1 Insect Population

Euscelidius variegatus of the Torino (Italy) phytoplasma-free laboratory colonies (EvaTO) were originally collected in Piedmont (Italy) and reared on oat, *Avena sativa* (L.), inside plastic and nylon cages in growth chambers at 20–25 °C with a L16:D8 photoperiod.

3.5.2 DNA and RNA Extraction

DNA and total RNA were extracted from either whole bodies or dissected organs of emerged EvaTO adults, as described by Marzachì et al. (1998) and Ottati et al. (2020), respectively. In order to distinguish the encapsidated phage DNA (lytic infection) from the phage DNA integrated into the host chromosome (lysogenic infection), we proceeded as follows. Bacterial colonies were resuspended in sterile water and filter-sterilized with a 0.22 µm filter. Such step should eliminate bacterial hosts and enrich the aqueous phase with phage particles. The suspension was then treated with TURBO™ DNase (Thermo Fisher

Scientific, Waltham, MA, USA) for 1 h at 37 °C to digest any residual free DNA and subjected to DNA extraction with one volume of phenol:chloroform:isoamyl alcohol (25:24:1 v/v) followed by a wash step with one volume of chloroform:isoamyl alcohol (24:1 v/v) to remove any trace of phenol. Finally, DNA was precipitated with sodium acetate/ethanol, washed with 70% ethanol, and resuspended in 10 mM Tris-HCl pH 8.2. The same DNase treatment and DNA extraction protocol were also used on semipurified viral particles.

3.5.3 RNA-Seq and Bioinformatic Analysis

Six micrograms of total RNA were sent to Macrogen (South Korea) for cDNA library construction and sequencing, as detailed in (Abba et al., 2017). At least 100 million 100-nt paired-end reads were obtained for each dataset. The two datasets were merged and the pre-assembly steps were performed using BBTools suite v38.70, as previously described (S Ottati et al., 2020). BBMap, in particular, was used to remove reads mapping to the *Euscelidius variegatus* transcriptome shotgun assembly (TSA Accession number: GFTU00000000.1) before the assembling steps with Trinity v2.9.1 (Grabherr et al., 2011). The resulting sequences were further assembled by CAP3 v3 (overlap length cutoff = 60; overlap percent identity cutoff n = 90) (X. Q. Huang & Madan, 1999). As a result, around 120,000 assembled sequences were obtained and queried against the NCBI non redundant "nr" protein database (Last access February 2021) with DIAMOND v0.9.24.125 (Buchfink, Xie, & Huson, 2015) using an E-value cut-off of 0,0001. Bowtie2 (Langmead & Salzberg, 2012)was used to map reads against the putative phage transcripts with default parameters. Reads mapping onto the selected transcripts were expressed as RPK (Reads Per Kilobase of transcript). VipTree (Nishimura et al., 2017) was used to automatically generate the annotation of the selected transcripts. Given that the tool used the RefSeq release 93, the predicted coding sequences and the corresponding deduced proteins were analyzed using NCBI RefSeq Release 205 (February 2021).

3.5.4 Accession Numbers

Reads were deposited into the NCBI's Sequence Read Archive (SRA) database with BioSample accessions SAMN18744878 and SAMN18744879 as part of BioProject PRJNA393620. The partial 16S ribosomal RNA sequence of Candidatus Symbiopectobacterium strain EvaTO and the 12 phage transcripts were submitted to NCBI GenBank with accessions MW936016 (16S rRNA) and MW965281 MW965292 (phage sequences).

3.5.5 Phylogenetic Analysis

Phylogenetic relationships were inferred on the basis of the amino acid sequences of phage major capsid proteins. The three newly identified major capsid proteins were aligned with MUSCLE (Edgar, 2004) to their best blastx hits and the first ten hits identified by blastp analysis against the NCBI RefSeq protein limited to the taxon "Viruses (Taxid:10239)". Phylogenetic trees were then generated using the maximum likelihood (ML) approach, implemented in IQ-TREE (Trifinopoulos et al., 2016) with default parameters through the

CIPRES Science Gateway V. 3.3 (Miller, Pfeiffer, & Schwartz, 2012). Bootstrap analyses involving 1000 replicates were used with the Dayhoff substitution matrix to estimate the pairwise distances.

3.5.6 PCR and RT-PCR Amplifications

PCR was used to verify the presence of the three genes, encoding the major capsid proteins in EvaTO insects, phage DNA, and bacterial colonies. Universal 16S rRNA bacterial primers were first used, and then BEV3/ BEV4 primers were used to identify the bacterial host harboring EVP-1 phage by colony PCR. BEV primers were also used to exclude the presence of residual bacterial host DNA integrated into the bacterial chromosome. For each sample, cDNA was synthesized from total RNA (500 ng) with EvaTO_phage1r primer using the RevertAid Reverse Transcriptase (Thermo Fisher Scientific, Waltham, MA, USA). The absence of contaminating genomic DNA was verified including, in the PCR step, sample without the reverse transcription step. All primer sequences and amplification conditions used in this work are listed in Table 3.2 The resulting amplicons were validated by Sanger sequencing at BMR Genomics (Padua, Italy).

3.5.7 Bacterial Isolation

CO_2-anesthetized leafhoppers were surface-sterilized by submerging them first in 95% ethanol for 1 to 2 min, then in 1.2 to 1.5% sodium hypochlorite solutions for 2 min and eventually, rinsing them 2 or 3 times in sterile water (Purcell et al., 1986). Under a dissecting microscope the hemolymph was aspirated with a fine, flame-drawn needle inserted into the insect body, between the thorax and the abdomen. The fluid was transferred to a tube containing 1X PBS. The hemolymph of five individuals was combined, then split in two and plated onto chocolate (Blood Agar Base—Sigma Aldrich—added with 7% horse defibrinated blood) and purple agar (Bromocresol Purple Broth—Sigma Aldrich—added with 1.5% agar) solid medium. The hemolymph of a total of 40 individuals was obtained. Plates were kept at 26°C in the dark for up to 14 days. Colonies were numbered (using C when isolated from chocolate agar and P when isolated from purple agar plates) and transferred onto new chocolate and purple plates. For subcultures and maintenance, a Tryptic Soy Agar (TSA) medium (Sigma Aldrich) was eventually used.

3.5.8 Transmission Electron Microscopy

Viral particles were partially purified following the protocol previously described by (Abba et al., 2017). Insect guts were collected under a dissecting microscope and crushed in 0.1 M phosphate buffer pH 7, added with 2% PVP, to obtain a crude extract. A portion of the bacterial colonies was collected with a toothpick from cultures on solid medium plates and suspended in 20 µL of liquid growth medium. A drop of the viral partial purification, the gut crude extract, or the bacterial suspension was deposited on carbon and formvar coated copper-palladium grids and left to stand for about 3 min. Grids were washed with water and negatively stained with 0.5% aqueous uranyl acetate. Observations and image acquisition were done using a CM 10 electron microscope (Philips, Eindhoven, The

Netherlands) operating at 80kV. Micrograph films were developed and then digitally acquired at high resolution with a D800 Nikon camera. Images were trimmed and adjusted for brightness and contrast using GIMP 2 software. Particle measurements were done using Fiji software.

3.6 Author contributions

Conceptualization, S.A., M.V., M.R.; methodology, S.A., M.V., M.R., S.O., G.M., L.G.; data curation, S.A.; writing—original draft preparation, S.A., M.V., M.R.; writing—review and editing, S.A., M.V., M.R., L.G., C.M., S.O., G.M.; visualization, S.A., M.V.; funding acquisition, C.M., M.V. All authors have read and agreed to the published version of the manuscript.

3.7 Figures and Tables

Figure 3.1. (**a**) TEM micrograph of siphovirus-like particles observed in negatively stained partial viral purification from *Euscelidius variegatus* Torino population; bar = 100 nm. (**b**) PCR on the DNA extracted from viral particles (Lanes 1-4) and *E. variegatus* whole insect (Lanes 6-9). Lanes 1,6: PCR with BEV 3/4 primers; Lanes 2,7: PCR with EvaTO_phage1 primers; Lanes 3,8: PCR with EvaTO_phage2 primers; Lanes 4,9: PCR with EvaTO_phage3 primers. Lane 5: 1 Kb Plus DNA Ladder

(Invitrogen).

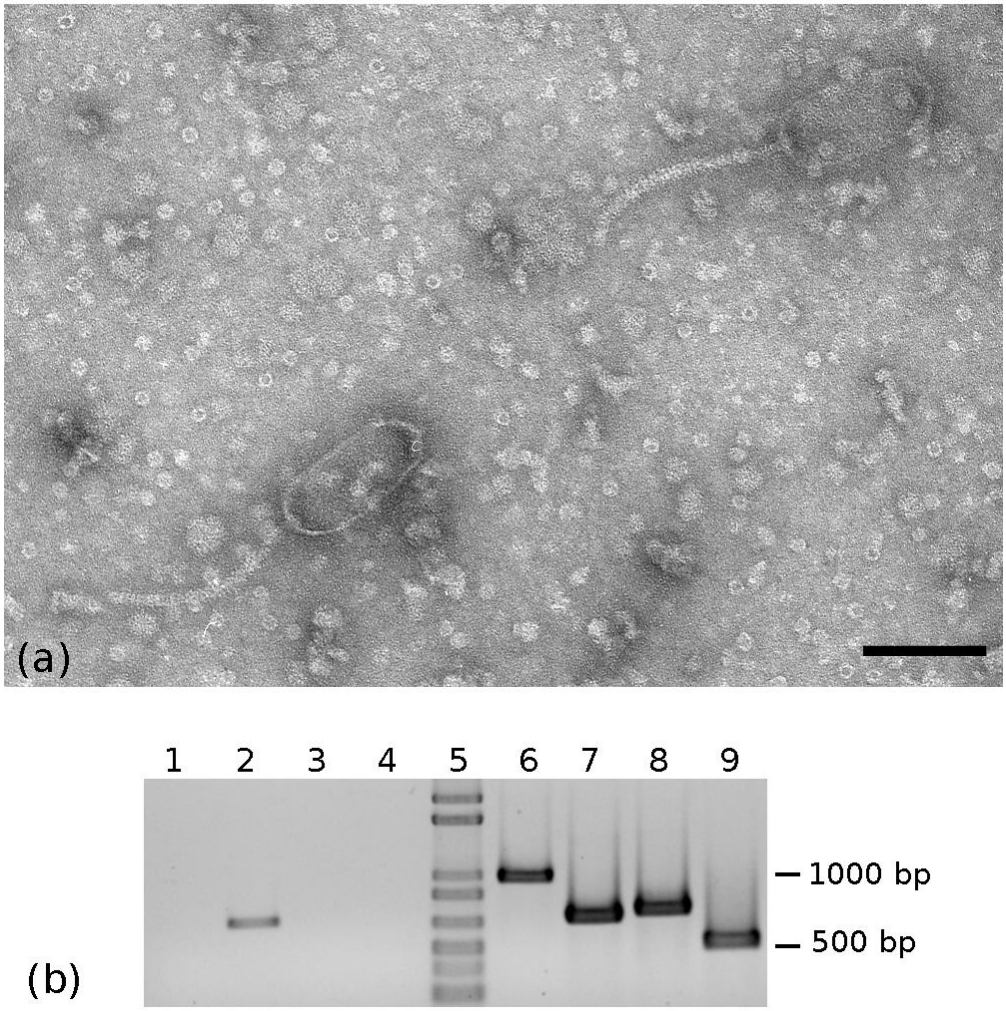

Figure 3.2. Phylogenetic analysis of the deduced amino acid sequences of the three identified major capsid proteins. Major capsid proteins were aligned by MUSCLE and the phylogeny was inferred by the maximum-likelihood method using the CIPRES Science Gateway V. 3.3. Bootstrap analyses with 1000 iterations were used with the Dayhoff substitution matrix to estimate pairwise distances. Only bootstrap values higher than 70 are shown. The three identified major capsid proteins are in bold. As regards MW965289 and MW965291, which are both polycistronic transcripts, only the deduced amino acid sequences corresponding to the major capsid proteins were included in the alignment, i.e., ORF2 and ORF3, respectively. The scale bar indicates the evolutionary distance for 0.3 amino acid substitutions per site. The collapsed branch grouped nine sequences: BCI49740.1, Stx2a-converting phage Stx2 EH2201; BCI49860.1, Stx1a-converting phage Stx1 EH199; QIW91675.1,

Escherichia phage Lys8385Vzw; YP_001449293.1, Enterobacteria phage BP-4795; YP_009909243.1 Enterobacteria phage 2851; YP_002274188.1, Enterobacteria phage YYZ-2008; BAT31949.1, Stx2-converting phage Stx2a F349; YP_009909397.1, Stx2-converting phage Stx2a WGPS6; and YP_009909320.1, Stx2-converting phage Stx2a WGPS8. GenBank accession numbers of the other major capsid proteins are: WP_135684645.1, *Klebsiella pneumoniae*; YP_002284337.1, Pseudomonas phage PAJU2; WP_164114194.1, *Serratia marcescens*; YP_009324719.1, Salmonella phage 118970 sal3; NP_700379.1, Salmonella phage ST64B; YP_008766869.1, Shigella phage SfIV; YP_009147453.1, Enterobacteria phage SfI; YP_008318484.1, Shigella phage SfII; NP_543092.1, Enterobacteria phage phiP27; YP_355412.1, Burkholderia phage Bcep176; YP_001686874.1, Azospirillum phage Cd; YP_009304034.1, Brucella phage BiPBO1; YP_009010476.1, Geobacillus phage GBK2; NP_599037.1, Enterobacteria phage SfV; YP_003090181.1, Burkholderia phage KS9; YP_764476.1, Geobacillus phage GBSV1; MBG6243159.1, *Candidatus* Symbiopectobacterium sp. Dall1.0.

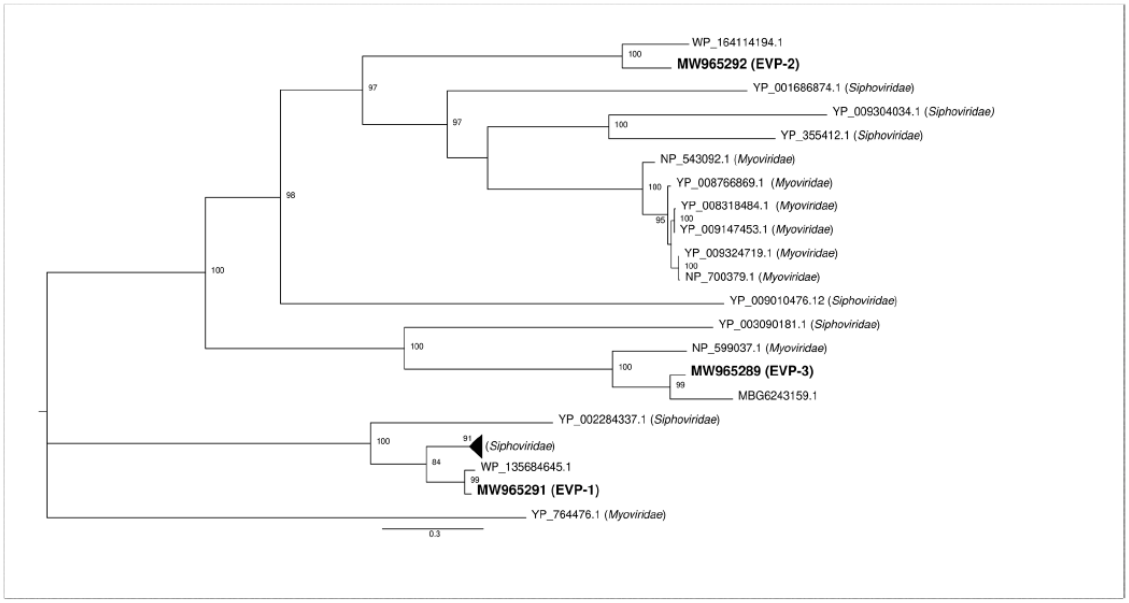

Figure 3.3. (**a**) PCR and RT-PCR experiments on *E. variegatus* dissected guts with EvaTO_phage1 primers. Lanes 1–3: RT-PCR on RNA extracted from three pools (five samples each) of *E. variegatus* guts. Lanes 6–8: PCR on the same RNA sample as in lanes 1–3 without the retrotranscription step. Lane 4: PCR on DNA extracted from a pool of five *E. variegatus* guts. Lane 5: negative control (no DNA) (**b**) TEM micrograph of siphovirus-like particles observed in negatively stained crude extract from dissected gut of *E. variegatus* Torino; bar = 100 nm.

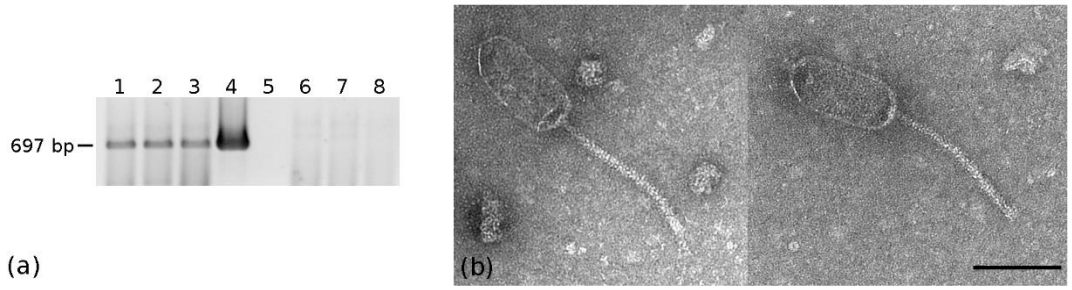

Figure 3.4. TEM micrographs of the negatively stained 4C colony showing bacterial cells (**a**), myovirus-like particles (**b**), siphovirus-like particle (**c**), and podovirus-like particles (**d**). Scale bars correspond to 1 µm (**a**) or 100 nm (b–d). (**e**) PCR on DNA extracted after the enrichment of viral particles from bacterial colony 4C (Lanes 1,4) and PCR on the bacterial colony 4C (Lanes 6–9). Lanes 1,6: PCR with BEV3/BEV4 primers; Lanes 2,7: PCR with EvaTO_phage1 primers; Lanes 3,8: PCR with EvaTO_phage2 primers; Lanes 4,9: PCR with EvaTO_phage3 primers. Lane 5: 1 Kb Plus DNA Ladder (Invitrogen).

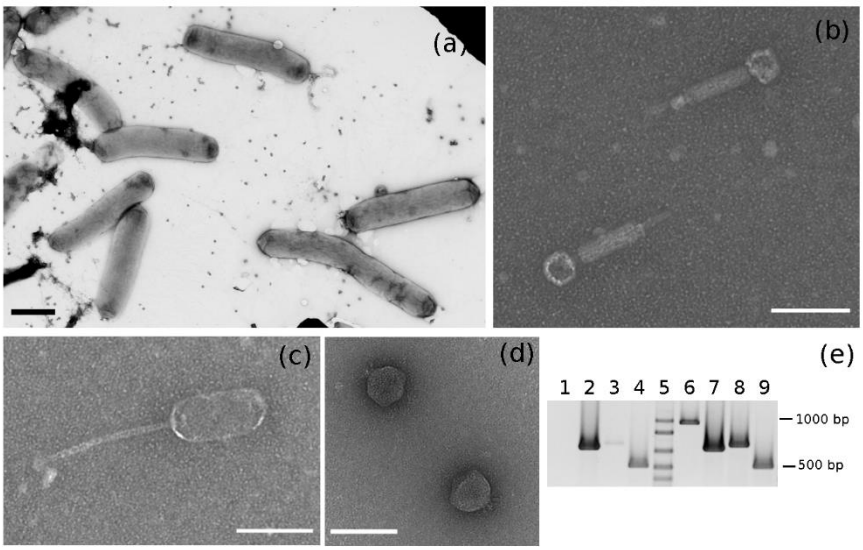

Figure 3.5. TEM micrographs of a negatively stained portion of the 4C colony showing bacterial cells (**a**,**b**, **$**), podovirus-like particles (**a**,**b**, asterisks), a siphovirus-like particle without tail (**a**, #), a myovirus-like particle with contracted tail (**b**, @). Bars represent 200 nm.

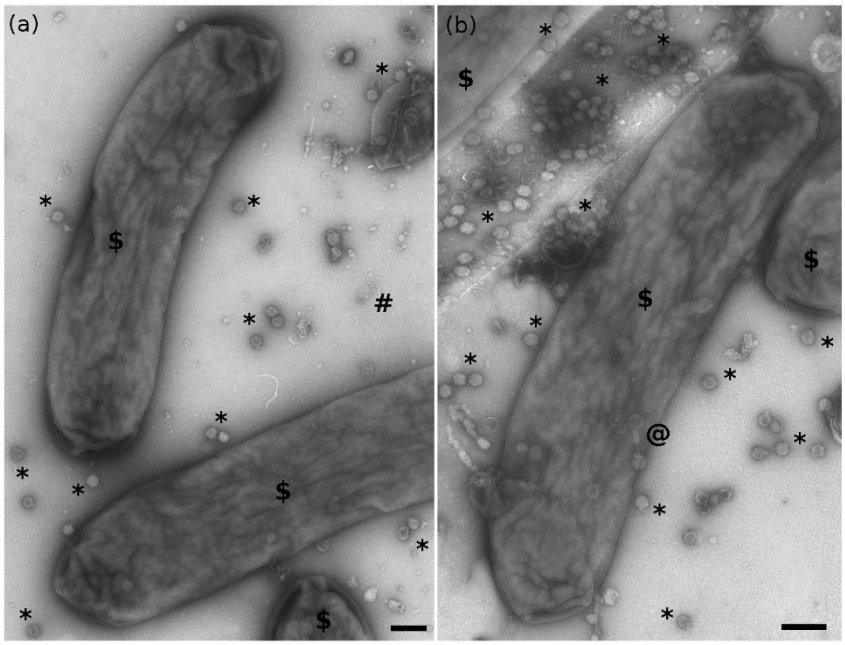
(a)
(b)

Table 3.1: ViPTree Gene ORF Prediction and Blastx Analysis of the 12 Selected Phage Sequences.

Table 1. ViPTree Gene ORF Prediction and Blastx Analysis of the 12 Selected Phage Sequences.

Transcripts IDs and Predicted ORFs	Length (bp)	Range	RPK	Hit Description [Organism]	% Identities	E-Value	% Query Coverage
MW965290	5544		111.7				
ORF1	398	1–398		WP_195316289.1 phage tail tape measure protein [*Serratia marcescens*]	70	2×10^{-51}	97
ORF2 #	357	398–754		WP_039351538.1 phage tail protein [*Pectobacterium fontis*]	90	1×10^{-75}	97
ORF3 #	753	804–1556		MBG6243408.1 phage minor tail protein L [*Candidatus* Symbiopectobacterium sp. Dall1.0]	96	0.0	100
ORF4 #	576	1713–2288		MBG6243407.1 peptidase P60 [*Candidatus* Symbiopectobacterium sp. Dall1.0]	95	8×10^{-165}	94
ORF5 #	606	2272–2877		WP_104212022.1 tail assembly protein [*Pectobacterium brasiliense*]	81	2×10^{-85}	100
ORF6	2611	2934–5544		WP_104212026.1 phage tail protein [*Pectobacterium brasiliense*]	91	2×10^{-70}	100
MW965281	2188		112				
ORF1	318	255–572		WP_021179416 fimbrial protein TcfA [*Serratia fonticola*]	62	4×10^{-29}	90
ORF2 #	252	557–808		WP_146751463.1 ANR family transcriptional regulator [*Enterobacter cloacae* complex]	56	5×10^{-7}	60
ORF3 #	1089	859–1947		WP_187497555.1 phage tail protein [*Pantoea* Psp39-30]	43	2×10^{-82}	98
MW965289	1777		128.3				
ORF1	99	1–99		EFC4054519.1 HK97 family phage prohead protease [*Escherichia coli*]	81	2×10^{-9}	100
ORF2 #	1227	109–1335		MBG6243159.1 phage major capsid protein [*Candidatus* Symbiopectobacterium sp. Dall1.0]	85	0.0	99
ORF3 #	300	1426–1725		WP_044208854.1Phage gp6-like head-tail connector family protein [*Pectobacterium odoriferum*]	87	3×10^{-57}	100
MW965291	6115		213.4				
ORF1	580	1–580		WP_108703399 Terminase small subunit [*Enterobacter hormaechei*]	96	2×10^{-86}	96
ORF2 #	1659	583–2241		WP_108703400 terminase large subunit [*Citrobacter europaeus*]	98	0.0	100
ORF3 #	1935	2324–4258		WP_135684645.1 phage major capsid protein [*Klebsiella pneumoniae*]	95	0.0	99
ORF4 #	168	4297–4464		WP_181941880.1 hypothetical protein [*Klebsiella pneumoniae*]	89	8×10^{-28}	100
ORF5 #	1359	4464–5822		NIC64170.1 phage portal protein [*Klebsiella pneumoniae*]	94	0.0	100
ORF6	297	5819–6115		RTO54147.1 phage gp6-like head-tail connector protein, partial [*Enterobacter hormaechei*]	80	8×10^{-47}	100
MW965287	1419		71.2				
ORF1	482	1–482		MBD2797976.1 HK97 family phage prohead protease [*Xenorhabdus* sp. 18]	72	6×10^{-74}	96
ORF2	953	467–1419		QBY47020.1 phage portal protein [*Arsenophonus nasoniae*]	92	0.0	100
MW965282	770		61.0	WP_187497555.1 putative phage tail protein [*Plautia stali* symbiont]	99	1×10^{-158}	84
MW965283	3268		114.1	WP_113869621.1 phage tail tape measure protein [*Brenneria salicis*]	82	0.0	82
MW965286 *	251		47.8	SPW64604.1 putative head-tail adaptor [*Escherichia coli*]	98	1×10^{-20}	73
MW965288	768		50.8	MBJ9599707.1 phage portal protein [*Citrobacter werkmanii*]	99	4×10^{-179}	94
MW965292 #	1852		123.1	WP_164114194.1 phage major capsid protein [*Serratia marcescens*]	63	0.0	77
MW965285	299		23.4	WP_010281992.1 portal protein [*Pectobacterium brasiliense*]	95	8×10^{-55}	92
MW965284 *	345		46.4	SUH06759.1 portal protein [*Salmonella enterica* subsp. enterica]	87	1×10^{-27}	66

RPK: read counts divided by the length of each transcript in kilobases. * putative pseudogene (presence of frameshifts). # Complete CDS. Grey shaded cells represent different transcript IDs.

Table 3.2: List of primers used in this work

Primer Name	Sequence	Target	Product Size (bp)	Annealing T (°C)	Citation
EvaTO_phage1f	CCGGTGGGTTCACTTTCC	MW965291	697	64	This work
EvaTO_phage1r	CGTCCGCAGACCATTATCGG				
EvaTO_phage2f	CTTCTCTGGCTGGCCTACCC	MW965292	725	64	This work
EvaTO_phage2r	GAGTATCGCCGGTCATCACG				
EvaTO_phage3f	AGGGTACTAGCCAGGACGAC	MW965289	524	64	This work
EvaTO_phage3r	TGTGCCGCCATTTCGATAAG				
BEV3	TTATGAGGTCCGCTTGCTCT	BEV 16S ribosomal DNA sequence	1009	64	Galetto et al. 2009
BEV4	CGATCCCTAGCTGGTCTGAG				
27F	AGAGTTTGATCMTGGCTCAG	16S ribosomal DNA sequence	1507	58	Lane 1991
1494R	CTACGGCTACCTTGTTACGA				

Supplementary material

The following are available online at https://www.mdpi.com/article/10.3390/pathogens10050612/s1, Figure S1: (a) Examples of chocolate agar plates with colonies grown after plating hemolymph extracted from *Euscelidius variegatus* Torino population. (b) List and characteristics of all the isolated colonies from chocolate (C) and purple (P) agar plates; positivity to EVP-1 was determined by PCR with EVP-1 primers. Figure S2: Alignment of the 16S ribosomal sequence of the three colonies with the one from the "Bacterial parasite of *Euscelidius variegatus*" (BEV) GenBank accession number: Z14096; (Campbell and Purcell, 1993). Table S1: Blastn analysis of the 12 selected phage sequences against the BEV sequences submitted to the GenBank Trace Archive.

4 CONCLUSIONS

In this work we have achieved the isolation, morphological and molecular characterization of a set of phages active against Psa and Pph pathogens. We have begun then researching for a method of utilizing these phages as biocontrol agent in a greenhouse or field context.

To increase the availability of active phages genomes and lysins sequences against *Pseudomonas syringae* pathogens it would be advisable to conduct in future metagenomic analysis of other phylloviruses on bean and kiwifruit surfaces as it was performed on wheat (Forero-Junco et al., 2022), to increase the possibility to detect phages that are not easily retrieved with the classical microbiology phage isolation methods, as phages with RNA based genomes.

Another field worth of future investigation would be the use of phages in parallel with other new plant defence approaches as nanoparticles and phytoextracts. Three different kind of copper-based nanoparticles ($Cu_4(OH)_6Cl_2$ nanoparticles, $Cu(OH)_2$ nanowires and $Cu_3(PO_4)$ nanosheets) were successfully tested against Psa, showing a minimum bactericidal concentrations about one hundredth times lower than the classical commercial agent thiodiazole copper (Ren et al., 2022). Maybe it will be possible a synergistic use of these copper forms and phages, remaining compliant with the stricter regulation that will be applied in future in Europe on copper usage. As discussed in chapter two it would be advisable to test the possibility of phage synergy with biostimulants or phytoextracts. Caraway (*Carum carvi*) essential oil was tested against *Pseudomonas aeruginosa*, and resulted in a reduction of biofilm formation and of quorum sensing (Fekry et al., 2022). A possible future use of phages for curing soil dysmicrobism as is currently studied to modulate and manipulate the human microbiome (Krishnamurthy et al., 2016; Mirzaei & Deng, 2022; Starr et al., 2019). Furthermore, a phage-mediated regulation of the microbiome of insects could be applied to control pathogen or vector insect population. Phages from their importance to the birth of molecular biology have arrived today to a possible role of therapeutic agents able to evolute and adapting to the pathogens that threaten our crops.

5 REFERENCES

Abba, S., Galetto, L., Vallino, M., Rossi, M., Turina, M., Sicard, A., et al. (2017). Genome sequence, prevalence and quantification of the first iflavirus identified in a phytoplasma insect vector. *Archives of Virology, 162*(3), 799-809.

Abedon, S. T. (2021). Detection of bacteriophages: Phage plaques. *Bacteriophages: Biology, Technology, Therapy*, 507-538.

Abedon, S. T., Thomas-Abedon, C., Thomas, A., & Mazure, H. (2011). Bacteriophage prehistory: is or is not Hankin, 1896, a phage reference? *Bacteriophage, 1*(3), 174-178.

Adriaenssens, E. M., Sullivan, M. B., Knezevic, P., van Zyl, L. J., Sarkar, B. L., Dutilh, B. E., et al. (2020). Taxonomy of prokaryotic viruses: 2018-2019 update from the ICTV Bacterial and Archaeal Viruses Subcommittee. *Archives of Virology, 165*(5), 1253-1260.

Afgan, E., Baker, D., Batut, B., van den Beek, M., Bouvier, D., Cech, M., et al. (2018). The Galaxy platform for accessible, reproducible and collaborative biomedical analyses: 2018 update. *Nucleic Acids Research, 46*(W1), W537-W544.

Aitana, A., Joana, P., Eva, G., Joana, C., & Igor, T. (2021). The Leaf Bacterial Microbiota of Female and Male Kiwifruit Plants in Distinct Seasons: Assessing the Impact of *Pseudomonas syringae* pv. *actinidiae*. *https://doi.org/10.1094/PBIOMES-09-20-0070-R*.

Alcalá-Briseño, R. I., Casarrubias-Castillo, K., López-Ley, D., Garrett, K. A., & Silva-Rosales, L. (2020). Network analysis of the papaya orchard virome from two agroecological regions of Chiapas, Mexico. *Msystems, 5*(1), e00423-00419.

Altschul, S., Wootton, J., Gertz, E., Agarwala, R., Morgulis, A., Schäffer, A., et al. (2005). Protein database searches using compositionally adjusted substitution matrices. *The FEBS journal, 272*(20).

Argov, T., Sapir, S. R., Pasechnek, A., Azulay, G., Stadnyuk, O., Rabinovich, L., et al. (2019). Coordination of cohabiting phage elements supports bacteria–phage cooperation. *Nature communications, 10*(1), 1-14.

Arnold, D. L., Lovell, H. C., Jackson, R. W., & Mansfield, J. W. (2011). *Pseudomonas syringae* pv. *phaseolicola*: from 'has bean' to supermodel. *Molecular Plant Pathology, 12*(7), 617-627.

Audy, P., Braat, C. E., Saindon, G., Huang, H. C., & Laroche, A. (1996). A rapid and sensitive PCR-based assay for concurrent detection of bacteria causing common and halo blights in bean seed. *Phytopathology, 86*(4), 361-366.

Badawy, M. E., & Rabea, E. I. (2011). A biopolymer chitosan and its derivatives as promising antimicrobial agents against plant pathogens and their applications in crop protection. *International Journal of Carbohydrate Chemistry, 2011*.

Bae, J. Y., Wu, J., Lee, H. J., Jo, E. J., Murugaiyan, S., Chung, E., et al. (2012). Biocontrol potential of a lytic bacteriophage PE204 against bacterial wilt of tomato. *Journal of microbiology and biotechnology, 22*(12), 1613-1620.

Bailly-Bechet, M., Vergassola, M., & Rocha, E. (2007). Causes for the intriguing presence of tRNAs in phages. *Genome research, 17*(10).

Balestra, G. (2004). Use of copper formulations to limit bacterial diseases in kiwifruit. (Speciale *Actinidia*). *Rivista di Frutticoltura e di Ortofloricoltura, 66*, 35-41.

Balestra, G., & Varvaro, L. (1995). *Epiphytic survival and control of Pseudomonas viridiflava on Actinidia deliciosa.* Paper presented at the III International Symposium on Kiwifruit 444.

Balestra, G., & Varvaro, L. (1997). *Pseudomonas syringae* pv. *syringae* causal agent of disease on floral buds of *Actinidia deliciosa* (A. Chev) Liang et Ferguson in Italy. *Journal of Phytopathology, 145*(8-9), 375-378.

Balogh, B., Jones, J. B., Iriarte, F. B., & Momol, M. T. (2010). Phage Therapy for Plant Disease Control. [Review]. *Current Pharmaceutical Biotechnology, 11*(1), 48-57.

Bankevich, A., Nurk, S., Antipov, D., Gurevich, A., Dvorkin, M., Kulikov, A., et al. (2012). SPAdes: a new genome assembly algorithm and its applications to single-cell sequencing. *Journal of computational biology: a journal of computational molecular cell biology, 19*(5).

Bardell, D. (1982). An 1898 report by Gamaleya for a lytic agent specific for *Bacillus anthracis*. *Journal of the history of medicine and allied sciences, 37*(2), 222-225.

Bauer, K., Garbe, D., & Surburg, H. (2003). Flavors and Fragrances, Ullmann's Encyclopedia of Industrial Chemistry: Wiley-VCH, Weinheim.

Beatrice, C., Linthorst, J., Cinzia, F., & Luca, R. (2017). Enhancement of PR1 and PR5 gene expressions by chitosan treatment in kiwifruit plants inoculated with *Pseudomonas syringae* pv. *actinidiae*. *European Journal of Plant Pathology, 148*(1), 163-179.

Bellucci, E., Bitocchi, E., Rau, D., Rodriguez, M., Biagetti, E., Giardini, A., et al. (2014). Genomics of origin, domestication and evolution of *Phaseolus vulgaris*. *Genomics of plant genetic resources*, 483-507.

Benler, S., & Koonin, E. V. (2020). Phage lysis-lysogeny switches and programmed cell death: danse macabre. *BioEssays, 42*(12), 2000114.

Berg, G., Rybakova, D., Fischer, D., Cernava, T., Vergès, M.-C. C., Charles, T., et al. (2020). Microbiome definition re-visited: old concepts and new challenges. *Microbiome, 8*(1), 1-22.

Berge, O., Monteil, C. L., Bartoli, C., Chandeysson, C., Guilbaud, C., Sands, D. C., et al. (2014). A user's guide to a data base of the diversity of *Pseudomonas syringae* and its application to classifying strains in this phylogenetic complex. *PloS one, 9*(9), e105547.

Bhowmick, T. S., Das, M., Heinz, K. M., Krauter, P. C., & Gonzalez, C. F. (2016). Transmission of phage by glassy-winged sharpshooters, a vector of *Xylella fastidiosa*. *Bacteriophage, 6*(3), e1218411.

Bhunchoth, A., Phironrit, N., Leksomboon, C., Chatchawankanphanich, O., Kotera, S., Narulita, E., et al. (2015). Isolation of *Ralstonia solanacearum*-infecting bacteriophages from tomato fields in Chiang Mai, T hailand, and their experimental use as biocontrol agents. *Journal of Applied Microbiology, 118*(4), 1023-1033.

Biondi, E., Kuzmanovic, N., Galeone, A., Ladurner, E., Benuzzi, M., Minardi, P., et al. (2012). Potential of *Bacillus amyloliquefaciens* strain d747 as control agent against *Pseudomonas syringae* pv. *actinidiae*. *Journal of Plant Pathology, 94*(4).

Bitocchi, E., Nanni, L., Bellucci, E., Rossi, M., Giardini, A., Zeuli, P. S., et al. (2012). Mesoamerican origin of the common bean (*Phaseolus vulgaris* L.) is revealed by sequence data. *Proceedings of the National Academy of Sciences, 109*(14), E788-E796.

Black, M., Casonato, S., & Bent, S. (2014). *Opportunities for environmental modification to control Pseudomonas syringae pv. actinidiae in kiwifruit.* Paper presented at the XXIX International Horticultural Congress on Horticulture: Sustaining Lives, Livelihoods and Landscapes (IHC2014): 1105.

Boeckaerts, D., Stock, M., Criel, B., Gerstmans, H., De Baets, B., & Briers, Y. (2021). Predicting bacteriophage hosts based on sequences of annotated receptor-binding proteins. *Scientific Reports, 11*(1).

Bolger, A., Lohse, M., & Usadel, B. (2014). Trimmomatic: a flexible trimmer for Illumina sequence data. [Article]. *Bioinformatics, 30*(15), 2114-2120.

Borges, A. L. (2021). How to train your bacteriophage. *Proceedings of the National Academy of Sciences, 118*(28).

Borin, J. M., Avrani, S., Barrick, J. E., Petrie, K. L., & Meyer, J. R. (2021). Coevolutionary phage training leads to greater bacterial suppression and delays the evolution of phage resistance. *Proceedings of the National Academy of Sciences, 118*(23).

Bouvier, T., & Del Giorgio, P. (2007). Key role of selective viral-induced mortality in determining marine bacterial community composition. *Environmental microbiology, 9*(2), 287-297.

Breitbart, M., Salamon, P., Andresen, B., Mahaffy, J. M., Segall, A. M., Mead, D., et al. (2002). Genomic analysis of uncultured marine viral communities. *Proceedings of the National Academy of Sciences of the United States of America, 99*(22), 14250-14255.

Brettin, T., Davis, J., Disz, T., Edwards, R., Gerdes, S., Olsen, G., et al. (2015). RASTtk: a modular and extensible implementation of the RAST algorithm for building custom annotation pipelines and annotating batches of genomes. *Scientific reports, 5*.

Buchfink, B., Xie, C., & Huson, D. H. (2015). Fast and sensitive protein alignment using DIAMOND. *Nature Methods, 12*(1), 59-60.

Burkholder, W. H. (1926). A new bacterial disease of the bean. *Phytopathology, 16*(12).

Burkholder, W. H. (1930). The bacterial diseases of the Beau. A comparative study. *Memoir. Cornell Agricultural Experiment Station, 127*.

Burmeister, A. R., Fortier, A., Roush, C., Lessing, A. J., Bender, R. G., Barahman, R., et al. (2020). Pleiotropy complicates a trade-off between phage resistance and antibiotic resistance. *Proceedings of the National Academy of Sciences, 117*(21), 11207-11216.

Burns, N., James, C. E., & Harrison, E. (2015). Polylysogeny magnifies competitiveness of a bacterial pathogen in vivo. *Evolutionary applications, 8*(4), 346-351.

Calendar, R. (2012). *The Bacteriophages: Volume 1*: Springer Science & Business Media.

Cameron, A., Zoysa, G. H. D., & Sarojini, V. (2014). Antimicrobial peptides against *Pseudomonas syringae* pv. *actinidiae* and Erwinia amylovora: Chemical synthesis, secondary structure, efficacy, and mechanistic investigations. *Peptide Science, 102*(1), 88-96.

Campbell, B. C., & Purcell, A. H. (1993). Phylogenetic affiliation of BEV, a bacterial parasite of the leafhopper *Euscelidius variegatus*, on the basis of 16S rDNA sequences. *Current microbiology, 26*(1), 37-41.

Carvalho, L. J., Corrêa, M., Pereira, E., Nutti, M., Carvalho, J. V., Ribeiro, E. G., et al. (2012). Iron and zinc retention in common beans (*Phaseolus vulgaris* L.) after home cooking. *Food & nutrition research, 56*(1), 15618.

Cellini, A., Fiorentini, L., Buriani, G., Yu, J., Donati, I., Cornish, D., et al. (2014). Elicitors of the salicylic acid pathway reduce incidence of bacterial canker of kiwifruit caused by *Pseudomonas syringae* pv. actinidae. *Annals of Applied Biology, 165*(3), 441-453.

Cellini, A., Giacomuzzi, V., Donati, I., Farneti, B., Rodriguez-Estrada, M. T., Savioli, S., et al. (2019). Pathogen-induced changes in floral scent may increase honeybee-mediated dispersal of *Erwinia amylovora*. *The ISME journal, 13*(4), 847-859.

Ceyssens, P., & Lavigne, R. (2010). Bacteriophages of Pseudomonas. *Future microbiology, 5*(7).

Chan, B. K., Turner, P. E., Kim, S., Mojibian, H. R., Elefteriades, J. A., & Narayan, D. (2018). Phage treatment of an aortic graft infected with *Pseudomonas aeruginosa*. *Evolution, medicine, and public health, 2018*(1), 60-66.

Chapman, J., Taylor, R., Weir, B., Romberg, M., Vanneste, J., Luck, J., et al. (2012). Phylogenetic relationships among global populations of *Pseudomonas syringae* pv. *actinidiae*. *Phytopathology, 102*(11), 1034-1044.

Chen, J., & Civerolo, E. L. (2008). Morphological evidence for phages in *Xylella fastidiosa*. *Virology Journal, 5*, 1-4.

Chen, Q., Yu, J.-J., He, J., Feng, T., & Liu, J.-K. (2022). Isobenzofuranones and isocoumarins from kiwi endophytic fungus *Paraphaeosphaeria sporulosa* and their antibacterial activity against *Pseudomonas syringae* pv. *actinidiae*. *Phytochemistry, 195*, 113050.

Cheung, W. W., & Purcell, A. H. (1993). Ultrastructure of the digestive system of the Le fhopper *Euscelidius variegatus* Kirshbaum (*Homoptera*: *Cicadellidae*), with and without congenital bacterial infections. *International Journal of Insect Morphology and Embryology, 22*(1), 49-61.

Chitwood, D. J. (2002). Phytochemical based strategies for nematode control. *Annual review of phytopathology, 40*(1), 221-249.
Chopin, M.-C., Chopin, A., & Bidnenko, E. (2005). Phage abortive infection in lactococci: variations on a theme. *Current opinion in microbiology, 8*(4), 473-479.
Chou-Fen, L., & Ferguson, A. (1986). The botanical nomenclature of the kiwifruit and related taxa. *New Zealand journal of botany, 24*(1), 183-184.
Cipollini, D., & Heil, M. (2010). Costs and benefits of induced resistance to herbivores and pathogens in plants. *CABI Reviews* (2010), 1-25.
Clavijo-Coppens, F., Ginet, N., Cesbron, S., Briand, M., Jacques, M.-A., & Ansaldi, M. (2021). Novel virulent bacteriophages infecting mediterranean isolates of the plant pest *Xylella fastidiosa* and *Xanthomonas albilineans*. *Viruses, 13*(5), 725.
Clearwater, M., Blattmann, P., Luo, Z., & Lowe, R. (2007). Control of scion vigour by kiwifruit rootstocks is correlated with spring root pressure phenology. *Journal of Experimental Botany, 58*(7), 1741-1751.
Clokie, M. R., Millard, A. D., Letarov, A. V., & Heaphy, S. (2011). Phages in nature. *Bacteriophage, 1*(1), 31-45.
Cohen, A., Williamson, D., & Oishi, K. (1987). SpV3 viruses of *Drosophila spiroplasmas*. *Israel journal of medical sciences, 23*(5), 429-433.
Collina, M., Donati, I., Bertacchini, E., Brunelli, A., & Spinelli, F. (2016). Greenhouse assays on the control of the bacterial canker of kiwifruit (*Pseudomonas syringae* pv. *actinidiae*). *Journal of Berry Research, 6*(4), 407-415.
Colombi, E., Straub, C., Künzel, S., Templeton, M., McCann, H., & Rainey, P. (2017). Evolution of copper resistance in the kiwifruit pathogen *Pseudomonas syringae* pv. *actinidiae* through acquisition of integrative conjugative elements and plasmids. *Environmental microbiology, 19*(2).
Conrath, U. (2009). Priming of induced plant defense responses. *Advances in botanical research, 51*, 361-395.
Cooper, B. (2022). The Detriment of Salicylic Acid to the *Pseudomonas savastanoi* pv. *phaseolicola* Proteome. *Molecular Plant-Microbe Interactions*(ja).
Cooper, B., & Yang, R. (2021). Genomic Resources for *Pseudomonas savastanoi* pv. *phaseolicola* Races 5 and 8. *Phytopathology®, 111*(5), 893-895.
Coplin, D., & Majerczak, D. (1990). Extracellular polysaccharide genes in *Erwinia stewartii*: directed mutagenesis and complementation analysis. *Mol. Plant-Microbe Interact, 3*, 286-292.
Cotrut, R., Renzi, M., Taratufolo, M., Mazzaglia, A., Balestra, G., & Stanica, F. (2013). *Actinidia arguta* ploidy level variation in relation to *Pseudomonas syringae* pv. *actinidiae* susceptibility. *Lucrări Ştiinţifice, 56*, 29-38.
Cui, Z. (1993). Chinese Kiwifruit. *Shandong Science and Technology Press*.
Culpepper, S. A., & Aguinis, H. (2011). R is for revolution: A cutting-edge, free, open source statistical package. *Organizational research methods, 14*(4), 735-740.
Cunty, A., Poliakoff, F., Rivoal, C., Cesbron, S., Fischer-Le Saux, M., Lemaire, C., et al. (2015). Characterization of *Pseudomonas syringae* pv. *actinidiae* (P sa) isolated from France and assignment of Psa biovar 4 to a de novo pathovar: *Pseudomonas syringae* pv. *actinidifoliorum* pv. nov. *Plant pathology, 64*(3), 582-596.

Cusumano, A., Bella, P., Peri, E., Rostás, M., Guarino, S., Lievens, B., et al. (2022). Nectar-inhabiting bacteria affect olfactory responses of an insect parasitoid by altering nectar odors. *Microbial Ecology*, 1-13.

Czajkowski, R., Jackson, R. W., & Lindow, S. E. (2019). Environmental bacteriophages: From biological control applications to directed bacterial evolution (Vol. 10, pp. 1830): Frontiers Media SA.

d'Herelle, M. (1917). Sur un microbe invisible antagoniste des bacilles dysentériques. *Acta Kravsi*.

Danhorn, T., & Fuqua, C. (2007). Biofilm formation by plant-associated bacteria. *Annual review of microbiology, 61*.

Daranas, N., Roselló, G., Cabrefiga, J., Donati, I., Francés, J., Badosa, E., et al. (2019). Biological control of bacterial plant diseases with *Lactobacillus plantarum* strains selected for their broad-spectrum activity. *Annals of Applied Biology, 174*(1), 92-105.

Das, M., Bhowmick, T. S., Ahern, S. J., Young, R., & Gonzalez, C. F. (2015). Control of Pierce's Disease by Phage. *Plos One, 10*(6).

de Jong, H., Reglinski, T., Elmer, P. A., Wurms, K., Vanneste, J. L., Guo, L. F., et al. (2019). Integrated use of *Aureobasidium pullulans* strain CG163 and acibenzolar-S-methyl for management of bacterial canker in kiwifruit. *Plants, 8*(8), 287.

De Mendiburu, F., & Reinhard, S. (2015). Agricolae - Ten years of an open source statistical tool for experiments in breeding, agriculture and biology. (e1748).

Degnan, P. H., Bittleston, L. S., Hansen, A. K., Sabree, Z. L., Moran, N. A., & Almeida, R. P. (2011). Origin and examination of a leafhopper facultative endosymbiont. *Current microbiology, 62*(5), 1565-1572.

Degnan, P. H., & Moran, N. A. (2008). Diverse phage-encoded toxins in a protective insect endosymbiont. *Applied and environmental microbiology, 74*(21), 6782-6791.

Degnan, P. H., Yu, Y., Sisneros, N., Wing, R. A., & Moran, N. A. (2009). *Hamiltonella defensa*, genome evolution of protective bacterial endosymbiont from pathogenic ancestors. *Proceedings of the National Academy of Sciences, 106*(22), 9063-9068.

Di Lallo, G., Evangelisti, M., Mancuso, F., Ferrante, P., Marcelletti, S., Tinari, A., et al. (2014). Isolation and partial characterization of bacteriophages infecting *Pseudomonas syringae* pv. *actinidiae*, causal agent of kiwifruit bacterial canker. [Article]. *Journal of Basic Microbiology, 54*(11), 1210-1221.

Diallo, M. D., Monteil, C. L., Vinatzer, B. A., Clarke, C. R., Glaux, C., Guilbaud, C., et al. (2012). *Pseudomonas syringae* naturally lacking the canonical type III secretion system are ubiquitous in nonagricultural habitats, are phylogenetically diverse and can be pathogenic. *Isme Journal, 6*(7), 1325-1335.

Dillon, M., Thakur, S., Almeida, R., Wang, P., Weir, B., & Guttman, D. (2019). Recombination of ecologically and evolutionarily significant loci maintains genetic cohesion in the *Pseudomonas syringae* species complex. *Genome biology, 20*(1).

Dion, M., Oechslin, F., & Moineau, S. (2020). Phage diversity, genomics and phylogeny. *Nature reviews. Microbiology, 18*(3).

Domingo-Calap, M. L., Aure, C. M., Navarro-Herrero, I., Domingo-Calap, P., & Marco-Noales, E. (2021). Isolation and characterization of bacteriophages against *Xylella fastidiosa.* Paper presented at the 3rd European conference on *Xylella fastidiosa* and XF-ACTORS.

Donati, I., Buriani, G., Cellini, A., Mauri, S., Costa, G., & Spinelli, F. (2014). New insights on the bacterial canker of kiwifruit (*Pseudomonas syringae* pv. *actinidiae*). *Journal of Berry Research, 4*(2), 53-67.

Donati, I., Buriani, G., Cellini, A., Raule, N., & Spinelli, F. (2017). Screening of microbial biocoenosis of *Actinidia chinensis* for the isolation of candidate biological control agents against *Pseudomonas syringae* pv. *actinidiae.* Paper presented at the IX International Symposium on Kiwifruit 1218.

Donati, I., Cellini, A., Buriani, G., Mauri, S., Kay, C., Tacconi, G., et al. (2018). Pathways of flower infection and pollen-mediated dispersion of *Pseudomonas syringae* pv. *actinidiae*, the causal agent of kiwifruit bacterial canker. *Horticulture Research, 5*.

Donati, I., Cellini, A., Sangiorgio, D., Caldera, E., Sorrenti, G., & Spinelli, F. (2020). Pathogens associated to kiwifruit vine decline in Italy. *Agriculture, 10*(4), 119.

Donati, I., Cellini, A., Sangiorgio, D., Vanneste, J. L., Scortichini, M., Balestra, G. M., et al. (2020). *Pseudomonas syringae* pv. *actinidiae*: Ecology, Infection Dynamics and Disease Epidemiology. *Microbial ecology, 80*(1).

Donati, I., Mauri, S., Buriani, G., Cellini, A., & Spinelli, F. (2017). Role of *Metcalfa pruinosa* as a vector for *Pseudomonas syringae* pv. *actinidiae*. *The plant pathology journal, 33*(6), 554.

Dong, H., Delaney, T. P., Bauer, D. W., & Beer, S. V. (1999). Harpin induces disease resistance in *Arabidopsis* through the systemic acquired resistance pathway mediated by salicylic acid and the NIM1 gene. *The Plant Journal, 20*(2), 207-215.

Dowson, W. (1943). On the generic names *Pseudomonas*, *Xanthomonas* and *Bacterium* for certain bacterial plant pathogens. *Transactions of the British Mycological Society, 26*(1-2).

Duman, K., & Soylu, S. (2019). Characterization of plant growth-promoting traits and antagonistic potentials of endophytic bacteria from bean plants against *Pseudomonas syringae* pv. *phaseolicola*. *Plant Protection Bulletin, 59*(3), 59-69.

Dutilh, B. E., Cassman, N., McNair, K., Sanchez, S. E., Silva, G. G., Boling, L., et al. (2014). A highly abundant bacteriophage discovered in the unknown sequences of human faecal metagenomes. *Nature communications, 5*(1), 1-11.

D'Accolti, M., Soffritti, I., Mazzacane, S., & Caselli, E. (2021). Bacteriophages as a potential 360-degree pathogen control strategy. *Microorganisms, 9*(2), 261.

D'Ippolito, I., Mininni, A., Dichio, B., Reyes, F., Xylogiannis, E., Mastroleo, M., et al. (2021). Moria del kiwi: alterazione della struttura anatomica e morfologica delle radici di actinidia sottoposte a condizioni di asfissia del suolo. Paper presented at the XIII Giornate Scientifiche della Società di Ortoflorifrutticoltura Italiana (SOI).

Edgar, R. C. (2004). MUSCLE: multiple sequence alignment with high accuracy and high throughput. *Nucleic Acids Research, 32*(5), 1792-1797.

Edwards, R. A., McNair, K., Faust, K., Raes, J., & Dutilh, B. E. (2016). Computational approaches to predict bacteriophage–host relationships. *FEMS microbiology reviews, 40*(2), 258-272.

EFSA, E. F. S. A., Vogelaar, M., Schenk, M., Delbianco, A., Graziosi, I., & Vos, S. (2020). Pest survey card on *Pseudomonas syringae* pv. *actinidiae*. *EFSA Supporting Publications, 17*(12), 1986E.

Eman, O. H., & Afaf, Z. A. E. (2014). Biocontrol of halo blight of bean caused by *Pseudomonas phaseolicola*.

Ercolani, G. L., & Crosse, J. E. (1966). The Growth of *Pseudomonas phaseolicola* and Related Plant Pathogens in vivo. *Microbiology, 45*(3), 429-439.

Everett, K., Pushparajah, I., & Vergara, M. (2012). *Pseudomonas syringae* pv *actinidiae* on surfaces in the orchard. *New Zealand Plant Protection, 65*, 19-24.

Fekry, M., Yahya, G., Osman, A., Al-Rabia, M. W., Mostafa, I., & Abbas, H. A. (2022). GC-MS Analysis and Microbiological Evaluation of Caraway Essential Oil as a Virulence Attenuating Agent against *Pseudomonas aeruginosa*. *Molecules, 27*(23), 8532.

Feng, T., Yu, J.-J., Zhang, Y., Cox, R. J., He, J., & Liu, J.-K. Terpenoids from Kiwi Endophytic Fungus *Bipolaris* sp. and Their Antibacterial Activity against *Pseudomonas syringae* pv. *actinidiae*. *Frontiers in Chemistry*, 1069.

Ferguson, A., & MacRae, E. (1991). *Vitamin C in actinidia.* Paper presented at the II International Symposium on Kiwifruit 297.

Ferguson, A. R. (1984). Kiwifruit: a botanical review. *Horticultural reviews, 6*, 1-64.

Fernández-Ruiz, I., Coutinho, F., & Rodriguez-Valera, F. (2018). Thousands of Novel Endolysins Discovered in Uncultured Phage Genomes. *Frontiers in microbiology, 9*.

Fernández-Sanz, A., MR, R., & AJ, G. (2016). *Pseudomonas syringae* pv. *phaseolicola* isolated from weeds in bean crop fields. *Letters in applied microbiology, 62*(4).

Fernández-Sanz, A. M., Rodicio, M. R., & González, A. J. (2016). *Pseudomonas syringae* pv. *phaseolicola* isolated from weeds in bean crop fields. *Letters in applied microbiology, 62*(4).

Ferrante, P., Fiorillo, E., Marcelletti, S., Marocchi, F., Mastroleo, M., Simeoni, S., et al. (2012). The importance of the main colonization and penetration sites of *Pseudomonas syringae* pv. *actinidiae* and prevailing weather conditions in the development of epidemics in yellow kiwifruit, recently observed in central Italy. *Journal of plant pathology*, 455-461.

Ferrante, P., & Scortichini, M. (2009). Identification of *Pseudomonas syringae* pv. *actinidiae* as causal agent of bacterial canker of yellow kiwifruit (*Actinidia chinensis* Planchon) in central Italy. *Journal of Phytopathology, 157*(11-12), 768-770.

Ferrante, P., & Scortichini, M. (2010). Molecular and phenotypic features of *Pseudomonas syringae* pv. *actinidiae* isolated during recent epidemics of bacterial canker on yellow kiwifruit (*Actinidia chinensis*) in central Italy. *Plant pathology, 59*(5), 954-962.

Ferrante, P., & Scortichini, M. (2014). Frost promotes the pathogenicity of *Pseudomonas* syringae pv. *actinidiae* in *Actinidia chinensis* and *A. deliciosa* plants. *Plant pathology, 63*(1), 12-19.

Ferrante, P., & Scortichini, M. (2014). Redefining the global populations of *Pseudomonas syringae* pv. *actinidiae* based on pathogenic, molecular and phenotypic characteristics - Ferrante - 2015 - Plant Pathology - Wiley Online Library.

Ferrante, P., & Scortichini, M. (2015). Redefining the global populations of *Pseudomonas syringae* pv. *actinidiae* based on pathogenic, molecular and phenotypic characteristics. *Plant Pathology, 64*(1), 51-62.

Flores, O., Retamales, J., Nunez, M., Leon, M., Salinas, P., Besoain, X., et al. (2020). Characterization of Bacteriophages against *Pseudomonas syringae* pv. *actinidiae* with Potential Use as Natural Antimicrobials in Kiwifruit Plants. *Microorganisms, 8*(7).

Fonseca, P. L., Badotti, F., De Oliveira, T. F., Fonseca, A., Vaz, A., Tomé, L. M., et al. (2018). Virome analyses of *Hevea brasiliensis* using small RNA deep sequencing and PCR techniques reveal the presence of a potential new virus. *Virology journal, 15*(1), 1-9.

Forero-Junco, L. M., Alanin, K. W. S., Djurhuus, A. M., Kot, W., Gobbi, A., & Hansen, L. H. (2022). Bacteriophages Roam the Wheat Phyllosphere. *Viruses, 14*(2), 244.

Frampton, R., Taylor, C., Holguín, M. A., Visnovsky, S., Petty, N., Pitman, A., et al. (2014). Identification of bacteriophages for biocontrol of the kiwifruit canker phytopathogen *Pseudomonas syringae* pv. *actinidiae*. *Applied and environmental microbiology, 80*(7).

Frampton, R. A., Acedo, E. L., Young, V. L., Chen, D. N., Tong, B., Taylor, C., et al. (2015). Genome, Proteome and Structure of a T7-Like Bacteriophage of the Kiwifruit Canker Phytopathogen *Pseudomonas syringae* pv. *actinidiae*. [Article]. *Viruses-Basel, 7*(7), 3361-3379.

Francati, S., Masetti, A., Martinelli, R., Mirandola, D., Anteghini, G., Busi, R., et al. (2021). *Halyomorpha halys* (Hemiptera: Pentatomidae) on kiwifruit in northern Italy: Phenology, infestation, and natural enemies assessment. *Journal of Economic Entomology, 114*(4), 1733-1742.

Froud, K. J., Everett, K. R., Tyson, J. L., Beresford, R. M., & Cogger, N. (2015). Review of the risk factors associated with kiwifruit bacterial canker caused by *Pseudomonas syringae* pv *actinidiae*. [Papers]. *New Zealand Plant Protection, 68*.

Fujikawa, T., & Sawada, H. (2016). Genome analysis of the kiwifruit canker pathogen *Pseudomonas syringae* pv. *actinidiae* biovar 5. *Scientific reports, 6*(1), 1-11.

Fujikawa, T., & Sawada, H. (2019). Genome analysis of *Pseudomonas syringae* pv. *actinidiae* biovar 6, which produces the phytotoxins, phaseolotoxin and coronatine. *Scientific reports, 9*(1), 1-11.

Fujiwara, A., Fujisawa, M., Hamasaki, R., Kawasaki, T., Fujie, M., & Yamada, T. (2011). Biocontrol of *Ralstonia solanacearum* by treatment with lytic bacteriophages. *Applied and environmental microbiology, 77*(12), 4155-4162.

Galetto, L., Abbà, S., Rossi, M., Vallino, M., Pesando, M., Arricau-Bouvery, N., et al. (2018). Two phytoplasmas elicit different responses in the insect vector *Euscelidius variegatus* Kirschbaum. *Infection and immunity, 86*(5), e00042-00018.

Galetto, L., Nardi, M., Saracco, P., Bressan, A., Marzachì, C., & Bosco, D. (2009). Variation in vector competency depends on chrysanthemum yellows phytoplasma distribution within *Euscelidius variegatus*. *Entomologia experimentalis et applicata, 131*(2), 200-207.

Gallelli, A., L'Aurora, A., & Loreti, S. (2011). Gene sequence analysis for the molecular detection of *Pseudomonas syringae* pv. *actinidiae*: DEVELOPING DIAGNOSTIC PROTOCOLS. *Journal of Plant Pathology, 93*(2), 425-435.

Gao, X., Huang, Q., Zhao, Z., Han, Q., Ke, X., Qin, H., et al. (2016). Studies on the infection, colonization, and movement of *Pseudomonas syringae* pv. *actinidiae* in kiwifruit tissues using a GFPuv-labeled strain. *PloS one, 11*(3), e0151169.

Gašić, K., Kuzmanović, N., Ivanović, M., Prokić, A., Šević, M., & Obradović, A. (2018). Complete genome of the *Xanthomonas euvesicatoria* specific bacteriophage KΦ1, its survival and potential in control of pepper bacterial spot. *Frontiers in microbiology, 9*, 2021.

Gepts, P., Aragão, F. J., Barros, E. d., Blair, M. W., Brondani, R., Broughton, W., et al. (2008). Genomics of *Phaseolus* beans, a major source of dietary protein and micronutrients in the tropics *Genomics of tropical crop plants* (pp. 113-143): Springer.

Ginestet, C. (2011). ggplot2: elegant graphics for data analysis: Wiley Online Library.

Goldberg, J. B. (2000). 'Pseudomonas' 99, The Seventh International Congress on *Pseudomonas*: Biotechnology and Pathogenesis', organized by the American Society for Microbiology, was held in Maui, HI, USA, 1–5 September 1999. *Trends in microbiology, 8*(2), 55-57.

Gonella, E., Crotti, E., Mandrioli, M., Daffonchio, D., & Alma, A. (2018). *Asaia* symbionts interfere with infection by Flavescence dorée phytoplasma in leafhoppers. *Journal of Pest Science, 91*(3), 1033-1046.

Gonella, E., Tedeschi, R., Crotti, E., & Alma, A. (2019). Multiple guests in a single host: interactions across symbiotic and phytopathogenic bacteria in phloem-feeding vectors–a review. *Entomologia Experimentalis et Applicata, 167*(3), 171-185.

Gong, J.-T., Li, Y., Li, T.-P., Liang, Y., Hu, L., Zhang, D., et al. (2020). Stable Introduction of Plant-Virus-Inhibiting *Wolbachia* into Planthoppers for Rice Protection. *Current Biology, 30*(24), 4837-+.

González-Villalobos, E., & Balcázar, J. L. (2022). Does phage-mediated horizontal gene transfer represent an environmental risk? *Trends in Microbiology*.

Grabherr, M. G., Haas, B. J., Yassour, M., Levin, J. Z., Thompson, D. A., Amit, I., et al. (2011). Full-length transcriptome assembly from RNA-Seq data without a reference genome. [Article]. *Nature Biotechnology, 29*(7), 644-U130.

Guerin, E., Shkoporov, A., Stockdale, S. R., Clooney, A. G., Ryan, F. J., Sutton, T. D., et al. (2018). Biology and taxonomy of crAss-like bacteriophages, the most abundant virus in the human gut. *Cell host & microbe, 24*(5), 653-664. e656.

Gui, Y. (1981). Comparative morphological observations of *Actinidia chinensis* Planch. var. *chinensis* and *A. chinensis* Planch. var. *hispida* CF Liang. *Acta Phytotax. Sin, 19*, 304-307.

Guilbaud, C., Morris, C. E., Barakat, M., Ortet, P., & Berge, O. (2016). Isolation and identification of *Pseudomonas syringae* facilitated by a PCR targeting the whole P. syringae group. *FEMS microbiology ecology, 92*(1).

Gurney, J., Brown, S. P., Kaltz, O., & Hochberg, M. E. (2020). Steering phages to combat bacterial pathogens. *Trends in microbiology, 28*(2), 85-94.

Gurung, K., Wertheim, B., & Falcao Salles, J. (2019). The microbiome of pest insects: it is not just bacteria. *Entomologia Experimentalis et Applicata, 167*(3), 156-170.

Gurung, K., Wertheim, B., & Salles, J. F. (2019). The microbiome of pest insects: it is not just bacteria. *Entomologia Experimentalis Et Applicata, 167*(3), 156-170.

Gutiérrez, D., & Briers, Y. (2021). Lysins breaking down the walls of gram-negative bacteria, no longer a no-go. *Current Opinion in Biotechnology, 68*, 15-22.

Guy, L., Department of Molecular Evolution, U. U., Norbyvägen 18C, 75236 Uppsala, Sweden, Roat Kultima, J., Department of Molecular Evolution, U. U., Norbyvägen 18C, 75236 Uppsala, Sweden, Andersson, S. G. E., & Department of Molecular Evolution, U. U., Norbyvägen 18C, 75236 Uppsala, Sweden. (2020). genoPlotR: comparative gene and genome visualization in R. *Bioinformatics, 26*(18), 2334-2335.

Han, H.-S., Koh, Y.-J., Hur, J.-S., & Jung, J.-S. (2003). Identification and characterization of coronatine-producing *Pseudomonas syringae* pv. *actinidiae*. *Journal of microbiology and biotechnology, 13*(1), 110-118.

Hankin, E. H. (1896). L'action bactericide des eaux de la Jumna et du Gange sur le vibrion du cholera. *Ann Inst Pasteur, 10*(11).

Harper, D. R., Abedon, S. T., Burrowes, B. H., & McConville, M. L. (2019). *Bacteriophages: Biology, Technology, Therapy*: Springer International Publishing.

Hatfull, G. F., & Hendrix, R. W. (2011). Bacteriophages and their genomes. *Current opinion in virology, 1*(4), 298-303.

He, Z., Zhang, X., Zhong, Y., & Ye, L. (2000). Phylogenetic relationships of *Actinidia* and related genera based on micromorphological characters of foliar trichomes. *Genetic Resources and Crop Evolution, 47*(6), 627-639.

Health, E. P. o. P., Jeger, M., Bragard, C., Caffier, D., Candresse, T., Chatzivassiliou, E., et al. (2016). Risk to plant health of Flavescence dorée for the EU territory. *EFSA journal, 14*(12), e04603.

Hertwig, S., Hammer, J., Appel, B., & Alter, T. (2013). Post-harvest application of lytic bacteriophages for biocontrol of food-borne pathogens and spoilage bacteria. *Berliner und Münchener Tierärztliche Wochenschrift, 126*(9/10), 357-369.

Hofstatter, P., Tice, A., Kang, S., Brown, M., & Lahr, D. (2016). Evolution of bacterial recombinase A (recA) in eukaryotes explained by addition of genomic data of key microbial lineages. *Proceedings. Biological sciences, 283*(1840).

Holtappels, D., Kerremans, A., Busschots, Y., Van Vaerenbergh, J., Maes, M., Lavigne, R., et al. (2020). Preparing for the KIL: Receptor Analysis of *Pseudomonas syringae*

pv. *porri* Phages and Their Impact on Bacterial Virulence. *International Journal of Molecular Sciences, 21*(8).

Howard-Varona, C., Hargreaves, K. R., Abedon, S. T., & Sullivan, M. B. (2017). Lysogeny in nature: mechanisms, impact and ecology of temperate phages. *The ISME journal, 11*(7), 1511-1520.

Huang, H. (2016). *Kiwifruit: the genus Actinidia*: Academic Press.

Huang, H., & Ferguson, A. R. (2001). kiwifruit in China. *New Zealand Journal of Crop and Horticultural Science, 29*(1), 1-14.

Huang, X. Q., & Madan, A. (1999). CAP3: A DNA sequence assembly program. *Genome Research, 9*(9), 868-877.

Ichinose, Y., Taguchi, F., & Mukaihara, T. (2013). Pathogenicity and virulence factors of *Pseudomonas syringae*. *Journal of general plant pathology, 79*(5), 285-296.

Ingram, D. M., & Lu, S.-E. (2009). Evaluation of Foliar Sprays of Bacteriophages for the Management of Bacterial Canker in Greenhouse Tomatoes. *Plant Health Progress, 10*(1), 19.

Iriarte, F., Obradović, A., Wernsing, M., Jackson, L., Balogh, B., Hong, J., et al. (2012). Soil-based systemic delivery and phyllosphere in vivo propagation of bacteriophages: Two possible strategies for improving bacteriophage persistence for plant disease control. *Bacteriophage, 2*(4).

Ishii, Y., Matsuura, Y., Kakizawa, S., Nikoh, N., & Fukatsu, T. (2013). Diversity of bacterial endosymbionts associated with Macrosteles leafhoppers vectoring phytopathogenic phytoplasmas. *Applied and Environmental Microbiology, 79*(16), 5013-5022.

Jacquiod, S., Nunes, I., Brejnrod, A., Hansen, M. A., Holm, P. E., Johansen, A., et al. (2018). Long-term soil metal exposure impaired temporal variation in microbial metatranscriptomes and enriched active phages. *Microbiome, 6*(1), 1-14.

James, S., Rabiey, M., Neuman, B., Percival, G., & Jackson, R. (2020). Isolation, Characterisation and Experimental Evolution of Phage that Infect the Horse Chestnut Tree Pathogen, *Pseudomonas syringae* pv. *aesculi*. *Current microbiology, 77*(8).

Jie, Z., & Beuzenberg, E. (1983). Chromosome numbers in two varieties of *Actinidia chinensis* Planch. *New Zealand journal of botany, 21*(3), 353-355.

Joardar, V., Lindeberg, M., Jackson, R. W., Selengut, J., Dodson, R., Brinkac, L. M., et al. (2005). Whole-genome sequence analysis of *Pseudomonas syringae* pv. *phaseolicola* 1448A reveals divergence among pathovars in genes involved in virulence and transposition. *Journal of bacteriology, 187*(18), 6488-6498.

Joensen, K., Scheutz, F., Lund, O., Hasman, H., Kaas, R., Nielsen, E., et al. (2014). Real-time whole-genome sequencing for routine typing, surveillance, and outbreak detection of verotoxigenic *Escherichia coli*. *Journal of clinical microbiology, 52*(5).

Jones, J. B., Jackson, L. E., Balogh, B., Obradovic, A., Iriarte, F. B., & Momol, M. T. (2007). Bacteriophages for plant disease control *Annual Review of Phytopathology* (Vol. 45, pp. 245-262).

Jørgensen, J. B., Djurhuus, A. M., Carstens, A. B., Kot, W., Neve, H., Morris, C. E., et al. (2020). Presentation of Three Novel Tailed Phages Targeting Multiple Strains of *Pseudomonas syringae*. *PHAGE, 1*(4), 245-250.

Kagale, S., & Close, T. J. (2021). Legumes: Embracing the genome era (Vol. 3, pp. e113): Wiley Online Library.

Kami, J., Velásquez, V., Debouck, D., & Gepts, P. (1995). Identification of presumed ancestral DNA sequences of phaseolin in *Phaseolus vulgaris*. *Proceedings of the National Academy of Sciences of the United States of America, 92*(4).

Kawato, Y., Yasuike, M., Nakamura, Y., Shigenobu, Y., Fujiwara, A., Sano, M., et al. (2015). Complete genome sequence analysis of two *Pseudomonas plecoglossicida* phages, potential therapeutic agents. *Applied and Environmental Microbiology, 81*(3), 874-881.

Kelley, L. A., Mezulis, S., Yates, C. M., Wass, M. N., & Sternberg, M. J. E. (2015). The Phyre2 web portal for protein modeling, prediction and analysis. *Nature Protocols, 10*(6), 845-858.

Kembel, S. W., O'Connor, T. K., Arnold, H. K., Hubbell, S. P., Wright, S. J., & Green, J. L. (2014). Relationships between phyllosphere bacterial communities and plant functional traits in a neotropical forest. *Proceedings of the National Academy of Sciences, 111*(38), 13715-13720.

Kim, G. H., Kim, K.-H., Son, K. I., Choi, E. D., Lee, Y. S., Jung, J. S., et al. (2016). Outbreak and spread of bacterial canker of kiwifruit caused by *Pseudomonas syringae* pv. *actinidiae* biovar 3 in Korea. *The plant pathology journal, 32*(6), 545.

Kim, M.-J., Chae, D.-H., Cho, G., Kim, D.-R., & Kwak, Y.-S. (2019). Characterization of antibacterial strains against kiwifruit bacterial canker pathogen. *The plant pathology journal, 35*(5), 473.

Kim, Y. C., Leveau, J., McSpadden Gardener, B. B., Pierson, E. A., Pierson III, L. S., & Ryu, C.-M. (2011). The multifactorial basis for plant health promotion by plant-associated bacteria. *Applied and Environmental Microbiology, 77*(5), 1548-1555.

Kimmelshue, C., Goggi, A. S., & Cademartiri, R. (2019). The use of biological seed coatings based on bacteriophages and polymers against *Clavibacter michiganensis* subsp. *nebraskensis* in maize seeds. *Scientific reports, 9*(1), 1-11.

Koh, Y. (1994). Outbreak and spread of bacterial canker in kiwifruit. Korean. *J. Plant Pathol., 10*, 68-72.

Koh, Y. J., Lee, D. H., Shin, J. S., & Hur, J. S. (2001). Chemical and cultural control of bacterial blossom blight of kiwifruit caused by *Pseudomonas syringae* in Korea. *New Zealand Journal of Crop and Horticultural Science, 29*(1), 29-34.

Koh, Y. J., & Nou, I. S. (2002). DNA markers for identification of *Pseudomonas syringae* pv. *actinidiae*. *Molecules and Cells, 13*(2), 309-314.

Kortright, K. E., Chan, B. K., Koff, J. L., & Turner, P. E. (2019). Phage therapy: a renewed approach to combat antibiotic-resistant bacteria. *Cell host & microbe, 25*(2), 219-232.

Koskella, B., Hall, L. J., & Metcalf, C. J. E. (2017). The microbiome beyond the horizon of ecological and evolutionary theory. *Nature ecology & evolution, 1*(11), 1606-1615.

Krishnamurthy, S. R., Janowski, A. B., Zhao, G., Barouch, D., & Wang, D. (2016). Hyperexpansion of RNA Bacteriophage Diversity. *Plos Biology, 14*(3).

Kumar, S., Stecher, G., & Tamura, K. (2016). MEGA7: molecular evolutionary genetics analysis version 7.0 for bigger datasets. *Molecular biology and evolution, 33*(7), 1870-1874.

Kupczok, A., Neve, H., Huang, K., Hoeppner, M., Heller, K., Franz, C., et al. (2018). Rates of Mutation and Recombination in *Siphoviridae* Phage Genome Evolution over Three Decades. *Molecular biology and evolution, 35*(5).

Kutter, E., & Sulakvelidze, A. (2004). *Bacteriophages: biology and applications*: Crc press.

Lam, F., & Longnecker, M. (1983). A modified Wilcoxon rank sum test for paired data. *Biometrika, 70*(2), 510-513.

Langmead, B., & Salzberg, S. L. (2012). Fast gapped-read alignment with Bowtie 2. *Nature Methods, 9*(4), 357-U354.

Lavigne, R., Burkal'tseva, M., Robben, J., Sykilinda, N., Kurochkina, L., Grymonprez, B., et al. (2003). The genome of bacteriophage phiKMV, a T7-like virus infecting *Pseudomonas aeruginosa*. *Virology, 312*(1).

Lavigne, R., & Loessner, M. J. (2021). Editorial overview: Phage therapy in the 21st century-inspired by biotechnology! (Vol. 68, pp. vi-vii).

Leigh, B. A., Bordenstein, S. R., Brooks, A. W., Mikaelyan, A., & Bordenstein, S. R. (2018). Finer-scale phylosymbiosis: insights from insect viromes. *Msystems, 3*(6), e00131-00118.

LePage, D. P., Metcalf, J. A., Bordenstein, S. R., On, J., Perlmutter, J. I., Shropshire, J. D., et al. (2017). Prophage WO genes recapitulate and enhance *Wolbachia*-induced cytoplasmic incompatibility. *Nature, 543*(7644), 243-247.

Linden, J. C., Stoner, R. J., Knutson, K. W., & Gardner-Hughes, C. A. (2000). Organic disease control elicitors. *Agro food industry hi-tech, 11*(5), 32-34.

Linden, S. B., Alreja, A. B., & Nelson, D. C. (2021). Application of bacteriophage-derived endolysins to combat streptococcal disease: Current state and perspectives. *Current Opinion in Biotechnology, 68*, 213-220.

Lindow, S., Arny, D., & Upper, C. (1978). Distribution of ice nucleation-active bacteria on plants in nature. *Applied and environmental microbiology, 36*(6), 831-838.

Lindow, S. E., & Brandl, M. T. (2003). Microbiology of the phyllosphere. *Applied and environmental microbiology, 69*(4), 1875-1883.

Liu, W., Lin, Y. R., Lu, M. W., Sung, P. J., Wang, W. H., & Lin, C. S. (2014). Genome sequences characterizing five mutations in RNA polymerase and major capsid of phages φA318 and φAs51 of *Vibrio alginolyticus* with different burst efficiencies. *BMC genomics, 15*(1).

Loc-Carrillo, C., & Abedon, S. (2011). Pros and cons of phage therapy. Bacteriophage 1: 111–114.

Loponte, R., Pagnini, U., Iovane, G., & Pisanelli, G. (2021). Phage therapy in veterinary medicine. *Antibiotics, 10*(4), 421.

Louws, F., Wilson, M., Campbell, H., Cuppels, D., Jones, J., Shoemaker, P., et al. (2001). Field control of bacterial spot and bacterial speck of tomato using a plant activator. *Plant Disease, 85*(5), 481-488.

Lowe, T., & Chan, P. (2016). tRNAscan-SE On-line: integrating search and context for analysis of transfer RNA genes. *Nucleic acids research, 44*(W1).

Luti, S., Campigli, S., Ranaldi, F., Paoli, P., Pazzagli, L., & Marchi, G. (2021). Lscβ and lscγ, two novel levansucrases of *Pseudomonas syringae* pv. *actinidiae* biovar 3, the causal agent of bacterial canker of kiwifruit, show different enzymatic properties. *International Journal of Biological Macromolecules, 179*, 279-291.

Ma, J.-T., Du, J.-X., Zhang, Y., Liu, J.-K., Feng, T., & He, J. (2022). Natural imidazole alkaloids as antibacterial agents against *Pseudomonas syringae* pv. *actinidiae* isolated from kiwi endophytic fungus *Fusarium tricinctum*. *Fitoterapia, 156*, 105070.

Madeira, F., Park, Y., Lee, J., Buso, N., Gur, T., Madhusoodanan, N., et al. (2019). The EMBL-EBI search and sequence analysis tools APIs in 2019. *Nucleic acids research, 47*(W1).

Malone, L. M., Birkholz, N., & Fineran, P. C. (2021). Conquering CRISPR: how phages overcome bacterial adaptive immunity. *Current Opinion in Biotechnology, 68*, 30-36.

Manrique, P., Bolduc, B., Walk, S. T., van der Oost, J., de Vos, W. M., & Young, M. J. (2016). Healthy human gut phageome. *Proceedings of the National Academy of Sciences, 113*(37), 10400-10405.

Mansfield, J., Genin, S., Magori, S., Citovsky, V., Sriariyanum, M., Ronald, P., et al. (2012). Top 10 plant pathogenic bacteria in molecular plant pathology. *Molecular plant pathology, 13*(6).

Marcelletti, S., Ferrante, P., Petriccione, M., Firrao, G., & Scortichini, M. (2011). *Pseudomonas syringae* pv. *actinidiae* draft genomes comparison reveal strain-specific features involved in adaptation and virulence to *Actinidia* species. *PloS one, 6*(11), e27297.

Marcelletti, S., & Scortichini, M. (2014). Definition of plant-pathogenic *Pseudomonas* genomospecies of the *Pseudomonas syringae* complex through multiple comparative approaches. *Phytopathology, 104*(12), 1274-1282.

Mariz-Ponte, N., Regalado, L., Gimranov, E., Tassi, N., Moura, L., Gomes, P., et al. (2021). A Synergic Potential of Antimicrobial Peptides against *Pseudomonas syringae* pv. *actinidiae*. *Molecules, 26*(5), 1461.

Martinson, V. G., Gawryluk, R. M., Gowen, B. E., Curtis, C. I., Jaenike, J., & Perlman, S. J. (2020). Multiple origins of obligate nematode and insect symbionts by a clade of bacteria closely related to plant pathogens. *Proceedings of the National Academy of Sciences, 117*(50), 31979-31986.

Martínez-Aguilar, K., Ramírez-Carrasco, G., Hernández-Chávez, J. L., Barraza, A., & Alvarez-Venegas, R. (2016). Use of BABA and INA as activators of a primed state in the common bean (*Phaseolus vulgaris* L.). *Frontiers in Plant Science, 7*, 653.

Marzachì, C., Veratti, F., & Bosco, D. (1998). Direct PCR detection of phytoplasmas in experimentally infected insects. *Annals of Applied Biology, 133*(1), 45-54.

Masschalck, B., Van Houdt, R., Van Haver, E., & Michiels, C. (2001). Inactivation of gram-negative bacteria by lysozyme, denatured lysozyme, and lysozyme-derived peptides under high hydrostatic pressure. *Applied and environmental microbiology, 67*(1).

Masui, S., Kuroiwa, H., Sasaki, T., Inui, M., Kuroiwa, T., & Ishikawa, H. (2001). Bacteriophage WO and virus-like particles in *Wolbachia*, an endosymbiont of arthropods. *Biochemical and biophysical research communications, 283*(5), 1099-1104.

Mauchline, N., & Hill, M. (2005). Settlement of armoured scale insects on fruit of commercial *Actinidia* spp. *New Zealand Plant Protection, 58*, 294-298.

Mauri, S., Cellini, A., Buriani, G., Donati, I., Costa, G., & Spinelli, F. (2016). Optimization of cultural practices to reduce the development of *Pseudomonas syringae* pv. *actinidiae*, causal agent of the bacterial canker of kiwifruit. *Journal of Berry Research, 6*(4), 355-371.

McCann, H., Li, L., Liu, Y., Li, D., Pan, H., Zhong, C., et al. (2017). Origin and Evolution of the Kiwifruit Canker Pandemic. *Genome biology and evolution, 9*(4).

McClean, P. E., Lavin, M., Gepts, P., & Jackson, S. A. (2008). *Phaseolus vulgaris*: a diploid model for soybean *Genetics and genomics of soybean* (pp. 55-76): Springer.

McKight, P. E., & Najab, J. (2010). Kruskal-wallis test. *The corsini encyclopedia of psychology*, 1-1.

Melotto, M., Underwood, W., & He, S. Y. (2008). Role of stomata in plant innate immunity and foliar bacterial diseases. *Annu. Rev. Phytopathol., 46*, 101-122.

Merrill, B., Ward, A., Grose, J., & Hope, S. (2016). Software-based analysis of bacteriophage genomes, physical ends, and packaging strategies. *BMC genomics, 17*(1).

Miao, L., Genjia, T., Yao, L., & Lian, X. (2005). Resistance mechanism of kiwifruit cultivars to *Pseudomonas syringae*} pv. *actinidae*. *Acta Phytophylacica Sinica, 32*(1), 37-42.

Miao, Y.-h., Xiao, J.-h., & Huang, D.-w. (2020). Distribution and evolution of the bacteriophage WO and its antagonism with Wolbachia. *Frontiers in microbiology, 11*, 595629.

Miller, M. A., Pfeiffer, W., & Schwartz, T. (2012). *The CIPRES science gateway: enabling high-impact science for phylogenetics researchers with limited resources.* Paper presented at the Proceedings of the 1st Conference of the Extreme Science and Engineering Discovery Environment: Bridging from the extreme to the campus and beyond.

Mingeot-Leclercq, M.-P., Glupczynski, Y., & Tulkens, P. M. (1999). Aminoglycosides: activity and resistance. *Antimicrobial agents and chemotherapy, 43*(4), 727-737.

Mirzaei, M. K., & Deng, L. (2022). New technologies for developing phage-based tools to manipulate the human microbiome. *Trends in Microbiology, 30*(2), 131-142.

Mojardín, L., & Salas, M. (2016). Global transcriptional analysis of virus-host interactions between phage φ29 and *Bacillus subtilis*. *Journal of virology, 90*(20), 9293-9304.

Monteiro, R., Pires, D., Costa, A., & Azeredo, J. (2019). Phage Therapy: Going Temperate? *Trends in microbiology, 27*(4).

Morella, N. M., Gomez, A. L., Wang, G., Leung, M. S., & Koskella, B. (2018). The impact of bacteriophages on phyllosphere bacterial abundance and composition. *Molecular ecology, 27*(8), 2025-2038.

Morris, C., Sands, D., Vanneste, J., Montarry, J., Oakley, B., Guilbaud, C., et al. (2010). Inferring the evolutionary history of the plant pathogen *Pseudomonas syringae*

from its biogeography in headwaters of rivers in North America, Europe, and New Zealand. *mBio, 1*(3).
Morris, C. E., Sands, D. C., Vinatzer, B. A., Glaux, C., Guilbaud, C., Buffière, A., et al. (2008). The life history of the plant pathogen *Pseudomonas syringae* is linked to the water cycle. *The ISME journal, 2*(3).
Mukeshimana, G., Ma, Y., Walworth, A. E., Song, G.-q., & Kelly, J. D. (2013). Factors influencing regeneration and *Agrobacterium tumefaciens*-mediated transformation of common bean (*Phaseolus vulgaris* L.). *Plant Biotechnology Reports, 7*(1), 59-70.
Munoz-Adalia, E. J., Diez, J. J., Fernandez, M. M., Hantula, J., & Vainio, E. J. (2018). Characterization of small RNAs originating from mitoviruses infecting the conifer pathogen *Fusarium circinatum*. *Archives of Virology, 163*(4), 1009-1018.
Murphy, K. (2016). λ Recombination and Recombineering. *EcoSal Plus, 7*(1).
Myers, E., & Miller, W. (1988). Optimal alignments in linear space. *Computer applications in the biosciences: CABIOS, 4*(1).
Nadeem, M. A., Yeken, M. Z., Shahid, M. Q., Habyarimana, E., Yılmaz, H., Alsaleh, A., et al. (2021). Common bean as a potential crop for future food security: an overview of past, current and future contributions in genomics, transcriptomics, transgenics and proteomics. *Biotechnology & Biotechnological Equipment, 35*(1), 759-787.
Nakajima, M., Yamashita, S., Takikawa, Y., Tsuyumu, S., Hibi, T., & Goto, M. (1995). Similarity of streptomycin resistance gene (s) in *Pseudomonas syringae* pv. *actinidiae* with strA and strB of plasmid RSF1010. *Japanese Journal of Phytopathology, 61*(5), 489-492.
Narouei-Khandan, H. A., Worner, S. P., Viljanen, S. L., van Bruggen, A. H., Balestra, G. M., & Jones, E. (2022). The Potential Global Climate Suitability of Kiwifruit Bacterial Canker Disease (*Pseudomonas syringae* pv. *actinidiae* (Psa)) Using Three Modelling Approaches: CLIMEX, Maxent and Multimodel Framework. *Climate, 10*(2), 14.
Neri, U., Wolf, Y. I., Roux, S., Camargo, A. P., Lee, B. D., Kazlauskas, D., et al. (2022). A five-fold expansion of the global RNA virome reveals multiple new clades of RNA bacteriophages. *bioRxiv*.
Ng, T. F. F., Willner, D. L., Lim, Y. W., Schmieder, R., Chau, B., Nilsson, C., et al. (2011). Broad surveys of DNA viral diversity obtained through viral metagenomics of mosquitoes. *PloS one, 6*(6), e20579.
Ni, P., Wang, L., Deng, B., Jiu, S., Ma, C., Zhang, C., et al. (2020). Combined Application of Bacteriophages and Carvacrol in the Control of *Pseudomonas syringae* pv. *actinidiae* Planktonic and Biofilm Forms. *Microorganisms, 8*(6).
Ni, P., Wang, L., Deng, B., Jiu, S., Ma, C., Zhang, C., et al. (2021). Characterization of a Lytic Bacteriophage against *Pseudomonas syringae* pv. *actinidiae* and Its Endolysin. *Viruses, 13*(4).
Nishimura, Y., Yoshida, T., Kuronishi, M., Uehara, H., Ogata, H., & Goto, S. (2017). ViPTree: the viral proteomic tree server. *Bioinformatics, 33*(15), 2379-2380.
Noble, T. J., Williams, B., Douglas, C. A., Giblot-Ducray, D., Mundree, S., & Young, A. J. (2022). Evaluating molecular diagnostic techniques for seed detection of

Pseudomonas savastanoi pv. *phaseolicola*, causal agent of halo blight disease in mungbean (*Vigna radiata*). *Australasian Plant Pathology, 51*(4), 453-459.
Nunes da Silva, M., Carvalho, S. M., Rodrigues, A. M., Gómez-Cadenas, A., António, C., & Vasconcelos, M. W. (2022). Defence-related pathways, phytohormones and primary metabolism are key players in kiwifruit plant tolerance to *Pseudomonas syringae* pv. *actinidiae*. *Plant, Cell & Environment, 45*(2), 528-541.
O'Leary, B., Neale, H., Geilfus, C., Jackson, R., Arnold, D., & Preston, G. (2016). Early changes in apoplast composition associated with defence and disease in interactions between *Phaseolus vulgaris* and the halo blight pathogen *Pseudomonas syringae* Pv. *phaseolicola*. *Plant, cell & environment, 39*(10).
Obeng, N., Pratama, A. A., & van Elsas, J. D. (2016). The significance of mutualistic phages for bacterial ecology and evolution. *Trends in microbiology, 24*(6), 440-449.
OECD. (2016). *Common bean (Phaseolus vulgaris)*.
Onorato, R., Yu, J., Cornish, D., Spinelli, F., Max, S., Vanneste, J., et al. (2010). *Recent advances in the characterisation and control of Pseudomonas syringae pv. actinidiae, the causal agent of bacterial canker on kiwifruit.* Paper presented at the VII International Symposium on Kiwifruit 913.
Opgenorth, D., Lai, M., Sorrell, M., & White, J. (1983). *Pseudomonas* canker of kiwifruit. *Plant disease, 67*(11), 1283-1284.
Ottati, S., Chiapello, M., Galetto, L., Bosco, D., Marzachi, C., & Abba, S. (2020). New Viral Sequences Identified in the Flavescence Doree Phytoplasma Vector *Scaphoideus titanus*. [Article]. *Viruses-Basel, 12*(3).
Ottati, S., Persico, A., Rossi, M., Bosco, D., Vallino, M., Abba, S., et al. (2020). Biological characterization of *Euscelidius variegatus* iflavirus 1. *Journal of Invertebrate Pathology, 173*.
Ottesen, A. R., González Peña, A., White, J. R., Pettengill, J. B., Li, C., Allard, S., et al. (2013). Baseline survey of the anatomical microbial ecology of an important food plant: *Solanum lycopersicum* (tomato). *BMC microbiology, 13*, 1-12.
Paez-Espino, D., Eloe-Fadrosh, E. A., Pavlopoulos, G. A., Thomas, A. D., Huntemann, M., Mikhailova, N., et al. (2016). Uncovering Earth's virome. *Nature, 536*(7617), 425.
Palleroni, N. J. Pseudomonas *Bergey's Manual of Systematics of Archaea and Bacteria* (pp. 1-1).
Park, S. C., & Nakai, T. (2003). Bacteriophage control of *Pseudomonas plecoglossicida* infection in ayu *Plecoglossus altivelis*. *Diseases of aquatic organisms, 53*(1), 33-39.
Park, S. C., Shimamura, I., Fukunaga, M., Mori, K.-I., & Nakai, T. (2000). Isolation of bacteriophages specific to a fish pathogen, *Pseudomonas plecoglossicida*, as a candidate for disease control. *Applied and environmental microbiology, 66*(4), 1416-1422.
Parkinson, N., Bryant, R., Bew, J., & Elphinstone, J. (2011). Rapid phylogenetic identification of members of the *Pseudomonas syringae* species complex using the rpoD locus. *Plant Pathology, 60*(2), 338-344.
Patel, R. R., Kandel, P. P., Traverso, E., Hockett, K. L., & Triplett, L. R. (2021). *Pseudomonas syringae* pv. *phaseolicola* uses distinct modes of stationary-phase persistence to survive bacteriocin and streptomycin treatments. *Mbio, 12*(2), e00161-00121.

Pattemore, D., Goodwin, R., McBrydie, H., Hoyte, S., & Vanneste, J. (2014). Evidence of the role of honey bees (*Apis mellifera*) as vectors of the bacterial plant pathogen *Pseudomonas syringae*. *Australasian Plant Pathology, 43*(5), 571-575.

Peters, T. L., Song, Y., Bryan, D. W., Hudson, L. K., & Denes, T. G. (2020). Mutant and recombinant phages selected from in vitro coevolution conditions overcome phage-resistant *Listeria monocytogenes*. *Applied and environmental microbiology, 86*(22), e02138-02120.

Petriccione, M., Zampella, L., Mastrobuoni, F., & Scortichini, M. (2017). Occurrence of copper-resistant *Pseudomonas syringae* pv. *syringae* strains isolated from rain and kiwifruit orchards also infected by *P. s*. pv. *actinidiae*. *European Journal of Plant Pathology, 149*(4), 953-968.

Pinheiro, L., Pereira, C., Barreal, M., Gallego, P., Balcão, V., & Almeida, A. (2020). Use of phage φ6 to inactivate *Pseudomonas syringae* pv. *actinidiae* in kiwifruit plants: in vitro and ex vivo experiments. *Applied microbiology and biotechnology, 104*(3).

Pinheiro, L., Pereira, C., Frazão, C., Balcão, V., & Almeida, A. (2019). Efficiency of Phage ϕ6 for Biocontrol of *Pseudomonas syringae* pv. syringae: An in Vitro Preliminary Study. *Microorganisms, 7*(9).

Pinto, C., Pinho, D., Sousa, S., Pinheiro, M., Egas, C., & Gomes, A. C. (2014). Unravelling the diversity of grapevine microbiome. *PLoS One, 9*(1), e85622.

Purahong, W., Orrù, L., Donati, I., Perpetuini, G., Cellini, A., Lamontanara, A., et al. (2018). Plant microbiome and its link to plant health: Host species, organs and *Pseudomonas syringae* pv. *actinidiae* infection shaping bacterial phyllosphere communities of kiwifruit plants. *Frontiers in Plant Science, 9*, 1563.

Purcell, A. H., Steiner, T., Mégraud, F., & Bové, J. (1986). In vitro isolation of a transovarially transmitted bacterium from the leafhopper *Euscelidius variegatus* (Hemiptera: Cicadellidae). *Journal of Invertebrate Pathology, 48*(1), 66-73.

Qadri, M., Short, S., Gast, K., Hernandez, J., & Wong, A. C.-N. (2020). Microbiome Innovation in Agriculture: Development of Microbial Based Tools for Insect Pest Management. *Frontiers in Sustainable Food Systems, 4*.

Rabiey, M., Roy, S. R., Holtappels, D., Franceschetti, L., Quilty, B. J., Creeth, R., et al. (2020). Phage biocontrol to combat *Pseudomonas syringae* pathogens causing disease in cherry. *Microbial Biotechnology, 13*(5), 1428-1445.

Refardt, D. (2011). Within-host competition determines reproductive success of temperate bacteriophages. *The ISME journal, 5*(9), 1451-1460.

Reglinski, T., Vanneste, J. L., Wurms, K., Gould, E., Spinelli, F., & Rikkerink, E. (2013). Using fundamental knowledge of induced resistance to develop control strategies for bacterial canker of kiwifruit caused by *Pseudomonas syringae* pv. *actinidiae* (Vol. 4, pp. 24): Frontiers Media SA.

Reglinski, T., Wurms, K., & Elmer, P. (2011). Short report on commercially available elicitors, natural products and microbes for evaluation against *Pseudomonas syringae* pv. *actinidiae*: *Actinidiae*.

Ren, G., Ding, Z., Pan, X., Wei, G., Wang, P., & Liu, L. (2022). Evaluation of the Abilities of Three Kinds of Copper-Based Nanoparticles to Control Kiwifruit Bacterial Canker. *Antibiotics, 11*(7), 891.

Renzi, M., Copini, P., Taddei, A., Rossetti, A., Gallipoli, L., Mazzaglia, A., et al. (2012). Bacterial canker on kiwifruit in Italy: anatomical changes in the wood and in the primary infection sites. *Phytopathology, 102*(9).

Reva, O. N., Dixelius, C., Meijer, J., & Priest, F. G. (2004). Taxonomic characterization and plant colonizing abilities of some bacteria related to *Bacillus amyloliquefaciens* and Bacillus subtilis. *FEMS microbiology ecology, 48*(2), 249-259.

Rodriguez-Valera, F., Martin-Cuadrado, A.-B., Rodriguez-Brito, B., Pasic, L., Thingstad, T. F., Rohwer, F., et al. (2009). Explaining microbial population genomics through phage predation. *Nature Precedings*, 1-1.

Rombouts, S., Volckaert, A., Venneman, S., Devlercq, B., Vandenheuvel, D., Allonsius, C. N., et al. (2016). Characterization of Noval Bacteriophages for Biocontrol of Bacterial Blight in Leek Caused by *Pseudomonas syringae* pv. porri. [Article]. *Frontiers in Microbiology, 7*, 15.

Rostøl, J. T., & Marraffini, L. (2019). (Ph) ighting phages: how bacteria resist their parasites. *Cell host & microbe, 25*(2), 184-194.

Roux, S., Brum, J. R., Dutilh, B. E., Sunagawa, S., Duhaime, M. B., Loy, A., et al. (2016). Ecogenomics and potential biogeochemical impacts of globally abundant ocean viruses. *Nature, 537*(7622), 689-693.

Ryazansky, S., Kulbachinskiy, A., & Aravin, A. A. (2018). The expanded universe of prokaryotic Argonaute proteins. *MBio, 9*(6), e01935-01918.

Ryu, C.-M., Farag, M. A., Hu, C.-H., Reddy, M. S., Wei, H.-X., Paré, P. W., et al. (2003). Bacterial volatiles promote growth in Arabidopsis. *Proceedings of the National Academy of Sciences, 100*(8), 4927-4932.

S, R., A, V., S, V., B, D., D, V., CN, A., et al. (2016). Characterization of Novel Bacteriophages for Biocontrol of Bacterial Blight in Leek Caused by *Pseudomonas syringae* pv. porri. *Frontiers in microbiology, 7*.

Sacher, J. C., Flint, A., Butcher, J., Blasdel, B., Reynolds, H. M., Lavigne, R., et al. (2018). Transcriptomic analysis of the *Campylobacter jejuni* response to T4-like phage NCTC 12673 infection. *Viruses, 10*(6), 332.

Saettler, A., Stadt, S., & Pontius, L. (1981). Effects of inoculation time and cultivar on internal infection of bean seed by *Pseudomonas phaseolicola*. *Journal of Seed Technology*, 23-30.

Salinas, A. D., Bonet, A., & Gepts, P. (1988). The Wild Relative of *Phaseolus vulgaris* in Middle America. *Genetic resources of Phaseolus beans* (pp. 163-184): Springer.

Sambrook, J., Fritsch, E. F., & Maniatis, T. (1989). Molecular cloning a laboratory manual second edition VOLS. 1 2 AND 3. *Sambrook, J., E. F. Fritsch and T. Maniatis. Molecular Cloning: a Laboratory Manual, Second Edition, Vols. 1, 2 and 3. Xxxix+Pagination Varies(Vol. 1); Xxxiii+Pagination Varies(Vol. 2): Xxxii+Pagination Varies(Vol. 3) Cold Spring Harbor Laboratory Press: Cold Spring Harbor, New York, USA. Illus. Paper*, XXXIX+PAGINATION VARIES (VOL 1), XXXIII+PAGINATION VARIES (VOL 2), XXXII+PAGINATION VARIES (VOL 3).

Sanders, E. (2012). Aseptic laboratory techniques: plating methods. *Journal of visualized experiments : JoVE*(63).

Sarma, B. K., Yadav, S. K., Singh, S., & Singh, H. B. (2015). Microbial consortium-mediated plant defense against phytopathogens: readdressing for enhancing efficacy. *Soil Biology and Biochemistry, 87*, 25-33.

Savian, F., Ginaldi, F., Musetti, R., Sandrin, N., Tarquini, G., Pagliari, L., et al. (2020). Studies on the aetiology of kiwifruit decline: interaction between soil-borne pathogens and waterlogging. *Plant and Soil, 456*(1), 113-128.

Schmerer, M., Molineux, I. J., & Bull, J. J. (2014). Synergy as a rationale for phage therapy using phage cocktails. *Peerj, 2*.

Schmutz, J., McClean, P., Mamidi, S., Wu, G., Cannon, S., Grimwood, J., et al. (2014). A reference genome for common bean and genome-wide analysis of dual domestications. *Nature genetics, 46*(7).

Schneider, C., Rasband, W., & Eliceiri, K. (2012). NIH Image to ImageJ: 25 years of image analysis. *Nature methods, 9*(7).

Scholl. (2017). Phage Tail-Like Bacteriocins. *Annual review of virology, 4*(1).

Schwalbach, M. S., Hewson, I., & Fuhrman, J. A. (2004). Viral effects on bacterial community composition in marine plankton microcosms. *Aquatic Microbial Ecology, 34*(2), 117-127.

Scortichini, M. (1994). Occurrence of *Pseudomonas syringae* pv. *actinidiae* on kiwifruit in Italy. *Plant Pathology, 43*(6), 1035-1038.

Scortichini, M. (2016). Field efficacy of a zinc-copper-hydracid of citric acid biocomplex compound to reduce oozing from winter cankers caused by *Pseudomonas syringae* pv. *actinidiae* to Actinidia spp. *Journal of Plant Pathology*, 651-655.

Scortichini, M., Marcelletti, S., Ferrante, P., Petriccione, M., & Firrao, G. (2012). *Pseudomonas syringae* pv. *actinidiae*: a re-emerging, multi-faceted, pandemic pathogen (Vol. 13, pp. 631-640): Wiley Online Library.

Scortichini, M., & Rossi, M. P. (1991). In vitro susceptibility of *Erwinia amylovora* (Burrill) Winslow et al. to geraniol and citronellol. *Journal of applied bacteriology, 71*(2), 113-118.

Serizawa, S., & Ichikawa, T. (1993). Epidemiology of Bacterial Canker of Kiwifruit 1. Infection and Bacterial Movement in Tissue of New Canes. *Japanese Journal of Phytopathology, 59*(4), 452-459.

Serizawa, S., Ichikawa, T., Takikawa, Y., Tsuyumu, S., & Goto, M. (1989). Occurrence of bacterial canker of kiwifruit in Japan description of symptoms, isolation of the pathogen and screening of bactericides. *Japanese Journal of Phytopathology, 55*(4), 427-436.

Shen, Y., & Loessner, M. J. (2021). Beyond antibacterials–exploring bacteriophages as antivirulence agents. *Current Opinion in Biotechnology, 68*, 166-173.

Shi, M., Lin, X.-D., Tian, J.-H., Chen, L.-J., Chen, X., Li, C.-X., et al. (2016). Redefining the invertebrate RNA virosphere. *Nature, 540*(7634), 539-543.

Shropshire, J. D., On, J., Layton, E. M., Zhou, H., & Bordenstein, S. R. (2018). One prophage WO gene rescues cytoplasmic incompatibility in Drosophila melanogaster. *Proceedings of the National Academy of Sciences, 115*(19), 4987-4991.

Sieradzki, E. T., Ignacio-Espinoza, J. C., Needham, D. M., Fichot, E. B., & Fuhrman, J. A. (2019). Dynamic marine viral infections and major contribution to photosynthetic

processes shown by spatiotemporal picoplankton metatranscriptomes. *Nature communications, 10*(1), 1-9.
Singh, S. P., Gepts, P., & Debouck, D. G. (1991). Races of common bean (*Phaseolus vulgaris*, *Fabaceae*). *Economic Botany, 45*(3), 379-396.
Singh, S. P., & Schwartz, H. F. (2010). Breeding common bean for resistance to diseases: a review. *Crop Science, 50*(6), 2199-2223.
Sistrom, M., Park, D., O'Brien, H., Wang, Z., Guttman, D., Townsend, J., et al. (2015). Genomic and Gene-Expression Comparisons among Phage-Resistant Type-IV Pilus Mutants of *Pseudomonas syringae* pathovar *phaseolicola*. *PloS one, 10*(12).
Smith, A. R. W., Zamze, S. E., & Hignett, R. C. (1994). Morphology and hydrolytic activity of A7, a typing phage of *Pseudomonas syringae* pv. *morsprunorum*. *Microbiology, 140*(4), 905-913.
Spinelli, F., Donati, I., Vanneste, J., Costa, M., & Costa, G. (2010). Real time monitoring of the interactions between *Pseudomonas syringae* pv. *actinidiae* and *Actinidia* species. Paper presented at the VII International Symposium on Kiwifruit 913.
Starr, E. P., Nuccio, E. E., Pett-Ridge, J., Banfield, J. F., & Firestone, M. K. (2019). Metatranscriptomic reconstruction reveals RNA viruses with the potential to shape carbon cycling in soil. *Proceedings of the National Academy of Sciences of the United States of America, 116*(51), 25900-25908.
Stefan, H., Jens, H., Bernd, A., & Thomas, A. (2013). Post-harvest application of lytic bacteriophages for biocontrol of food-borne pathogens and spoilage bacteria. *Berliner und Münchener Tierärztliche Wochenschrift, 126*(9/10), 357-369.
Suttle, C. A. (2007). Marine viruses - major players in the global ecosystem. *Nature Reviews Microbiology, 5*(10), 801-812.
Sutton, T. D., & Hill, C. (2019). Gut bacteriophage: current understanding and challenges. *Frontiers in Endocrinology, 10*, 784.
Svircev, A., Roach, D., & Castle, A. (2018). Framing the Future with Bacteriophages in Agriculture. *Viruses, 10*(5).
Tacconi, G., Giacopini, A., Vittone, G., Nari, L., Spadaro, D., Savian, F., et al. (2019). Moria del kiwi": situazione disastrosa al nord, preoccupante nel resto d'Italia.
Taylor, J., Teverson, D. M., Allen, D. J., & Pastor-Corrales, M. A. (1996). Identification and origin of races of *Pseudomonas syringae* pv. *phaseolicola* from Africa and other bean growing areas. *Plant Pathology, 45*(3), 469-478.
Taylor, J. D., Teverson, D. M., & Davis, J. H. C. (1996). Sources of resistance to *Pseudomonas syringae* pv *phaseolicola* races in *Phaseolus vulgaris*. *Plant Pathology, 45*(3), 479-485.
Taylor, V. L., Fitzpatrick, A. D., Islam, Z., & Maxwell, K. L. (2019). The diverse impacts of phage morons on bacterial fitness and virulence. *Advances in virus research, 103*, 1-31.
Terán, H., Lema, M., Webster, D., & Singh, S. P. (2009). 75 years of breeding pinto bean for resistance to diseases in the United States. *Euphytica, 167*(3), 341-351.
Tomkins, M., Kliot, A., Maree, A. F., & Hogenhout, S. A. (2018). A multi-layered mechanistic modelling approach to understand how effector genes extend

beyond phytoplasma to modulate plant hosts, insect vectors and the environment. *Current opinion in plant biology, 44*, 39-48.

Trifinopoulos, J., Lam-Tung, N., von Haeseler, A., & Minh, B. Q. (2016). W-IQ-TREE: a fast online phylogenetic tool for maximum likelihood analysis. *Nucleic Acids Research, 44*(W1), W232-W235.

Trivedi, P., Trivedi, C., Grinyer, J., Anderson, I. C., & Singh, B. K. (2016). Harnessing host-vector microbiome for sustainable plant disease management of phloem-limited bacteria. *Frontiers in Plant Science, 7*, 1423.

Tsao, Y.-F., Taylor, V. L., Kala, S., Bondy-Denomy, J., Khan, A. N., Bona, D., et al. (2018). Phage morons play an important role in *Pseudomonas aeruginosa* phenotypes. *Journal of bacteriology, 200*(22), e00189-00118.

Turner, D., Kropinski, A., & Adriaenssens, E. (2021). A Roadmap for Genome-Based Phage Taxonomy. *Viruses, 13*(3).

Turner, N., Ritchie, L., Bresalier, R., & Chapkin, R. (2013). The microbiome and colorectal neoplasia: environmental modifiers of dysbiosis. *Current gastroenterology reports, 15*, 1-10.

Tvedte, E. S., Walden, K. K., McElroy, K. E., Werren, J. H., Forbes, A. A., Hood, G. R., et al. (2019). Genome of the parasitoid wasp *Diachasma alloeum*, an emerging model for ecological speciation and transitions to asexual reproduction. *Genome biology and evolution, 11*(10), 2767-2773.

Twort, F. W. (1915). An investigation on the nature of ultra-microscopic viruses. *Acta Kravsi*.

Tynecki, P., Guziński, A., Kazimierczak, J., Jadczuk, M., Dastych, J., & Onisko, A. (2020). PhageAI - Bacteriophage Life Cycle Recognition with Machine Learning and Natural Language Processing.

Valente, M., Ortugno, C., Tosi, L., Scannavini, M., Pelliconi, F., Fagioli, L., et al. (2014). Bion® 50WG (acibenzolar-S-methyl), systemic acquired resistance inducer: efficacy in field against bacterial kiwifruit vine disease, caused by *Pseudomonas syringae* pv. *actinidiae*. *Atti, Giornate Fitopatologiche, Chianciano Terme (Siena), 18-21 marzo 2014, Volume secondo*, 147-156.

Van Der Wilk, F., Dullemans, A. M., Verbeek, M., & Van Den Heuvel, J. F. (1999). Isolation and characterization of APSE-1, a bacteriophage infecting the secondary endosymbiont of *Acyrthosiphon pisum*. *Virology, 262*(1), 104-113.

van Lenteren, J. C., Bolckmans, K., Kohl, J., Ravensberg, W. J., & Urbaneja, A. (2018). Biological control using invertebrates and microorganisms: plenty of new opportunities. *Biocontrol, 63*(1), 39-59.

Vanneste, J. (2012). *Pseudomonas syringae* pv. *actinidiae* (Psa): a threat to the New Zealand and global kiwifruit industry. *New Zealand Journal of Crop and Horticultural Science, 40*(4), 265-267.

Vanneste, J., Cornish, D., Yu, J., & Stokes, C. (2014). First report of *Pseudomonas syringae* pv. *actinidiae* the causal agent of bacterial canker of kiwifruit on Actinidia arguta vines in New Zealand. *Plant disease, 98*(3), 418-418.

Vanneste, J., Oldham, J., Clark, G., & Felman, C. (2013). Survival of *Pseudomonas syringae* pv *actinidiae* in nonkiwifruit green compost. *New Zealand Plant Protection, 66*, 178-183.

Vanneste, J., Yu, J., Cornish, D., Oldham, J., Spinelli, F., Pattemore, D., et al. (2013). Survival of *Pseudomonas syringae* pv. *actinidiae* in the environment*.* Paper presented at the I International Symposium on Bacterial Canker of Kiwifruit 1095.

Vanneste, J. L. (2017). The scientific, economic, and social impacts of the New Zealand outbreak of bacterial canker of kiwifruit (*Pseudomonas syringae* pv. *actinidiae*). *Annual Review of Phytopathology, 55*, 377-399.

Varghese, F. S., & Rij, R. P. v. (2018). Insect virus discovery by metagenomic and cell culture-based approaches *Viral Metagenomics* (pp. 197-213): Springer.

Vassallo, C. N., Doering, C. R., Littlehale, M. L., Teodoro, G. I., & Laub, M. T. (2022). A functional selection reveals previously undetected anti-phage defence systems in the E. coli pangenome. *Nature microbiology, 7*(10), 1568-1579.

Vayssier-Taussat, M., Albina, E., Citti, C., Cosson, J.-F., Jacques, M.-A., Lebrun, M.-H., et al. (2014). Shifting the paradigm from pathogens to pathobiome: new concepts in the light of meta-omics. *Frontiers in Cellular and Infection Microbiology, 4*.

Venturini, C., Petrovic Fabijan, A., Fajardo Lubian, A., Barbirz, S., & Iredell, J. (2022). Biological foundations of successful bacteriophage therapy. *EMBO Molecular Medicine*, e12435.

Vidaver, A., Koski, R., & Van Etten, J. (1973). Bacteriophage phi6: a Lipid-Containing Virus of *Pseudomonas phaseolicola*. *Journal of virology, 11*(5).

Vikram, A., Woolston, J., & Sulakvelidze, A. (2021). Phage biocontrol applications in food production and processing. *Current issues in molecular biology, 40*(1), 267-302.

Von Bodman, S. B., Bauer, W. D., & Coplin, D. L. (2003). Quorum sensing in plant-pathogenic bacteria. *Annual review of phytopathology, 41*(1), 455-482.

Vu, N. T., & Oh, C.-S. (2020). Bacteriophage usage for bacterial disease management and diagnosis in plants. *The Plant Pathology Journal, 36*(3), 204.

Völksch, B., & May, R. (2001). Biological control of *Pseudomonas syringae* pv. *glycinea* by epiphytic bacteria under field conditions. *Microbial ecology, 41*, 132-139.

Walker, P., Siddell, S., Lefkowitz, E., Mushegian, A., Adriaenssens, E., Dempsey, D., et al. (2020). Changes to virus taxonomy and the Statutes ratified by the International Committee on Taxonomy of Viruses (2020). *Archives of virology, 165*(11).

Wan, X., Hendrix, H., Skurnik, M., & Lavigne, R. (2021). Phage-based target discovery and its exploitation towards novel antibacterial molecules. *Current Opinion in Biotechnology, 68*, 1-7.

Wang, F., Li, J., Ye, K., Liu, P., Gong, H., Jiang, Q., et al. (2019). An in vitro Actinidia bioassay to evaluate the resistance to *Pseudomonas syringae* pv. *actinidiae*. *The plant pathology journal, 35*(4), 372.

Wang, X., Wei, Z., Yang, K., Wang, J., Jousset, A., Xu, Y., et al. (2019). Phage combination therapies for bacterial wilt disease in tomato. *Nature Biotechnology, 37*(12), 1513-+.

Wattam, A. R. (2016). Improvements to PATRIC, the all-bacterial Bioinformatics Database and Analysis Resource Center.

Webster, D., Atkin, J., & Cross, J. (1983). Bacterial Blights of Snap Beans. *Plant Disease, 67*(9), 935.

Weinbauer, M. G. (2004). Ecology of prokaryotic viruses. *FEMS microbiology reviews, 28*(2), 127-181.

Weiss, B., & Aksoy, S. (2011). Microbiome influences on insect host vector competence. *Trends in parasitology, 27*(11), 514-522.

Williamson, K. E., Schnitker, J. B., Radosevich, M., Smith, D. W., & Wommack, K. E. (2008). Cultivation-based assessment of lysogeny among soil bacteria. *Microbial ecology, 56*(3), 437-447.

Wilton, M., Subramaniam, R., Elmore, J., Felsensteiner, C., Coaker, G., & Desveaux, D. (2010). The type III effector HopF2 Pto targets Arabidopsis RIN4 protein to promote *Pseudomonas syringae* virulence. *Proceedings of the National Academy of Sciences, 107*(5), 2349-2354.

Wojtus, J., Frampton, R., Warring, S., Hendrickson, H., & Fineran, P. (2019). Genome Sequence of a Jumbo Bacteriophage That Infects the Kiwifruit Phytopathogen *Pseudomonas syringae* pv. *actinidiae*. *Microbiology resource announcements, 8*(22).

Wommack, K. E., & Colwell, R. R. (2000). Virioplankton: viruses in aquatic ecosystems. *Microbiology and molecular biology reviews, 64*(1), 69-114.

Wright, A., Hawkins, C., Änggård, E., & Harper, D. (2009). A controlled clinical trial of a therapeutic bacteriophage preparation in chronic otitis due to antibiotic-resistant *Pseudomonas aeruginosa*; a preliminary report of efficacy. *Clinical otolaryngology, 34*(4), 349-357.

Xin, X.-F., Kvitko, B., & He, S. Y. (2018). *Pseudomonas syringae*: what it takes to be a pathogen. *Nature Reviews Microbiology, 16*(5), 316-328.

Yaish, M. W. F., Sosa, D., Vences, F. J., & Vaquero, F. (2006). Genetic mapping of quantitative resistance to race 5 of *Pseudomonas syringae* pv. *phaseolicola* in common bean. *Euphytica, 152*(3), 397-404.

Yin, Y., Ni, P. e., Deng, B., Wang, S., Xu, W., & Wang, D. (2019). Isolation and characterization of phages against *Pseudomonas syringae* pv. *actinidiae*. *Acta Agriculturae Scandinavica, Section B—Soil & Plant Science, 69*(3), 199-208.

Yoshikawa, G., Askora, A., Blanc-Mathieu, R., Kawasaki, T., Li, Y., Nakano, M., et al. (2018). *Xanthomonas citri* jumbo phage XacN1 exhibits a wide host range and high complement of tRNA genes. *Scientific Reports, 8*.

Young, J. (2010). Taxonomy of *Pseudomonas syringae*. *Journal of plant pathology*, S5-S14.

Young, J. (2012). *Pseudomonas syringae* pv. *actinidiae* in New Zealand. *Journal of Plant Pathology, 94*(1sup), 1-5-S1. 10.

Young, J., Dye, D., Bradbury, J., Panagopoulos, C., & Robbs, C. (1978). A proposed nomenclature and classification for plant pathogenic bacteria. *New Zealand Journal of Agricultural Research, 21*(1), 153-177.

Yu, J. G., Lim, J. A., Song, Y. R., Heu, S., Kim, G. H., Koh, Y. J., et al. (2016). Isolation and Characterization of Bacteriophages Against *Pseudomonas syringae* pv. *actinidiae* Causing Bacterial Canker Disease in Kiwifruit. [Article]. *Journal of Microbiology and Biotechnology, 26*(2), 385-393.

Yutin, N., Makarova, K. S., Gussow, A. B., Krupovic, M., Segall, A., Edwards, R. A., et al. (2018). Discovery of an expansive bacteriophage family that includes the most abundant viruses from the human gut. *Nature microbiology, 3*(1), 38-46.

Zhang, Y.-Z., Shi, M., & Holmes, E. C. (2018). Using metagenomics to characterize an expanding virosphere. *Cell, 172*(6), 1168-1172.

Zhao, X., Chen, C., Shen, W., Huang, G., Le, S., Lu, S., et al. (2016). Global transcriptomic analysis of interactions between *Pseudomonas aeruginosa* and bacteriophage PaP3. *Scientific reports, 6*(1), 1-12.

Zhi-Yu, Z. (1983). A Report on the Chromosome Numbers of 2 Varieties of Actinidia chinensis Planch. *Journal of Systematics and Evolution, 21*(2), 161.

Álvarez, B., López, M. M., & Biosca, E. G. (2019). Biocontrol of the major plant pathogen *Ralstonia solanacearum* in irrigation water and host plants by novel waterborne lytic bacteriophages. *Frontiers in Microbiology, 10*, 2813.